PhD degree in Molecular Medicine

curriculum in Molecular Oncology

European School of Molecular Medicine (SEMM),

University of Milan and University of Naples "Federico II"

Faculty of Medicine (MED/04)

NPMc+ as a model system to investigate the role of quiescence in leukemia development

Maria Elena Boggio Merlo

European Institute of Oncology (IEO), Milan

Student ID: R10754 – R20

Supervisor: Prof. Pier Giuseppe Pelicci, MD, PhD

Added Supervisors: Dr. Emanuela Colombo, PhD

Academic year 2017-2018

Table of contents

List of Abbreviations

4-OHT	4-Hydroxy-tamoxifen
5-FU	5-fluorouracil
Abs	Antibodies
AML	Acute myeloid leukemia
Ara-C	Cytarabine
BM	Bone marrow
BM-MNCs	BM Mono-nucleated Cells
BMT	BM Transplantation
bp	Base Pair
BrdU	5-Bromo-2-deoxyuridine
CRU	Colony Repopulating Unit
DNMT3a	DNA methyltranferase a
ELDA	Extreme limiting dilution analysis
FAB	French-American-British classification
FACS	Fluorescence activated cell sorting
FLT3-ITD	FLT3 Internal Tandem Duplication
GSEA	Gene Set Enrichment Assay
HOX	Homeobox containing family of transcription factors
Hprt	hypoxanthine-guanine phosphor-ribosyl-transferase locus
HSC	Hematopoietic stem cell
HSPC	Hematopoietic stem and progenitor cell
IFN	Interferon
i.p.	Intraperitoneal
i.v.	Intravenous
KI	Knock-in
KO	Knock-out
LIC	Leukemia initiating cell
Lin	Lineage markers
LKS	Lin^-, $cKit^+$, $Sca\text{-}1^+$ (cells)
LTR	Long Term Retaining (cells)
LSC	Leukemia stem cell
LT-HSC	Long-term repopulating HSC
MEF	Mouse embryonic fibroblast
min	Minutes
MPN	Myeloproliferative neoplasm
MDS	Myelodysplastic syndrome
MPP	Multi Potent Progenitors
NES	Nuclear Export Signal
NGS	Next generation sequencing
NK-AML	Normal Karyotype AML
NPMc+	Nucleophosmin (cytoplasmic localization)
O/N	Overnight
PB	Peripheral blood

PCR	Polymerase chain reaction
pIpC	Polyinosinic:polycytidylic acid
RBC	Red Blood Cells
ROS	Reactive Oxygen Species
rpm	Round per minute
RT	Room Temperature
scRNAseq	Single Cell RNA sequencing
ST-HSC	Short-term repopulating HSC
TCGA	The Cancer Genome Atlas
TIC	Tumor initiating cell
TKI	tyrosine kinase inhibitors
VAF	Variant Allele Frequency
WBC	White Blood Cells
WHO	World Health Organization
WT	Wild-Type
YFP	Yellow fluorescent protein

List of Figures

List of Tables

Abstract

The evolution of Acute Myeloid Leukemia (AML) is a complex process characterized by the stepwise accumulation of mutations, primarily occurring in Hematopoietic Stem Cells (HSCs). Such mutations give rise to the so-called Leukemia Initiating Cell (LIC), characterized by enhanced self-renewal and impaired differentiation. The molecular mechanisms underlying this transition are still poorly understood but they are likely to be critical to understanding the leukemic stem cell (LSC) biology.

Recent functional and genetic studies on AML revealed NPMc+ as a critical driver oncogene, highly conserved at relapse, and characterizing the AML phenotype. Likely, NPMc+ has a pivotal role in the LIC evolution and LSC behavior.

Taking advantage of the extended pre-leukemic phase of our inducible NPMc+ mouse model, we elucidated the impact of NPMc+ expression on normal HSCs to define the early mechanisms of NPMc+ induced leukemogenesis. We have found that NPMc+ expression leads to the expansion of the HSC compartment by enforcing a stem-cell transcriptional program that promotes quiescence and increases self-renewal. Moreover, considering the strong co-occurrence of NPMc+ with FLT3-ITD in patients, we investigated the mechanisms of this cooperation in pre-leukemia. Strikingly, the expression of NPMc+ in the FLT3-ITD background *i)* prevents the HSCs exhaustion imposed by FLT3-ITD, *ii)* restores their repopulating capacity, *iii)* restores the same transcriptional program observed in the NPMc+ HSCs, including quiescence genes upregulation. These data strongly suggest that NPMc+ and FLT3-ITD mutations cooperate in inducing AML, thanks to the NPMc+ ability to limit LT-HSCs exhaustion and reconstitute a fully competent LT-HSC population in which the oncogenic activities of FLT3-ITD lead to a rapid selection of the LICs.

We thus hypothesized that enforced quiescence might be critical to maintain the transformed clone during both the pre-leukemic and the leukemic phase. In support, we

identified the TGFβ pathway, one of the most critical pathways that regulate HSCs quiescence, as being upregulated by NPMc+, either alone or in combination with FLT3-ITD. Moreover, we report that pharmacological inhibition of this pathway impacts on NPMc+/FLT3-ITD AML growth *in vivo*. Finally, we provide preliminary results suggesting that TGFβ inhibition might modify the fitness and/or the number of LSCs.

1 Introduction

1.1 Hematopoiesis and Hematopoietic Stem Cells

Mature circulating blood cells are short-lived and need to be continuously replaced. In a healthy individual more than 500 billion of new blood cells are daily produced through a process called hematopoiesis, which is based on the rare Hematopoietic Stem Cells (HSCs) population.

From a developmental point of view, HSCs arise from the embryo yolk sac, then move to the aorta-gonad-mesonephros (AGM) embryo region and, later to the placenta and the fetal liver. Subsequently, they move into the bone marrow (BM) which, finally, becomes the main site of hematopoiesis in the adult (Rieger and Schroeder 2012) (Fig1).

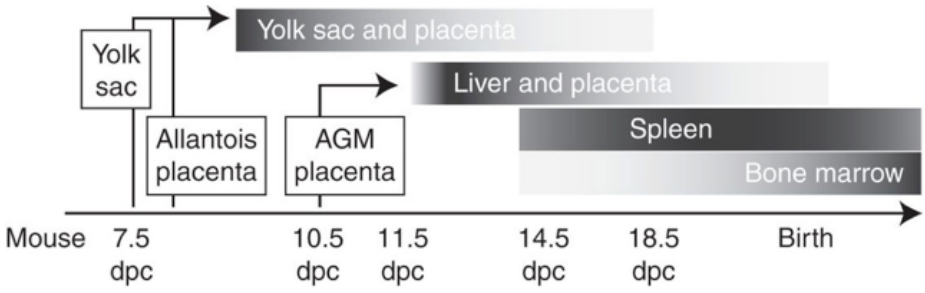

Figure 1 Embryonic hematopoietic development.
Organs and timing of the hematopoietic system development, from the embryo to the adult mouse. dpc= days after conception. (Adapted from Rieger and Schroeder, Cold Spring Harbor Perspectives in Biology, 2012)

Two sites in the BM have been found as the most enriched in HSCs and have been proposed as "niches": the endosteal osteoblastic niche (Calvi et al. 2003; Zhang et al. 2003) and the perivascular endothelial region (Kiel et al. 2005).

HSCs, and in general adult stem cells, are characterized by two unique cellular features: long-term self-renewal and differentiation potential (multipotency). Pioneering *in vivo* experiments by Till and McCulloch contributed to this definition (Till and McCulloch

1961); indeed, they observed the formation of "nodules" on the spleen surface of irradiated mice transplanted with syngeneic bone marrow mononucleated cells (BM-MNCs). Further analysis of these nodules demonstrated the existence, in the BM of adult mice, of a rare and mainly quiescent cell population, capable of generating multiple types of mature blood cells. Few years later, studies by Becker and Siminovitch demonstrated that this rare population gave rise to identical cells that could be re-transplanted to secondary hosts where they reconstitute all blood cell lineages (Becker, McCulloch, and Till 1963; Siminovitch, McCulloch, and Till 1963).

These observations introduced the concept of hematopoiesis as a hierarchical organized process: HSCs are at the apex of the process, which proceeds through a developmental organized series of branches, giving rise to progressively more committed progenitors that represent the basis of the pyramid (Fig2). The long-term maintenance of the HSC pool is guaranteed by the HSCs' property to produce, upon division, one (asymmetric division) or two (symmetric division) daughter cells that retain the capacity to self-renew.

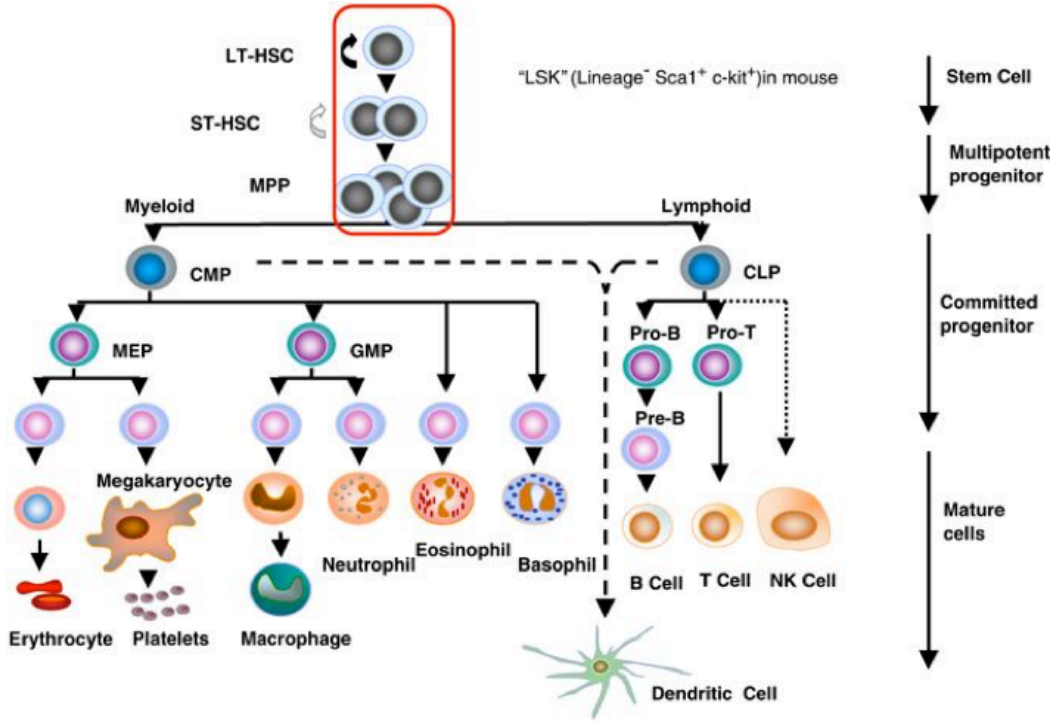

Figure 2 The hierarchical organization of the hematopoietic process.
In mice, the rare HSC population stands at the apex of the hierarchical hematopoietic process, depicted as a series of branches that progressively differentiate towards the hematopoietic lineages. (Adapted from Larsson and Karlsson, Oncogene, 2005).

Extensive studies gradually contributed to conceive the hematopoietic differentiation tree model as shown in Fig3b. With the introduction of the single-cell transcriptomic analysis (scRNA-seq), several groups are actively working on HSC and progenitor single cell transcriptomes and their mathematical interpretation. According to these analyses, we can now envision a "modern" hematological tree where the differentiation process becomes a continuum between lower and higher differentiated elements, and the rigid boundaries between distinct cell types in the tree are progressively relaxed (Fig3c) (Laurenti and Göttgens 2018).

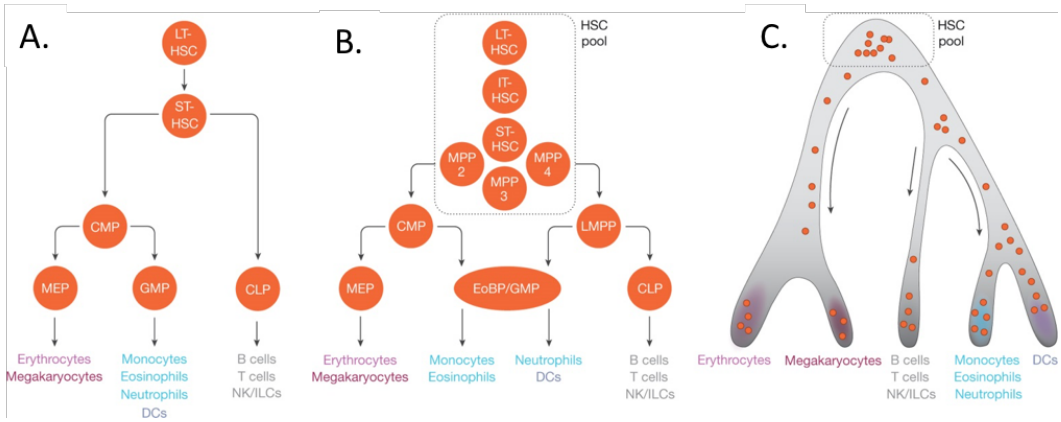

Figure 3 Hierarchical hematopoiesis, a developing model
A) The first hematological tree proposed, where HSCs are a discrete and homogenous population. B) The introduction of a higher heterogeneity in both the HSC and progenitor pools. C) The novel continuum differentiation model. (Adapted from Laurenti and Göttgen, Nature, 2018)

However, this new scenario is not free of puzzlements. In particular, the combination of cell surface markers allows the isolation of distinct Hematopoietic Stem and Progenitor cell (HSPC) subpopulations with specific functionality, even in the proposed continuum of low-primed cells analyzed by scRNA-seq. Thus, further studies are required to define a comprehensive hematopoietic differentiation model.

1.1.1 HSCs history and markers

Nowadays we are quite familiar with concepts like adult stem cells and hierarchical tissue organization, and hematopoiesis is considered the paradigm for the mammalian stem cell system. HSCs express a unique cell surface marker pattern and, since they are not interconnected in a tissue, can be easily separated and further characterized. Over the last decades, fluorescence-activated cell sorting (FACS) combined with robust monoclonal antibody against surface markers have been exploited to isolate a pure murine HSC population. From an historical point of view, in 1988 the initial prospective purification of HSCs from mouse BM was achieved by selecting the Lineage negative (Lin- [typically B220, CD4, CD8, Gr-1, Mac-1 and Ter-119], Sca-1+ and Thy-1-low population)

(Spangrude, Heimfeld, and Weissman 1988). These cells represented around 0.05% of the mouse BM and they were the only cells able to stably reconstitute lethally irradiated recipients (3 months after transplantation), thus retrospectively proving their true HSC identity. In the same years, a population with similar stem cell characteristics was isolated by c-Kit positive selection on Lin-/Sca-1+ BM cells, the so-called LKS population (Okada et al. 1992).

Although greatly enriched for HSC phenotype and activity, LKS cells contain only 10% of *bona fide* long-term HSCs (Morrison and Weissman 1994) and different strategies have been used to further enrich for HSCs. One approach is based on the introduction of the CD34 marker, previously identified as positive marker for human HSCs (Baum et al. 1992). By this approach, LKS can be divided in two classes of cells with long term ($CD34^-$, LT-HSCs) and short term ($CD34^+$, ST-HSCs) reconstitution potential. Notably, 1 out of 4 cells of the CD34 negative portion showed long-term reconstitution abilities, after single-cell transplantation (Osawa et al. 1996). Further, based on high expression level of the Flk receptor, multipotent progenitors (MPP) were isolated within LKS, and represent a population that has lost the self-renewal capacity (Adolfsson et al. 2001). Alternatively, relying on the expression of the two signaling lymphocyte activation molecules CD48 and CD150, a population characterized by 50% long-term HSCs purity (SLAM population) can be isolated within the LKS cells (Kiel et al. 2005). In addition, physical parameters (e.g. efflux of the Hoechst 33342 dye) have been used for prospective isolation of LT-HSCs with comparable purity and called side population (SP) (Goodell et al. 1996). More recently, Wilson and colleagues, combining the available markers, demonstrated that only 30% of SLAM HSCs were CD34-, thus isolating a novel subpopulation, highly enriched in functional HSCs, which accounted for the 0.0013% of the total BM (Wilson et al. 2008).

1.2 HSCs and quiescence

In the BM, two distinct HSC states can be defined: the proliferative state, necessary for differentiation and self-renewal ability, and the quiescence one, which enables lifelong hematopoietic cell production. Quiescence, or G0 phase, is defined as the cell exit from the cycle (characterized by the four phases G1, S, G2 and M) and is a critical property of adult HSCs (Pardee 1974). Indeed, in the embryo, HSCs incessantly divide asymmetrically to generate mature blood cells and reach the hematological homeostasis. They switch to a quiescent state only by the fourth week after birth (Pietras, Warr, and Passegué 2011). In the adult, initial studies on HSC cell cycle assessed that, in homeostatic conditions, about 75% of the HSCs are in the G0 phase and they are recruited into the cell cycle every 57 days (Cheshier et al. 1999). More recent studies highlighted a higher degree of heterogeneity with the existence of "active" HSCs and "dormant" HSCs, with the latter accounting for the 5-10% of the total HSC pool and entering the cell cycle once every 145days (Wilson et al. 2008; Foudi et al. 2009).

HSC quiescence represents a complete "switch off" status that relies on a slow metabolism (Suda, Arai, and Shimmura 2005), low rate of transcription and protein synthesis (Passegué et al. 2005), and low activity of the DNA replication machinery, including low transcripts for the DNA polymerases (Wilson et al. 2008).

Notably, quiescence is a reversible status, and cells might re-enter cell cycle if requested by injury signals. Quiescent HSCs, for instance, can be activated by cytokines, like granulocyte colony stimulating factor (G-CSF), or by chemotherapeutic agents that provoke myeloid depression (Wilson et al. 2008; Passegué et al. 2005), as well as by inflammatory signals, like interferon-1 (IFN-1) (Pietras et al. 2014). Inevitably, the progression into G1 phase causes a reduction of the long-term engraftment potential. Accordingly, dormant HSCs show a greater self-renewal capacity and long-term reconstitution potential than active ones (Wilson et al. 2008). The loss of stemness in

HSCs is proportional to their proliferation rate, as illustrated by the progressive exhaustion of aging HSCs (Rossi et al. 2005).

These studies underscore the critical importance of quiescence maintenance for proper hematopoiesis, and the need of a complex network of intrinsic and environmental factors that preserve the balance between HSC quiescence and proliferation potential (Fig4). Studies based on genetically modified mouse models uncovered many intrinsic molecular mechanisms linking loss of quiescence to the HSCs exhaustion (Pietras, Warr, and Passegué 2011). It is not surprising that a major role is played by the competing actions of two main classes of cell cycle regulators: cyclin-dependent kinases (CDKs) and their inhibitors (CKIs). During G1 phase, the rate of cell proliferation is largely determined, and two Cyclin-CDKs complexes are involved: the Cyclin D–CDK4/6 and the Cyclin E–CDK2 complex. CDKs phosphorylate and inactivate RB protein family members (e.g. p130), thus allowing the release of E2F transcription factor, which enables the progression into the S phase. CDKs activity is impeded by the INK4 family of kinase inhibitors (p16, p15, p18, and p19), which blocks the activity of Cyclin D–CDK4/6 complex, and by the CIP/KIP family (p21, p27, and p57), which inhibits Cyclin E–CDK2 complex.

In mice, ablation of all D-type Cyclins (*Ccnd1-3*) or of *Cdk4/6* is embryonic lethal and is accompanied by reduced proliferation in fetal progenitors (Malumbres et al. 2004; Kozar et al. 2004). Conversely, the deletion of only *Cdk6*, although not affecting the HSCs cell cycle at homeostasis, reduced the HSC activation upon proliferation signals and their functionality in competitive BMT (Scheicher et al. 2015). The deletion of *p21*, instead, increases the number of HSCs and reduces their G0 proportion, thus provoking a more rapid BM exhaustion upon myeloablative stress (Cheng et al. 2000). *p57*-null HSCs highly proliferate and lose self-renewal, a defective phenotype which can be corrected by knocking-in *p27* in the *p57* locus, suggesting a functional overlap between the two genes in the control of HSCs homeostasis (Matsumoto et al. 2011).

In this scenario, the family of homeobox(HOX)-containing transcription factors (TFs), particularly HOXB4, represents a counter-intuitive level of regulation capable of expanding HSCs, both *in vitro* and *in vivo*, though preserving their functionality in transplantation assay (Thorsteinsdottir, Sauvageau, and Humphries 1999; Antonchuk, Sauvageau, and Humphries 2002). HOXB4 exogenous over-expression in murine HSCs has been shown to upregulate *c-Myc*, *Cyclin D2*, *D3* and *E*, thus shortening the cell cycle and facilitating the HSC transition from early to late G1 (Satoh et al. 2004). Consistently with early G1 phase being the sensitive period where cell-fate decisions occur, *HOX* genes reduce the likelihood of differentiation in HSCs, thus favoring symmetric cell division (Orford and Scadden 2008).

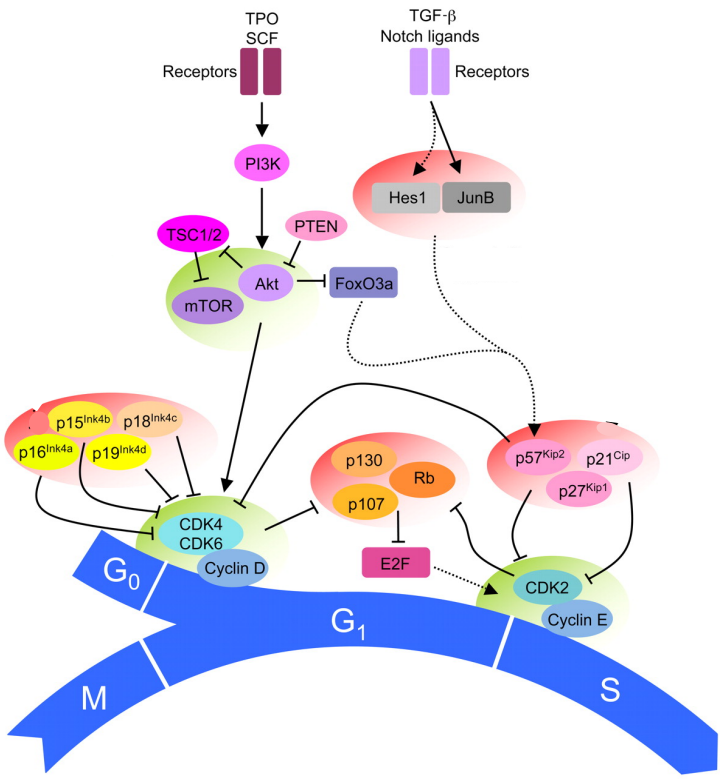

Figure 4 Complex network of intrinsic and environmental factors that regulate the HSCs cell cycle entry.
The regulatory machinery that controls HSCs cell cycle consists of three crucial hubs: 1. The PI3K/AKT/mTOR pathway, which is activated in response to numerous extrinsic signals and is inhibited by PTEN. 2. cyclin D–CDK4/6 complex which is negatively regulated by INK4 CKI family. 3. Cyclin E–CDK2 complex which regulates progression from the G1 to the S phase and is negatively regulated by CIP/KIP family of CDK inhibitors, as well as by the RB family. Functionally related groups of cell cycle activators are shaded in green; functionally related groups of cell cycle inhibitors are shaded in red. (Adapted from Pietras, Warr, and Passegué, Journal of Cell Biology, 2011)

In addition, factors produced by the niche, together with mediators produced by circulating immune cells**,** play a crucial role in the regulation of HSCs cell cycle.

The first demonstration derived from the BM knock-out (KO) for *Cdc42*, a molecule involved in the actin-filament formation, which showed a reduction in the number of HSCs and a consequent aberrant HSC homing into the niche, a phenotype coherent with the loss of CDC42 function (L. Yang et al. 2007). HSCs express specific receptors for factors released by niche cells, like the stromal cell-derived factor 1 (SDF1) (Nagasawa, Kikutani, and Kishimoto 1994), the stem cell factor (SCF) (Zsebo et al. 1990), Angiopoietin-1 (ANGPT1) (Suri et al. 1996) and thrombopoietin (TPO) (de Sauvage 1996). Mice deficient either for these ligands or their receptors showed increased cell cycle activity and progressive loss of the HSC compartment during adulthood (Ogawa et al. 1991; Yoshihara et al. 2007; Sugiyama et al. 2006; Arai et al. 2004).

A further level of regulation comes from the protein network involved in transducing the niche signals to the cells. In particular, the phosphatidylinositol-3 kinase (PI3K) is the main pathway responsible for the integration of external signals into the cell. PI3K induces HSCs proliferation by the activation of its downstream effectors AKT and mTOR and by the inhibition of its repressive factor FOXO. PI3K signaling results in the terminal stabilization of cyclin-D and its activity is restricted by the tumor suppressor phosphatase PTEN (Massagué 2004). Coherently, KO mice for *Pten* and *FoxO* genes showed increased HSCs proliferation rate followed by exhaustion of the HSC pool (K. Miyamoto et al. 2007; Yilmaz et al. 2006; Zhang et al. 2006). Furthermore, rapamycin, a pharmacological inhibitor of mTOR, is able to reverse many of the phenotypes associated with *Pten* deficiency, including the increased proliferation of HSCs (Yilmaz et al. 2006). Conversely, deletion of AKT results into an increased proportion of G0 HSCs, which can be rescued by increasing cellular reactive oxygen species (ROS) (Juntilla et al. 2010). Cellular oxygen level is indeed tightly connected with HSCs maintenance: HSC niche is mainly hypoxic and HSCs undertake anaerobic metabolism in order to limit ROS

production and maintain quiescence (Suda, Takubo, and Semenza 2011). Coherently, lack of hypoxia inducible factor 1 α (*Hif-1α*), part of the hypoxia-responsive regulatory pathway, in the murine BM results in reduced reconstitution abilities and lower stress tolerance (Takubo et al. 2010, 2013).

Furthermore, the TGFβ signal is considered the extrinsic master regulator of HSCs quiescence through a plethora of growth-repressive signals, including the transcriptional regulation of *p21* and *p57* genes (Blank and Karlsson 2015). Under stress conditions, TGFβ pharmacological inhibition delays HSCs re-entry into the G0 phase (Brenet et al. 2013) and the ablation of megakaryocytes in the niche leads to HSCs exit from quiescence, since they produce high level of TGFβ (Zhao et al. 2014).

As mentioned, also the metabolic status plays a role in modulating HSCs cell-cycle plasticity, including basic components of our diets. Indeed, both vitamin C and A signaling pathways have been shown to be enriched in HSCs and to regulate the balance between dormant and active status (Cabezas-Wallscheid et al. 2017, 2014; Agathocleous et al. 2017).

In conclusion, quiescence acts as a protective mechanism and the maintenance of the equilibrium between the different cell cycle phases is crucial to preserve a healthy hematopoietic system for the whole lifetime. Dividing HSCs undergo replicative stress and may both exhaust or accumulate mutations, thus becoming more prone to malignant transformation. Indeed, molecules such as CDK6 and PTEN, which actively sustain an efficient dynamic hematopoietic equilibrium, have been found mutated in cancer and in leukemia (Yilmaz et al. 2006; Scheicher et al. 2015). As a consequence, the further elucidation of the mechanisms controlling cell cycle activity in HSCs will significantly impact on the intersection between stem cell biology and oncology studies.

1.3 The pre-leukemic phase and pre-leukemic stem cells

The progression from dysplasia to cancer has been extensively investigated in solid tissues (e.g. colon rectal cancer (Vogelstein et al. 1988)) resulting in a linear evolution model where multiple somatic mutations, occurring in the same cell, culminate in its malignant transformation. Similarly, years of studies on leukemia evolution converge in a model where mutations progressively accumulate in normal HSCs, driving their transformation into Leukemia Initiating Cells (LICs). Given the low spontaneous mutation rate reported for human hematopoietic cells (Araten et al. 2005), the process of leukemogenesis is likely to occur over an extended time frame named "pre-leukemic" phase. We refer to HSCs harboring some, but not all, leukemia specific mutations as pre-leukemic HSCs (preL-HSCs) and they share quiescence, self-renewal and multipotency behaviors with their healthy counterpart.

The mutational event in the genome is stochastic. However, only mutations that provide advantageous changes tend to accumulate in the HSC population, such as those affecting differentiation or conferring unlimited proliferation potential (extended self-renewal). The mutation can also occur in a more differentiated cell, but it will be propagated only if it confers a novel self-renewal ability, otherwise it will be lost during differentiation (Fig5) (Corces-Zimmerman and Majeti 2014).

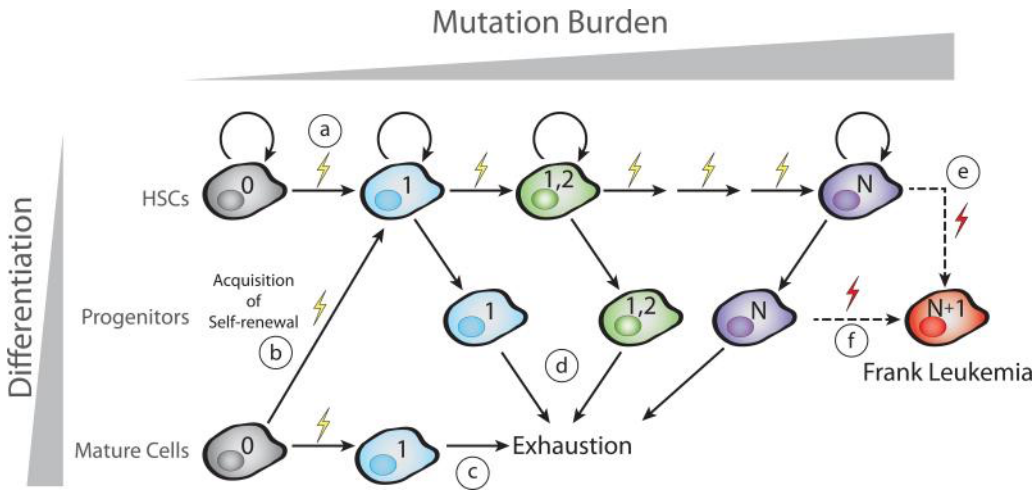

Figure 5 Model for evolution from pre-leukemic phase to frank leukemia.
Leukemia can originate from the accumulation of mutations in different cell types. The first mutation can occur in a normal HSC that retains self-renewal ability (a) or in a more differentiated cell that is "reprogrammed" into an HSC-like cell with self-renewal ability (b). If the mutation does not lead to "reprogramming" the mutated progenitors would likely be lost due to exhaustion (c). At each stage of the tumor evolution, the mutated self-renewing cells retain a certain level of capacity to differentiate, only the resultant leukemia cell loses this ability. (Adapted from Corces-Zimmerman and Majeti, Leukemia, 2014)

Pioneering studies by John Dick's lab formally demonstrated the presence of Leukemia Stem Cells (LSCs) in human Acute Myeloid Leukemia (AML), by the prospective isolation and xenotransplantation of different leukemic populations into immunocompromised mice. Based on blast antigen expression, they reported the CD34+ and CD38- as the only cell compartment that retains tumorigenic ability *in vivo* (Bonnet and Dick 1997; Lapidot et al. 1994). In '90s, clinical studies on both adult and pediatric leukemias reported the first evidences for the existence of preleukemic clones preceding overt AML. The recurrent AML translocation t(8;21), encoding for AML1 (Runt related Transcription Factor 1 [RUNX1])/ETO (RUNX1T1)) fusion protein, has been found in normal myeloid cells from patients in long-term remission. This represented the first formal demonstration that normal HSCs may harbor leukemic mutations and that pre-leukemic cells could persist during remission (T. Miyamoto et al. 1996; T. Miyamoto, Weissman, and Akashi 2000).

However, the greater step further in the investigation of pre-leukemia was represented by the discovery of leukemia-specific antigens that allowed the prospective isolation of normal HSCs from leukemia samples. Hence, by combining marker isolation strategy and xenotransplantation, Weissmann's group isolated, from the bulk tumor, residual normal HSCs capable of both myeloid and lymphoid differentiation lineages, both *in vitro* and *in vivo* (Jan et al. 2011; Majeti et al. 2009). The introduction of the high-throughput sequencing technology enabled to sequence these residual HSCs and demonstrate that they harbor only some of the leukemia specific mutations (Jan et al. 2012), confirming the existence of preL-HSCs in humans. Follow up studies further extended this revolutionary finding to broader AML patient cohorts, reporting that self-renewing HSCs serially acquire pre-leukemic mutations often conferring a growth advantage, allowing them to outcompete unmutated HSCs (Corces-Zimmerman et al. 2014; Shlush et al. 2014). Additionally, sequencing of paired diagnosis and remission AMLs revealed that only the pre-leukemic mutations identified at diagnosis were maintained in normal mature and immature hematopoietic cells during remission. Interestingly enough, also the patient-matched relapsed AML samples harbor the pre-leukemic mutations, either in combination with a mutational pattern similar to the primary leukemia (suggesting a clonal evolution during the relapse) or with a new pattern of relapsed specific mutations (suggesting the selection of a new LIC during relapse formation) (Corces-Zimmerman et al. 2014; Shlush et al. 2014). Together these evidences represented the first demonstration that preL-HSCs survive classical induction therapy and contribute to disease relapse, with important clinical implications.

PreL-HSCs share the same cellular features as normal HSCs, including quiescence. Since the standard cytarabine and anthracycline induction therapy permits only the rapid killing of the proliferating blasts, it is intrinsically unable to eliminate quiescent preL-HSCs. As a consequence, preL-HSCs survive in remission phase and likely contribute to relapse. In this setting, defining the spectrum of AML mutations, as well as understanding

their role in the transition from normal to malignant HSC and in selecting the leukemic founder clone, would contribute to the development of new therapies to potentially eradicate the preL-HSC pool.

1.4 Acute Myeloid Leukemia

Acute Myeloid Leukemia (AML) is the most common type of leukemia. In 2017, only in the United States, more than 20,000 new cases have been diagnosed and 10,000 patients died (Siegel, Miller, and Jemal 2017). AML is a hematological malignancy that occurs in the BM where the normal development of myeloid progenitors fails. This results in the rapid proliferation and accumulation of aberrant cells called blasts, which represent the hallmark of the disease.

As widely reported in the previous section, AML is now generally accepted as being a stepwise process. This model is coherent with the notion that AML is a disease of the elderly, with an average age at the time of diagnosis of 67 years. In this group, AML has a particularly poor outcome, with less than 5% of the patients surviving 5 years after the diagnosis, as compared to 40% in the young. The poor prognosis in older adults is due to a combination of both disease- and patient-related factors. Noteworthy, advanced age is often accompanied by frailty and comorbidities, which have an important impact on the tolerance of these patients to intensive treatment modalities. Hence, old AML patients receive chemotherapy less often than younger patients and show lower rates of complete remission with intensive chemotherapy (Almeida and Ramos 2016; Alibhai et al. 2009).

1.4.1 AML classification

AML stage definition is important to predict disease aggressiveness and patient therapy response. The French-American-British (FAB) classification was the first introduced in 1976, which subdivided AML in 8 sub-types (M0-M7) according to the cell type of origin and their level of maturation (Bennett et al. 1976). Even though it is quite basic, given its low price, the FAB system is still widely used today (Table1).

Type	Name
M0	Acute myeloblastic leukemia, undifferentiated
M1	Acute myeloblastic leukemia, without maturation
M2	Acute myeloblastic leukemia, with granulocytic maturati
M3	Acute promyelocytic leukemia (APL)
M4	Acute myelomonoytic leukemia
M5	Acute monocytic leukemia
M6	Acute erythroid leukemia
M7	Acute megakaryoblastic leukemia

Table 1. FAB classification of AML
(Adapted from Bennet et al, Britain Journal of Hematology, 1976)

Later, thanks to the pioneering studies by Rowley and colleagues, different chromosomal abnormalities in the leukemic cells have been discovered (e.g. t(8;21) and t(15;17), encoding for AML1-ETO and Promyelocytic Leukemia [PML]-Retinoic Acid Receptor α [RARα] oncogenes, respectively) and AML has become a genetic disease (Rowley 1973; Rowley, Golomb, and Dougherty 1977). In 2001 the World Health Organization (WHO) incorporated genetic information with morphologic, cytochemical, immunophenotypic, and clinical, to develop a more comprehensive patient risk-stratification classification (Table2) (D. A. Arber et al. 2016). Chromosomal aberrations became a powerful independent AML prognostic factor and AMLs with t(15;17), t(8;21), inv(16) or t(16;16) were assigned to favorable risk group. Complex karyotype, monosomy 5 or 7 or 11q changes other than t(9;11) were instead associated with poor prognosis, while the 50% of AML cases presenting normal karyotype (NK-AML) were originally assigned

to the intermediate risk outcome. Only the advent of novel techniques to investigate AML genome made possible to uncover the mutational complexity hidden within the NK-AML group, and to better allocate these patients to a specific risk class (H. Dohner et al. 2010; De Kouchkovsky and Abdul-Hay 2016).

Type	Cytogenetic, morphological and other characteristics
AML with recurrent genetic abnormalities	t(8;21)(q22;q22.1); *RUNX1 -RUNX1T1*
	inv(16)(p13.1q22) or t(16;16)(p13.1;q22); *CBFB -MYH11*
	PML-RARA (acute promyelocytic leukaemia, APL)
	t(9;11)(p21.3;q23.3); *MLLT3-KMT2A*
	t(6;9)(p23;q34.1); *DEK-NUP214*
	inv(3)(q21.3q26.2) or t(3;3)(q21.3;q26.2); *GATA2* , *MECOM*
	t(1;22)(p13.3;q13.3);*RBM15-MKL1* (megakaryoblastic AML)
	BCR-ABL1 (provisional entity)
	mutated *NPM1*
	biallelic mutations of *CEBPA*
	mutated *RUNX1* (provisional entity)
AML with myelodysplasia-related changes	Complex karyotype (3 or more abnormalities)
	Unbalanced abnormalities
	-7/del(7q)
	del(5q)/t(5q)
	i(17q)/t(17p)
	-13/del(13q)
	del(11q)
	del(12p)/t(12p)
	idic(X)(q13)
	Balanced abnormalities
	t(11;16)(q23.3;p13.3)
	t(3;21)(q26.2;q22.1)
	t(1;3)(p36.3;q21.2)
	t(2;11)(p21;q23.3)
	t(5;12)(q32;p13.2)
	t(5;7)(q32;q11.2)
	t(5;17)(q32;p13.2)
	t(5;10)(q32;q21.2)
	t(3;5)(q25.3;q35.1)
Therapy-related myeloid neoplasms	Therapy-related myelodysplastic syndrome (t-MDS)
	Therapy-related AML (t-AML)
AML, not otherwise specified	AML with minimal differentiation
	AML without maturation
	AML with maturation
	Acute myelomonocytic leukaemia
	Acute monoblastic/monocytic leukaemia
	Pure erythroid leukaemia
	Acute megakaryoblastic leukaemia
	Acute basophilic leukaemia
	Acute panmyelosis with myelofibrosis
Myeloid sarcoma	
Myeloid proliferations related to Down syndrome	Transient abnormal myelopoiesis (TAM)
	Myeloid leukaemia associated with Down syndrome

Table 2 WHO classification of AML and related neoplasms.
(Adapted from Arber et al., Blood, 2016)

1.4.2 The genetic landscape of AML

In the last 15 years, the definition of the genetic basis underlying the pathogenesis of AML has been tremendously improved. In particular, a large number of studies uncovered a huge heterogeneity within the intermediate risk NK-AML group, allowing the definition of different prognostic sub-groups based on the mutational landscape (Grimwade, Ivey, and Huntly 2016).

The first identified lesion with a prognostic meaning was the internal tandem duplication (ITD) in the juxta-membrane domain-coding sequence of the FMS-like Tyrosine Kinase 3 (FLT3) receptor that results in its constitutive activation (Nakao et al. 1996). Point mutations within the activation loop of the tyrosine kinase domain (TKD) have also been reported (Yamamoto et al. 2001) and, together, ITD and TDK represent the most frequent kinase mutations (30% and 7%, respectively) in AML. Both classes of mutations lead to constitutive activation of the receptor and mis-regulation of crucial functions such as apoptosis, proliferation and differentiation of hematopoietic cells. However, -TDK mutated patients have a better prognosis compared to -ITD ones (Mead et al. 2007). Indeed, the -ITD mutation is an independent predictor of high relapse rate and poor overall survival, which might get worse in case of acquisition of *FLT3-ITD* homozygosity (Whitman et al. 2001).

As for many other kinases involved in cancer, FLT3 tyrosine kinase inhibitors (TKI) emerged as a new therapeutic option in FLT3 mutated AML, and Midostaurin (Novartis) has been approved by FDA for the treatment of AML with mutated *FLT3* gene (Levis 2017). Unfortunately, several cancer resistance mechanisms are activated upon TKI administration. Thus a further effort is required in developing both more efficient TKIs and drugs targeting these resistance mechanisms to improve patients' prognosis (Gallogly, Lazarus, and Cooper 2017).

In early 2000, mutations in CCAAT/enhancer-binding-proteinα (*CEBP*α) and nucleophosmin (*NPM1*) genes have been discovered (Pabst et al. 2001; Falini et al. 2005)

(NPM is discussed in detail in the section 1.5). AMLs harboring such mutations are associated with favorable prognosis and thus, in 2016, have been accepted as novel AML classes in the WHO classification (D. A. Arber et al. 2016). Notably, the co-occurrence of *FLT3-ITD* in *CEBPA* or *NPM1* mutated patients results in a general worsening of the disease (De Kouchkovsky and Abdul-Hay 2016).

In 2009, the ten-eleven translocation 2 (*TET2*) gene, encoding for a methyl-cytosine dioxygenase, has been found mutated in the 20% of AML cases, representing one of the first evidences of the involvement of cell epigenetic regulatory machinery in AML pathogenesis (Delhommeau et al. 2009). *TET2* mutations correlate with NK-AML, older age and a general poor prognosis, worsened in the presence of *NPM1* and *CEBPA* mutations (Weissmann et al. 2012).

These initial clues on AML genomic architecture set the knowledge for the two-hit model of leukemogenesis that Griffin and Gilliland proposed in 2002 (Gilliland and Griffin 2002). They had observed that AML recurrent chromosomal alterations, affecting the normal hematopoietic development, fail to fully sustain AML onset and require the cooperation of mutated kinases, or signaling components, which confer survival and proliferative advantages to the aberrant myeloid progenitor. Therefore, they defined Class I mutations those conferring a proliferative advantage but no effect on differentiation (such as mutation in the *FLT3* or *NRAS* locus) and Class II mutations those impairing the hematopoietic differentiation (for example, *PML/RARα* and mixed lineage leukemia (*MLL)* gene fusions). According to their model, AML arises from two combined lesions, each belonging to a different class, while neither of them is sufficient to do so in isolation. The initiating lesions are thought to be Class II mutations, whereas class I mutations are typically later events.

This model, which is today widely accepted, has provided a useful framework to conceptualize the pathogenesis of AML as a disease characterized by block of differentiation and increased proliferation. However, a more comprehensive view of the

AML mutational scenario, obtained thanks to next generation sequencing (NGS) approaches, made this conceptualization slightly reductionist. In fact, a large number of alterations have been discovered that do not belong to any of the two groups, albeit further functional studies suggest that these new mutations could synergistically produce equivalent effects (Grove and Vassiliou 2014).

1.4.3 The next generation sequencing era in AML.

Since the publication of the first complete human genome sequence, cancer studies focused on a deeper analysis of the cancer genome compared to the normal counterpart. Thanks to these studies, a large number of new tumor associated mutations have been discovered in different cancer types, including AMLs.

As a milestone, in 2013 The Cancer Genome Atlas Consortium (TCGA) published the first AML mutations dataset based on whole genome sequencing of 200 adult *de novo* AMLs (The Cancer Genome Atlas Research Network 2013). This first comprehensive analysis revealed AML as the least mutated malignancy among all the sequenced cancer types, with an average of only 13 mutations/genome. Of these, an average of 5 are in genes that are recurrently mutated in AML. The big effort of TCGA study was the organization of mutated genes into homogeneous functional pathways with a likely role in AML pathogenesis (Fig6). Only 59% of the patients had a mutation in a gene encoding a signaling protein, thus revealing a weakness in the Gilliland model, which considered these mutations as necessary for AML pathogenesis (see section 1.4.2). On the other hand, this study strengthened the central role of the epigenetic status of AML genome, since 44% of mutated genes are involved in DNA methylation regulation.

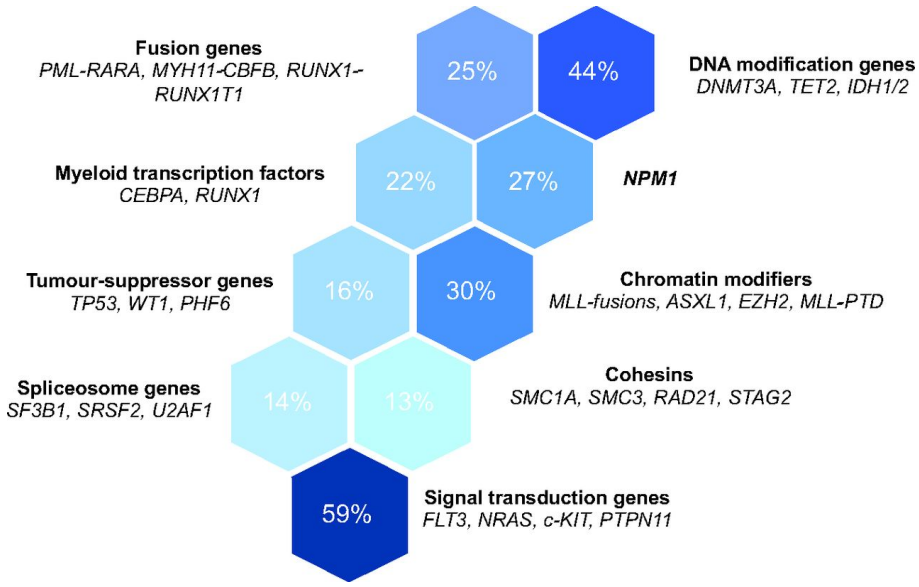

Figure 6 The TGCA functional categorization of *de novo* AML mutations.
The figure depicts the nine distinct functional groups of genes recurrently mutated in AML, as defined by TCGA. For each group is displayed *i)* the most prominent function, *ii)* the most important related genes and *iii)* the proportion of AMLs belonging to each group (Adapted from Grove and Vassiliou, Disease Models & Mechanisms, 2014).

In 2016, the sequencing of 1540 AML samples represented one step further in understanding the AML genome complex scenario (Papaemmanuil et al. 2016). This study identified 5234 driver mutations across 76 genes or regions, with at least one driver mutation in the majority of patients (>96%). Even so, only 48% of sequenced AMLs fitted in the WHO classification (Table 2). Therefore, they proposed a more comprehensive classification for AML, solely on the basis of genomic features. Distinct patterns of mutation co-occurrence or mutual exclusivity led to the definition of 11 AML classes with relevant clinical features. In addition to the ones already recognized by the WHO classification, they defined three new disease groups: *i)* AML with mutated chromatin, RNA-splicing genes, or both (18%), *ii) TP53* mutations/chromosomal aneuploidies or both (13%), and *iii)* $IDH2^{R172}$ mutations (1% of cases). According to this schema, 80% of patients were unambiguously classified in a single subgroup, and 4% met criteria for two or more categories.

These large genomic studies represent the first step toward the definition of a new AML classification scheme, which should fully integrate information from the genome, the

epigenome, the clinical outcome and the treatment, in order to avoid massive chemotherapy treatment and favor the introduction of target therapies into patient's management.

1.4.4 AML clonal heterogeneity

Large sequencing studies revealed specific mutational patterns with both co-occurring or mutually exclusive alterations. Interestingly, the latter often reveals common oncogenic pathways as in the case of mutations in *IDH1/2* and *TET2* genes. Indeed, mutated IDH1 forms the "oncometabolite" 2-hydroxyglutarate, which inhibits TET2 enzymatic activity (Figueroa et al. 2010). Moreover, both *IDH1/2* and *TET2* mutations, along with other recurrent mutations in *NPM1*, *CEPBA* and *RUNX1* genes, have been found mutually exclusive with translocations involving transcription-factor genes (e.g. *MLL1*, *RARα*), suggesting that these mutations may share similar oncogenic activities critical for AML development (The Cancer Genome Atlas Research Network 2013). On the other hand, *NPM1* mutations often associate with both *FLT3-ITD* and mutated DNA methyl transferase 3a (*DNMT3A*) (see section 1.5). The genotype with mutated *NPM1*, *DNMT3A* and *FLT3* is the most frequent three-gene co-occurrence, accounting the 6% of all AMLs and thus defining a unique AML subtype with a worst prognosis when compared to *NPMc+/FLT3-ITD* or *DNMT3A/FLT3-ITD* combinations. In contrast, the AMLs carrying the three mutations in *NPM1*, *DNMT3A* and *NRAS* genes have a more benign prognosis (Papaemmanuil et al. 2016).

Extensive sequencing studies of preL-HSCs isolated from AML patients helped in organizing the mutational events into a temporal line along the AML development. If a mutation is frequently found in the preL-HSCs it is likely to be an early event during leukemogenesis. Conversely, if a mutation is rarely seen, or absent, in the preL-HSCs it would be considered a later event. As a main finding, in two independent studies, genes

involved in the epigenome regulation (e.g. DNA methylation, histone modification or regulation of chromatin topology) have been often found mutated in preL-HSC, indicating them as early events in leukemogenesis. On the other side, mutations in *FLT3* and *NRAS*, as well as other signaling genes, were found to be later events (Corces-Zimmerman et al. 2014; Shlush et al. 2014).

Additional studies on the mutational spectrum between diagnosis and relapsed AMLs led to the definition of early events as the ones conserved at the relapse, and late events as the ones lost at the relapse. Coherently with previous findings, Krönke and colleagues reported *IDH1/2* and *DNMT3A* mutations as the most stably maintained at relapse, whilst *FLT3* and *NRAS* mutations appeared to be frequently gained or lost. Interestingly, mutated *NPM1* is rarely lost at relapse, thus indicating it as early event in leukemogenesis, even if it has never been found in preL-HSCs (see section 1.5) (Krönke et al. 2013).

More recently, the mathematical modeling of high-throughput sequencing data documented the stepwise acquisition of mutations that shape AML development. AML mutations are not identically shared by all the cells within the bulk tumor at diagnosis. Sub-groups of cells, the so-called clones, display each mutation co-occurring with others in different proportions. The mathematical analysis of NGS data enable to quantify the proportion of cells harboring a mutation as the Variant Allele Frequency (VAF) index, which indicates the frequency of a mutated allele in the whole tumor population compared with the wild-type (WT) allele. Then, the relative proportion of mutation VAFs allows the inference of tumor clonal architecture. Such analysis, showing the emergence of new clones carrying novel mutations at different times during AML evolution, provided the first evidence of a temporal relationship among different tumor clones, with the relative dominance of each sub-clone that varies throughout the course of disease (Grove and Vassiliou 2014). In particular, Papaemmanuil and co-workers, based on the NGS data of more than 1500 AMLs, confirmed that mutations in the epigenetic modifiers *DNMT3A*,

ASXL1, *IDH1/2* and *TET2* tend to be acquired early. Indeed, these mutations are in common with all the tumor clones and are almost never found alone, suggesting that they are not sufficient for leukemia development. Later, mutations in receptor tyrosine kinase–*RAS* pathway genes occur, with variable VAF values but always lower than 0.2. Regarding mutated *NPM1*, it emerges as a separate entity, secondary to epigenetic lesions and never found mutated in isolation (Fig7) (Papaemmanuil et al. 2016).

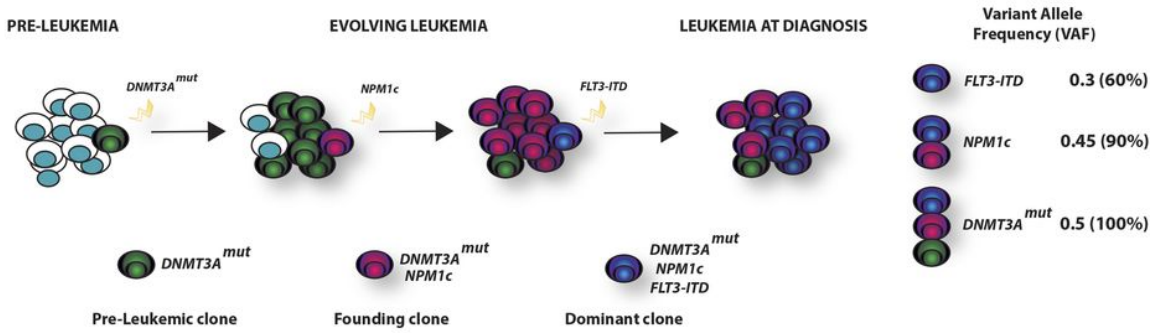

Figure 7 Clonal evolution and clonal heterogeneity of AML.
The quantification of the VAF of each mutation within a patient allows to demonstrate the temporal acquisition of mutations and the clonal hierarchy of the bulk tumor.
The figure depicts an example of the stepwise AML development in a patient that harbors mutations in *DNMT3a*, *NPM1*, and *FLT3* genes (most frequent three genes co-occurrence in AML). Mutation in *DNMT3a* is the earliest event that facilitates clonal expansion prior to overt disease development (VAF 0.5). Subsequently, *NPM1* mutation occurs and it represents the genetic event that provokes the switch to leukemia in the founding clone (VAF 0.45). Then, *FLT3* mutation occurs, conferring high proliferative rate to a sub-clone, which becomes dominant at diagnosis (VAF0.3). (Adapted from Grimwade, Ivey and Huntly, Blood, 2016)

Interestingly, mutations in epigenetic modifiers and RNA splicing factors had been found as initial event in myelodysplastic syndromes (MDSs). Since around 20% of MDS patients experience the progression into AML (Papaemmanuil et al. 2013), this finding corroborates the role of epigenetic modifiers as early events favoring cancer evolution. Moreover, mutations in *DNMT3A*, *TET2* and *AXSL1* characterize the clonal hematopoiesis occurring in elderly healthy individuals, thus confirming their ability to induce HSCs clonal expansion and drive a predisposition to later hematological malignancies (Genovese et al. 2014; Jaiswal et al. 2014).

1.5 NPM and hematological malignancies

NPM is a ubiquitously expressed phosphoprotein, mainly localized in nucleoli (Kang, Olson, and Busch 1974; Spector, Ochs, and Busch 1984), but continuously shuttling between nucleus and cytoplasm. It is member of the nucleoplasmin family of chaperone proteins (Frehlick, Eirín-López, and Ausió 2007) and interacts with a plethora of proteins, indicating its involvement in diverse cellular functions. Beyond its function in maintaining the nucleolar structure once located within nucleoli, NPM has been found involved in rRNA expression and maturation, in ribosome assembly, in centrosome duplication, in chromatin remodeling, in DNA replication, transcription and repair and in molecular chaperoning for histones and other proteins. Coherently with its numerous functions, NPM protein has several functional domains and undergoes various post-translational modifications (Colombo, Alcalay, and Pelicci 2011).

NPM has been associated with tumorigenesis (Grisendi et al. 2006). Consistently with the large number of processes it controls, both NPM oncogenic and tumor suppressor functions have been reported, depending on the cell type and the protein levels. In support of its oncogenic activities, NPM has been found overexpressed in different solid tumors (Yung 2007) where it contributes to increase the rate of ribosome biogenesis and protein synthesis that typically occurs during cancer progression (Roussel 1994). Evidences in favor of the tumor-suppressor role, instead, come from *in vitro* studies on *Npm1*-null mouse embryonic fibroblast (MEF) showing high DNA damage level, p53 activation, apoptosis (Colombo et al. 2005) and accumulation of mitotic figures with multiple centrosomes, consistent with p53-mediated post-mitotic tetraploid cell-cycle arrest (Grisendi et al. 2005). Moreover, loss of *Npm1* accelerates oncogenesis, as indicated by mice carrying a single inactivated *Npm1* allele ($Npm1^{+/-}$) which have an increased risk for lymphoma and myeloid malignancy development (Grisendi et al. 2005).

The *NPM1* locus is translocated in hematologic malignancies. The most frequent translocation was found in 30% of anaplastic large cell lymphomas (ALCLs), where the 5' portion of the *NPM1* locus is fused to the 3' end of the anaplastic lymphoma kinase (*ALK*) gene (Morris et al. 1994). Moreover, myeloid leukemia factor 1 (*MLF1*) and *RARα* are *NPM* fusion partners in myelodysplasia (Daniel A. Arber et al. 2003) and acute promyelocytic leukemia (APL) (Redner et al. 1996), respectively. The contribution of the NPM portion to the oncogenic activity of these fusion proteins is still under investigation. However, it must be considered that, by binding to WT NPM, these chimeric proteins cause haploinsufficiency for the WT *NPM1* and alter the WT protein localization.

The most recent indication that NPM activity is involved in tumor pathogenesis comes from the discovery of heterozygous *NPM1* mutations in AML (Falini et al. 2005). Virtually all the reported mutations (>40 types) occur at the exon 12 of the gene and involve its C-terminal region. In particular, the duplication of the TCTG tetranucleotide at position 956-959 of the sequence (Mutation A) is the most frequent, accounting for 75-80% of incidence. The frame-shift introduced by the mutations causes the loss of 2 tryptophan residues (W288 and W290), critical for the nucleolar localization of NPM, and the formation of a novel nuclear export signal (NES). This novel NES drives the delocalization of the NPM protein into the cytoplasm, which represents the hallmark of AML with mutated *NPM1*, leading to the definition of NPMc+ (cytoplasmic positive) AML (Fig8).

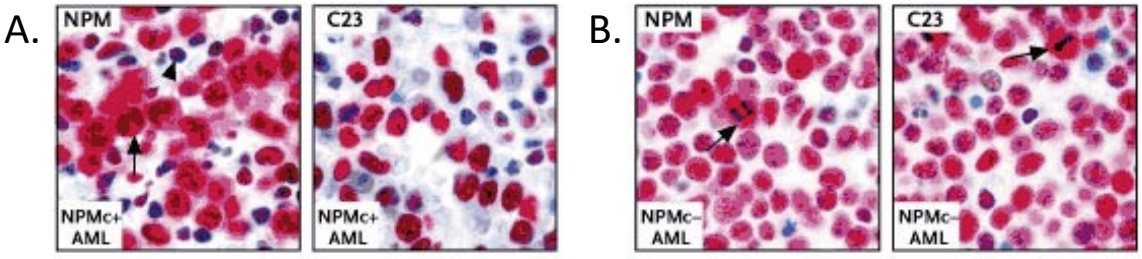

Figure 8 Subcellular patterns of expression of NPM in AML.
The subcellular patterns of expression of NPM in specimens from AML patients is obtained by the alkaline phosphatase anti-alkaline phosphatase (APAAP) staining method. A) NPMc+ AML: the majority of blasts (as indicated by the arrow) show the cytoplasmic localization of NPM in addition to regular nuclear/nucleolar NPM expression. The arrowhead highlights the presence of residual cells with only WT nucleolar localization of NPM. Nucleolin (C23) is always restricted to the nucleus.
B) NPMc- AML: blasts show both NPM and C23 expression restricted to the nucleus and the arrows highlight mitotic figures that show the expected cytoplasmic expression the two proteins. (Adapted from Falini et al, New England Journal of Medicine, 2005)

NPMc+ AMLs are associated with a better response to therapy and longer overall survival (Thiede 2006). Mutations in *NPM1* represent the most common alteration in adult AMLs (about 30% of cases), whereas are less frequent in pediatric AMLs (around 7% of cases) (Cazzaniga 2005). Pediatric studies have also shown that *NPM1* mutation frequency proportionally increased with the patient age at diagnosis, with the conspicuous absence of NPMc+ in children under 3 years of age (P. Brown et al. 2007). Interestingly, NPMc+ appears to be restricted to AML and to arise only in *de novo* cases (Falini et al. 2005; Liso et al. 2008). In fact, according to a recent retrospective study, the reported cases of MDSs or myeloproliferative neoplasms (MPNs) with mutated *NPM1* most likely are underdiagnosed AMLs (Forghieri et al. 2015). *NPM1* mutations are stable over the course of the disease (Falini, Martelli, et al. 2008; Chou et al. 2006) and they are largely conserved at relapse (Meloni et al. 2009; Krönke et al. 2013). Notably, the rare cases of AML that lose *NPM1* mutation at relapse likely represent *de novo* AMLs evolved from a common ancestral clone (K. Dohner and Bullinger 2017; Krönke et al. 2013). Furthermore, mutated *NPM1* is always mutually exclusive with AML recurrent genomic abnormalities and it is significantly associated with a normal karyotype (about 85% of NPMc+ AMLs)

(Falini, Mecucci, et al. 2008). On the other hand, a significant correlation has been found between mutated *NPM1* and other two frequent AML genetic abnormalities, mutated *DNMT3A* (e.g. *DNMT3A*^{R882}) and *FLT3-ITD* (54% and 39% of NPMc+ AMLs, respectively), with the latter strongly worsening the NPMc+ AML prognosis due to a lower response rate to chemotherapy (Papaemmanuil et al. 2016; Thiede 2006). NPMc+ AMLs are frequently CD34 negative (Falini et al. 2005) and they often show multi-lineage involvement (Pasqualucci et al. 2006). Overall, NPMc+ AMLs appear as a distinct AML subtype with specific pathological, phenotypic and prognostic features and, accordingly, it has been introduced as independent entity in the WHO classification.

1.5.1 NPMc+ and its role during leukemogenesis.

Three different mouse models bearing NPMc+ have been developed in the last years to support the pivotal role of this mutation in AML development. In the conditional transgenic model developed in Falini's group (Sportoletti et al. 2013), NPMc+ expression does not drive leukemia onset after 1.5-year follow-up, but it affects the megakaryocytic development. Our group generated a similar transgenic conditional model harboring the mutated *NPM1* human cDNA into the hypoxanthine-guanine phosphor-ribosyl-transferase (*Hprt*) locus. The mutated *NPM1* cDNA is under the control of a constitutive promoter, followed by a stop codon flanked by two LoxP sites. Upon Cre-mediated conditional expression, our NPMc+ mice develop leukemia at low penetrance (33.3% of animals) and with a long latency (median survival of 564 days) (Mallardo et al. 2013). Similarly, the knock-in model reported by Vassiliou and colleagues also developed AML with long latency and low penetrance (Vassiliou et al. 2011). Moreover, in both models the co-expression with the FLT3-ITD drives a fully penetrant and aggressive disease (Mallardo et al. 2013; Mupo et al. 2013). Although not fully transforming *per se*, these models support the pivotal role of NPMc+ in the selection and in the maintenance of the leukemic founder

clone. However, it is still lacking a detailed characterization of the prolonged pre-leukemic phase of these models that could provide important insights on the oncogenic pathways triggered by NPMc+ in the preL-HSC, possibly critical also for AML growth and maintenance.

Regarding the molecular mechanism underling the oncogenic role of NPMc+, so far, only *in vitro* studies on murine samples have been conducted. The cytoplasmic localization appears as critical for leukemic transformation. Under physiological conditions NPM is required for the nucleolar accumulation and stability of F-box proteins 7 (Fbw7γ) and $p19^{ARF}$ (Arf), involved in c-Myc turnover and in Mdm2-mediated p53 degradation, respectively. Both WT and mutated NPM bind to Fbw7γ and Arf, however NPMc+ binding leads to their abnormal cytoplasmic delocalization and degradation. As a consequence, Mdm2, which is inactivated by ARF in normal condition, can induce ubiquitination/degradation of p53; c-Myc, otherwise degraded by Fbw7γ, accumulates and activates its target genes (Fig9). Therefore, NPMc+ expression in MEFs attenuates an onco-suppressor pathway (Arf) and enhances an oncogenic one (c-Myc) (Colombo et al. 2005; Bonetti et al. 2008).

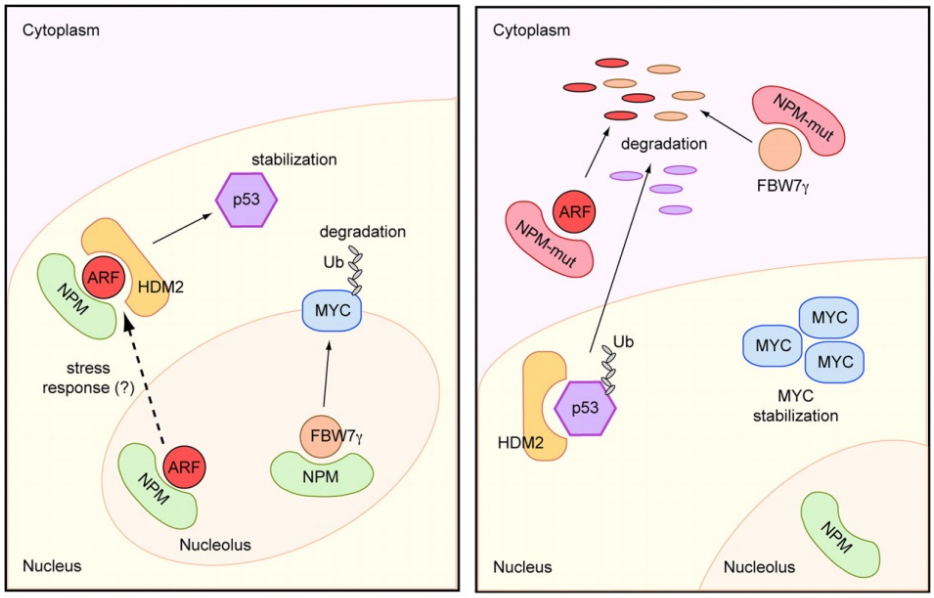

Figure 9 Oncogenic role of the cytoplasmic localization of NPMc+
Normal cell (left panel): NPM in the nucleolus stabilizes Fbw7γ and Arf protein. This is relevant for the control of c-Myc turnover, and provides an active pool of Arf ready to inactivate the HDM2-mediated p53 degradation in response to cellular stress.
AML blast (right panel): NPMc+ causes degradation of Fbw7 and Arf in the cytoplasm. As a consequence, Mdm2 can induce ubiquitination/degradation of p53, and c-Myc accumulates in the cell and activates its target genes (Adapted from Di Fiore, Journal of Cell Biology, 2008).

It is worth noting that, in AML, *NPM1* mutations are mutually exclusive with mutations in the *TP53* gene, further supporting the hypothesis of a functional inactivation of this pathway through the ARF-MDM2 axis (The Cancer Genome Atlas Research Network 2013). Moreover, *NPM1* mutations occur always in heterozygosis, and the NPM mutated protein dimerizes with the WT, modifying its localization and, likely, its activities. However, how and which activities are modified by this interaction and to which extent they are critical for leukemia development is still matter of investigation.

It is further known that, although NPMc+ in many cases is not a primary lesion, when it occurs, it strongly defines the AML phenotype. Indeed, NPMc+ imposes a specific gene expression signature mainly characterized by higher levels of *HOX* genes, known to be involved in stem cell maintenance (the compartment where AML development is thought to originate) and have a critical role in AML development (Alcalay 2005). Accordingly, it has been shown that HOX expression (Dovey et al. 2017) and activities

(Kuhn et al. 2016) are required for NPMc+ AML growth. Interestingly, HOX expression in NPMc+ AML blasts strongly correlates with its cytoplasmic localization, and the forced re-localization of NPMc+ in the nucleus is sufficient to induce the blast differentiation and the downregulation of *HOX* genes (Brunetti et al. 2018).

In summary, NPMc+ appears as a stable oncogene that characterizes the leukemic phenotype and fuels the leukemogenesis process. Therefore, furthers studies are required to elucidate the oncogenic pathways elicited by NPMc+ to drive AML. According to the view that considers AML as a stepwise process, NPMc+ oncogenic potential is likely to occur in the early stages of LICs clonal evolution, leading to the selection of the main leukemic clone. In this respect, NPMc+ may represent a critical pharmacological target to tackle the primary AML and hopefully to prevent relapse.

2 Materials and Methods

2.1 Animal Experimentation

Mouse colonies were maintained in a certified pathogen-free animal facility at the European Institute of Oncology. All experimental procedures including mice have been approved by the Italian Ministry of Health and have been performed in accordance with the Italian Legislation and with the international guidelines for the care and use of animals. All mice were euthanized by high concentrations of CO_2 inhalation.

2.1.1 Transgenic Mouse Models

All genetic modified murine strains were backcrossed in the C57BL/6J background. The NPMc+ transgenic mouse model harbors the human *NPM1* mutation A cDNA (NPMc+) in the *Hprt* locus, under the control of the ubiquitous CAG promoter. NPMc+ expression is inducible upon CRE-mediated excision of the floxed STOP cassette cloned between the pCAG promoter and the NPMc+ cDNA (Mallardo et al. 2013). Conditional NPMc+ mice were crossed with conditional *Rosa26-eYFP* (yellow fluorescent protein) mice (Srinivas et al. 2001) to obtain $NPM1c+^{fl/fl}/YFP^{fl/-}$ mice. The expression of both YFP and NPMc+ proteins is induced by *ex vivo* TAT-CRE treatment on $NPM1c+^{fl/fl}/YFP^{fl/-}$ (and $YFP^{fl/}$) BM-MNCs as described in section 2.2.2. To induce *in vivo* both NPMc+ and YFP expression, $NPM1c+^{fl/fl}/YFP^{fl/-}$ and control $YFP^{fl/-}$ mice were crossed with the *CMV-CreER*^{T} strain (Feil et al. 1996) and the resulting $NPM1c+^{fl/fl}/YFP^{fl/-}/Cre^{+/-}$ mice were treated with Tamoxifen (see section 2.1.3.1). Both $NPM1c+^{fl/fl}/YFP^{fl/-}$ and $NPM1c+^{fl/fl}/YFP^{fl/-}/Cre^{+/-}$ conditional models depend on FACS-sorting of YFP positive BM-MNCs followed by transplantation in recipient animals (sections 2.3.3 and 2.1.4.1). *Flt3-ITD* constitutive KI mouse model has been kindly provided by Prof. Gilliland group and has been kept in heterozygous condition ($Flt3\text{-}ITD^{+/-}$) (Lee et al. 2007). Both our *NPM1c+* and the $Flt3\text{-}ITD^{+/-}$ mice have been mated with the *Mx-Cre* strain (Kühn et al.

1995) to generate *NPM1c+$^{fl/fl}$/Mx-Cre$^{+/-}$*, *Flt3-ITD$^{+/-}$/Mx-Cre$^{+/-}$* mice. The breeding of *NPMc+$^{fl/fl}$/Mx-Cre$^{+/-}$* and *Flt3-ITD$^{+/-}$* generated double mutant *NPM1c+$^{fl/fl}$/Flt3-ITD$^{+/-}$/Mx-Cre$^{+/-}$* mice (Fig21). Mx promoter activity depends on pIpC injection (see section 2.1.3.2). 7 to 12 weeks old mice were used throughout the study with age-matched, littermate controls.

2.1.2 DNA extraction from tail-biopsies and genotyping strategy

Tails of 21-day-old mice were biopsied and kept in 80% ethanol until ready to elute DNA. Lysis was performed at 56°C in 200µl lysis buffer (100mM Tris-HCl [pH 8]; 5mM EDTA; 200mM NaCl; 0.1% Triton-X; 100mg/ml Proteinase K), overnight (O/N) in a Thermomixer, then followed by 10 minutes (min) at 95°C incubation for Proteinase K inactivation. Undissolved debris were pelleted and the supernatant containing the mouse genomic DNA used for further polymerase chain reaction (PCR). For amplification, primers summarized in Table3 were used. PCR conditions summarized in Table4 and in Table5 were applied for the PCR run in automatic TProfessionalTRIO® thermocycler (Biometra-analytikjena). Separation of DNA fragments by size was achieved by electrophoresis in agarose gel (1% - 3%; 1xTAE; 1xSYBR® Safe [Thermo Fisher]). As a size marker for gel electrophoresis 1kb or 100bp plus ladder (NEB, USA) was used.

Primer name	Sequence	Annealin °C (T_A)	Amplicon Size (bp)
NPMmut_FW	TGTCCATGTCCATCGAATCTTCCATCG	65	800
NPMmut_RV	AAATCTGTGCGGAGCCGAAATCTGG		
CRE_FW	GTGAAACAGCATTGCTGTCACTT	58	450
CRE_RV	GCGGTCTGGCAGTAAAAACTATC		
HPRT_FW	GGCAGAGTTCACATTGGATTTGTC	60	150
HPRT_RV	CCTATCACACCCAGGTTTCATCAG		
FLT3_FW	AGGTACGAGAGTCAGCTGCAGATG	60	(250) ITD; 220(WT)
FLT3_RV	TGTAAAGATGGAGTAAGTGCGGGT		
YFP_FW	GCCATGCCCGAAGGCTACGTCC	60	250
YFP_RV	AGCTGCACGCTGCCGTCCTCGATG		

Table 3 Genotyping primers, annealing temperatures and amplicons

Step	Temperature (°C)	Time (min)	
1	95	5	
2	94	00:30	
3	T_A	00:30	
4	72	00:30	2-->4 (35 cycles)
5	72	07:00	
6	4	pause	

Table 4 PCR condition for CRE-ER-TM, FLT3-ITD, HPRT, YFP genotypes

Step	Temperature (°C)	Time (min)	
1	95	5	
2	94	00:30	
3	65	00:30	
4	68	05:00	2-->4 (35 cycles)
5	72	08:00	
6	4	pause	

Table 5 PCR condition for NPMc+ genotype

2.1.3 Mouse Treatments

2.1.3.1 4-Hydroxy-tamoxifen (4-OHT) treatment

The murine strains containing *CMV-CreER*^{T} can be *in vivo* treated with 4-OHT to allow the Cre recombinase activity. Thus, *NPM1c+*$^{fl/fl}$*/YFP*$^{fl/-}$*/Cre*$^{+/-}$ and *YFP*$^{fl/-}$*/Cre*$^{+/-}$ mice were daily subjected to intraperitoneal injection (i.p.) with 1mg of 4-OHT (Sigma) to allow Cre mediated recombination of both NPMc+ and YFP transgenes. The CMV promoter is ubiquitously expressed and we limited the NPMc+ expression to the hematopoietic system collecting BM-MNCs from treated animals, FACS-sorting the YFP positive portion, and finally transplanting in recipient animals (see section 2.3.3. and 2.1.4.1).

2.1.3.2 Polyinosinic:polycytidylic acid (pIpC) treatment

The MX promoter is responsive to IFN, usually released during infections. The pIpC represents a costless analog of viral specific double stranded RNA which stimulates IFN synthesis and thus MX promoter activity. To allow the Cre transcription, all the

murine strains containing the *Mx-Cre* transgene were injected i.p. with 250ug pIpC (GE-Helthcare) every other day for 10 days total (5 injections).

2.1.3.3 5-Fluorouracil (5-FU) treatment

5-FU is a chemotherapy drug largely used in the treatment of several solid tumors (e.g. breast, head and neck, and colorectal cancer). It acts inhibiting the enzyme thymidylate synthase, consequently blocking the thymidine formation required for DNA synthesis and resulting in the elimination of rapidly dividing cells (Longley, Harkin, and Johnston 2003). This is true also in the normal murine BM where 5-FU treatment kills proliferating progenitor cells thus stimulating the subsequent cell-cycle entry of the quiescent LT-HSCs. Therefore, to force LT-HSCs proliferation in our mice we used 5-FU as stressor. 5-FU was administrated at dosage of 150mg/kg by i.p. injection the day after BMT, every 7 days. The level of engraftment was routinely checked in the peripheral blood (PB) of the recipients (see section 2.1.5) and the recovery ability from serial 5-FU stimuli were monitored until mice suffering was ethically tolerable.

2.1.3.4 5-Bromo-2-deoxyuridine (BrdU) administration

BrdU is a synthetic analog of thymidine commonly used in the detection of actively dividing cells in a tissue, because it is incorporated into the newly synthesized DNA during the S phase. BrdU is a stable chemical compound that is passed to daughter cells and diluted in the tissue through serial cell divisions. Thus, BrdU can be also employed to quantify cells which are slowly dividing and that, once incorporated BrdU in a pulse period, will not rapidly dilute it through replication. This assay is named BrdU Labeling Retaining and has been developed by Trumpp's lab to identify quiescent HSC over an extended time frame as Long Term Retaining (LTR) cells (Wilson 2004). Briefly, mice were i.p. injected with a single dose (180µg) of BrdU (Sigma-Aldrich) at the first day of treatment, then 800µg/ml BrdU were continuously administered with water (supplemented with 5% glucose) for the entire pulse period (13days for the mice cohorts including the

NPM1c+$^{fl/-}$/YFP$^{fl/-}$ model and 10days for the mice cohorts including the *NPM1c+$^{fl/fl}$/Flt3-ITD$^{+/-}$/MxCre$^{+/-}$* model). Then, after a variable chasing period, BM-MNCs have been collected and both surface markers and intracellular BrdU staining have been performed as illustrated in section 2.3.4.2.

2.1.3.5 TGFb inhibitor treatment

The TGFb inhibitor LY_364947 (Selleckem) was prepared 5mg/ml stock solution in DMSO. Mice transplanted with NPMc+ and FLT3-ITD expressing blasts (see section 2.1.4.4) were injected i.p. with the LY_364947 (or vehicle alone) diluted in 1xPBS at 10 mg/kg (of body weight) every other day for a total of 10 days (5 injections).

2.1.3.6 Combined cytarabine (Ara-C) and doxorubicin treatment

The majority of AML patients received 7+3 induction therapy that combines Ara-C (7 days, continuous intravenous) with an anthracycline (3 days, intravenous push). In mice transplanted with NPMc+ and FLT3-ITD expressing blasts (see section 2.1.4.4), chemotherapy was initiated upon detection of 10-15% PB infiltration as assessed by FACS. To mimic human induction treatment, mice were treated for 5 days with i.p injections of Ara-C (100mg/kg); during the first 3 days, doxorubicin (3 mg/kg) was administered in the same Ara-C i.p. injection. Mouse weight was checked daily during treatment to ensure that the mice received the correct dose of chemotherapy (Zuber et al. 2009).

2.1.4 Bone Marrow Transplantation (BMT)

C57 BL/6-Ly5.1 mice from Charles River were used as recipients for all transplantation procedures described in this study. This mouse strain expresses the alloantigen 1 of the CD45 surface antigen, while all our transgenic strains express the alloantigen 2. Recipients were lethally irradiated (7.5 cGy) 24h before the intravenous

(i.v.) delivery of donor cells. For AML blasts transplantation, recipient mice were sub-lethally irradiated (4.5cGy) 6-15h before the i.v. delivery of blasts.

2.1.4.1 YFP positive cells BMT

After *ex-vivo* TAT-CRE treatment (see section 2.2.2), *NPM1c+$^{fl/fl}$/YFP^{fl}* cells and control *YFP$^{fl/-}$* BM-MNCs were FACS sorted for YFP positivity (see section 2.3.3), then 2 million YFP+ cells were delivered into recipient animals. Moreover, in order to limit the NPMc+ expression to the hematopoietic system, the same BMT procedure was applied to the *NPM1c+$^{fl/fl}$/YFP$^{fl/-}$/Cre$^{+/-}$* and *YFP$^{fl/-}$/CRE$^{+/-}$* BM-MNCs *in vivo* treated with 4-OHT (see section 2.1.3.1). All transplanted animals were sacrificed for further analysis 4 months after transplantation.

2.1.4.2 Limiting number BMT

In the setting of BMT with limiting numbers of HSCs, 10,000 YFP+ sorted cells were mixed with 500,000 CD45.1 BM helper cells and injected i.v. in lethally irradiated recipients. 4 months post BMT, the YFP+ cell frequency in the PB of engrafted mice was ≥0.1%. LT-HSC frequency was calculated according to the Extreme Limiting Dilution Analysis (ELDA) web tool (Hu and Smyth 2009) .

2.1.4.3 Competitive BMT

For the competitive BMT assay, CD45.1 lethally irradiated mice were injected i.v. with a mixture of 1x10^6 CD45.2 (*MxCre$^{+/-}$*, *Flt3-ITD$^{+/-}$/MxCre$^{+/-}$* or *NPM1c+$^{fl/fl}$/Flt3-ITD$^{+/-}$/MxCre$^{+/-}$*) and 1x10^6 competitive WT CD45.1 BM-MNCs (competition ratio 1:1).

2.1.4.4 NPMc+/FLT3-ITD AML blasts transplantation

For all the experiments on NPMc+/FLT3-ITD AML reported in this study, primary blasts, derived from spleens of *NPM1c+$^{fl/fl}$/Flt3-ITD$^{+/-}$/MxCre$^{+/-}$* that developed AML, have been expanded in recipient animals that represent the secondary spleen donors. These

blasts have been transplanted ($1x10^6$ blasts) in CD45.1 sub-lethally irradiated mice. In the setting of AML transplantation with limiting numbers, CD45.1 sub-lethally irradiated mice were transplanted i.v. with $0.5x10^6$ blasts derived from spleens treated with LY_364947 or vehicle (see section 2.3.1.5).

2.1.5 Peripheral Blood collection

Donor contribution to the hematopoietic system reconstitution in recipient mice was assessed in the PB collected from the tail-veins of injected mice (max 150µl) at regular intervals, starting from 15 days after BMT. EDTA (0.5 M, pH 8.0) was used as anticoagulant. Red blood cells (RBCs) were lysed in a hypotonic salt solution (8.125 mg/ml NH_4Cl, 1 mg/ml $KHCO_3$, 0.13 mM EDTA in dH_2O) for 3 min on ice and centrifuged at 1200 rounds per min (rpm) at 4°C. The remaining white blood cells (WBCs) were stained for FACS analysis (see section 2.3.1).

2.1.6 Cytology and Histology

PB smears were stained with May-Grünwald-Giemsa according to the standard protocol. Spleen and ulna were fixed in 4% formalin and embedded in paraffin. Hematoxylin and Eosin staining were performed on 5µm tissue slices, according to the standard protocol. Samples were analyzed by pathologists for morphological characterization and AML diagnosis.

2.2 Cell Culture Procedures

2.2.1 Bone marrow and spleen single cell suspension protocols

Bones from posterior limbs, anterior limbs and sternum were crushed with a mortar and pestle, re-suspended in 1xPBS and filtered through 70 mm nylon cell strainers to obtain a total BM single cell suspension. Spleens were smashed in 1xPBS and filtered few

times in 70µm nylon meshes. As previously reported, both BM and spleen RBCs were lysed in a hypotonic salt solution (see section 2.1.5). For BM-MNCs suspension, total BM cells were layered onto density gradient (Histopaque®1083, Sigma-Aldrich) and centrifuged at 1500 rpm, 45min at 4°C. While erythrocytes aggregate with the poly-sucrose Histopaque® matrix and rapidly sediment, lymphocytes and other mononuclear cells remain at the1xPBS-Histopaque® interface which can be collected. Live cells were counted using Trypan blue dye (0.4% solution [Thermo Fisher]) to distinguish live and dead cells. Cell suspensions were either freshly used in further applications or stored in freezing medium (10% DMSO, [Merck] in fetal bovine serum (FBS) [Microgem]) in liquid nitrogen.

2.2.2 *Ex vivo* TAT-CRE recombination

In the *NPM1c+*$^{fl/fl}$*/YFP*$^{fl/-}$ strain the transcription of both transgenes is blocked by a STOP cassette flanked by two Lox-P sites. In order to drive the two transgenes expression, BM-MNCs derived from these mice (and control *YFP*$^{fl/-}$) were treated *ex vivo* with TAT-CRE, a recombinant version of CRE recombinase fused with the HIV protein TAT. Briefly, BM-MNCs, obtained as described above, were re-suspended 5x10^6/ml in serum-free media (Hyclone, USA) and incubated for 45 min at 37°C with 100µg/ml of TAT-CRE. Transduction was stopped diluting samples with 10 volumes of BM-MNCs medium (IMDM [Gibco, Carlsbad, CA.] 12.5% heat inactivated FBS, 12.5% Horse serum, 1% L-glutamine, 100ng/ml SCF, 20ng/ml IL3, and 20ng/ml IL6 [PeproTech] 0.1% β-mercapto-ethanol, and Hydrocortisone 10ng/ml). Then cells were spun down, re-suspended in BM-MNCs medium and cultured at a density of 2x10^{6}cells/ml for 24hours. The following day, cells underwent the same procedure. Deletion efficiency was evaluated 24-48 hours later by flow cytometry. At 96h from collection cells were FACS sorted for YFP positivity and transplanted in irradiated recipients (see 2.3.3 and 2.1.4.1 for further details).

2.3 Flow cytometry analysis

Cells collected from PB, BM and spleen were stained for surface marker and intracellular antigens as reported in this section. FACSCalibur ™ or a FACSCanto™ (BD Biosciences, USA) were used for multi-parametric and cell-cycle flow cytometry data acquisition. Dead cells were excluded from the analysis based on forward and side scatter parameters. Sorting of labeled cells, as well as YFP expressing cells, was performed using FACSAria™ (BD Biosciences, USA) and MoFlo® Astrios™ (Beckman Coulter). All flow cytometry data were analyzed with FlowJo™ 8.8.7 platform (Tree Star, USA).

2.3.1 Engraftment analysis (in the PB)

The unique expression of the CD45.2 alloantigen on the surface of donor cells was used as a marker to evaluate the donor contribution to recipient mice reconstitution since they express the CD45.1 isoform. Cells (collected as reported in section 2.1.5) were stained 30min on ice with antibodies specific for the mouse CD45.2 and for the mouse CD45.1 surface antigen. Samples were freshly FACS analyzed or fixed with 4% para-formaldehyde (PFA).

2.3.2 Immune-phenotype analysis

BM-MNCs were isolated as previously described (see section 2.2.1). To analyze stem cell and progenitor populations we relied on their unique setting of surface markers (as described in the Introduction section 1.1.2). In details, Lin- cell were identified according to the low expression of Mac-1; Gr1; B220; CD3; Ter119. LT-HSC were identified according to the following immuno-phenotype: Lin-; Sca-1+; cKit+; CD34-; Flk-. ST-HSC were identified according to the following immune-phenotype: Lin-; Sca-

1+; cKit+; CD34+; Flk-. MPP were identified according to the following immune-phenotype: Lin-; Sca-1+; cKit+; CD34-; Flk+. First, BM-MNCs were incubated at 4°C for at least 30min in blocking buffer (10% Bovine Serum Albumin (BSA) in 1xPBS). Then cells were incubated at 4°C for 30min at the concentration of $8x10^7$ cells *per* 1 ml of staining buffer (1% BSA in1xPBS) containing the appropriate mixture of fluorescently labeled antibodies (Abs). Two-step staining was performed when biotinylated Abs were detected using fluorescently-labeled streptavidin as secondary reagent. List of Abs, as well as working dilutions, are listed in Table 6. Monoclonal Abs were purchased from eBioscience. Samples were freshly FACS analyzed or fixed with 4% para-formaldehyde (PFA).

Antigen	Dye/conjugation	Brand	Dilution Factor	Clone
CD11b	PE-CY7	eBioscience	1:300	M1/70
Ly-6G (GR1)	PE-CY7	eBioscience	1:300	RB6-8C5
Ter-119	PE-CY7	eBioscience	1:300	Ter119
CD3e	PE-CY7	eBioscience	1:300	145-2C11
CD45R(B220)	PE-CY7	eBioscience	1:300	RA3-6B2
Ly-6A/E (Sca1)	PerCP-CY5.5	eBioscience	1:100	D7
cKit	APC-eFluor780	eBioscience	1:75	2B8
	APC	eBioscience	1:125	
CD135 (FLK)	PE	eBioscience	1:50	A2F10
CD34	biotinilated	eBioscience	1:100	RAM34
	FITC	eBioscience	1:200	
streptavidin	eFluor450	eBioscience	1:100	
CD45.1	PE, FITC, APC	eBioscience	1:200	A20
CD45.2	PE, FITC, APC	eBioscience	1:200	104

Table 6 List of antibodies used for flow cytometry.

2.3.3 Fluorescence activated cell sorting

Sorting procedure combines the FACS analysis of a bulk population with the possibility to isolate a specific fraction of cells according to the fluorescence signal and to collect it for further applications. We largely applied this strategy for the generation of the NPMc+/YFP experimental model: *in vitro* TAT-CRE treated *NPM1c+*$^{fl/fl}$*/YFP*$^{fl/-}$ and control YFP$^{fl/-}$ BM-MNCs were FACS-sorted for their YFP positivity and then transplanted into recipient animals (see section 2.1.4.1). Since CMV promoter is ubiquitously expressed, *in vivo* 4-OHT treated *NPM1c+*$^{fl/-}$*/YFP*$^{fl/-}$*/CreE*$^{+/-}$ BM-MNCs (and control) were sorted for YFP expression and transplanted in recipient animals to limit the transgene expression to the hematopoietic system. Moreover, we used FACS sorting strategy to isolate LT-HSCs for RNA extraction and gene expression analysis. Samples were surface labeled as reported in the previous section. All BM samples were filtered right before the sorting procedure and re-suspended in the EDTA containing Sorting Buffer (2% BSA in1xPBS, 0.4% 5mM EDTA).

2.3.4 Cell cycle analysis

2.3.4.1 Ki-67 analysis

Ki-67 expression is strictly associated with cell proliferation. The antigen is found in the nucleus of cycling cells (G1, S, G2, M cell-cycle phases), but has not been detected during G0 (Gerdes et al. 1984). To identify the G0 population in our samples, we stained our surface labeled BM-MNCs samples (see section 2.3.2.) for intracellular ki67, using the BrdU Flow Kit (BD Bioscience). In detail, 1x10^7 BM-MNCs were fixed in Cytofix/Cytoperm^{TM} buffer for 20min at room temperature (RT), washed by 1X Perm/Wash^{TM} Buffer (P/W) (BD Perm/Wash^{TM} buffer 10X diluted in dH_2O) and re-fixed in Cytofix/Cytoperm^{TM}Plus buffer for 10min at RT, protected from light. Cells were washed with P/W and incubated 5min with Cytofix/Cytoperm^{TM} buffer at RT, light

protected, and washed again with P/W. Fixed cells were stained with anti-ki67 (Alexafluor647® conjugated, clone 16A8, Biolegend) diluted 1:125 in 1X P/W buffer for 1hour at RT. After a final washing step with1xPBS, the cells were stained for total DNA levels with the DNA binding dye Hoechst 33342 diluted in 1XPBS (Sigma-Aldrich) at 4°C until FACS analysis.

2.3.4.2 BrdU incorporation analysis

BrdU incorporation analysis coupled with total DNA content staining enhances the resolution of S-phase from G0/G1 and G2/M events. For this purpose, $1x10^7$ BrdU labeled BM-MNCs stained for surface antigens (see section 2.3.2.) were fixed and permeabilized as described for ki67 analysis. To expose the incorporated BrdU, fixed and permeabilized BM-MNCs were treated with DNAse (diluted to 150µg/ml in 1xPBS) for 1 hour at 37°C. Then cells were incubated with an anti-BrdU antibody (APC BrdU Flow kit, BD; dilution 1:100 in 1X Perm/Wash buffer), 1 hour on ice. Stained cells were washed, re-suspended in 1 ml of 1xPBS containing Hoechst 33342 and incubated at 4°C until FACS analysis.

2.4 Immunofluorescence

Mutated NPM is aberrantly expressed only in the cytoplasm (Falini et al. 2005) and the protein can be detected by staining with a homemade antibody specific for the mutated form of the NPM protein. For WBCs immunofluorescence, cells were fixed in suspension with 4% PFA for 10min. After washing, cells were spun onto microscope slide with the help of the Cytospin centrifuge (300rpm, 3min, RT), a method which allows a better visualization of cytoplasm area where mutated NPM is confined. Area covered by cells were delimitated by DAKOPen (Agilent). Cells were then permeabilized 5min with 0.1% TritonX100 in 1xPBS at RT, washed 3 times in 1xPBS and blocked with 5% BSA in 1xPBS (blocking solution) O/N at 4°C. Staining with the anti-NPMc+ primary antibody

(homemade rabbit polyclonal immunopurified ab, dilution 1:1000) was performed in a humid chamber for 4-5 hour at RT and followed by 3 washes in 1xPBS. Coverslips were then stained with the secondary antibody (Alexa488 Fluor® or Alexa647 Fluor®) for 50min at RT, washed 3 times in 1xPBS, counterstained with DAPI and mounted in MOWIOL. Samples were acquired under an AX-70 Provis (Olympus) fluorescence microscope equipped with a b/w cooled CCD camera (Hamamatsu c5985) and analyzed by ImageJ 1.x (Schneider, Rasband, and Eliceiri 2012). For LKS immunofluorescence, cells were FACS sorted, resuspended in 5ul 1xPBS and plated on poly-lysine treated coverslips. Cells were allowed to deposit by gravity for 15min. Then cells were fixed in 4% PFA for 10min and stained as reported for WBCs. For quantification of the NPMc+ signal, widefield images have been collected by Olympus BX61 fully motorized fluorescence microscope controlled by the image screening Scan^R software. The analysis has been carried out by a computational platform developed by our group and named Automated Microscopy for Image-Cytometry (A.M.I.CO.) (Furia, Pelicci, and Faretta 2013).

2.5 Gene Expression Profiling

2.5.1 Microarray gene expression analysis

RNA was purified from 10-15,000 FACS-sorted *NPM1c+*$^{fl/fl}$*/YFP*$^{fl/-}$ and control YFP$^{fl/-}$ LT-HSCs using QIAGEN RNeasy kit following the manufacturer protocol. DNAse (QIAGEN) digestion step was added before elution to ensure the complete elimination of contaminant DNA. The integrity of RNA was analyzed by Bioanalyzer (Agilent). Double stranded cDNA synthesis was performed with Nugen®Pico WTA Systems V2 (NuGEN Technologies, Inc.). Hybridization was performed using the Affymetrix GeneChip® Mouse Gene ST 2.0 Array.

2.5.2 Whole transcriptome sequencing (RNAseq)

RNA was purified from 3-7,000 FACS-sorted *MxCre*$^{+/-}$, *Flt3-ITD*$^{+/-}$*/MxCre*$^{+/-}$ or *NPM1c+*$^{fl/fl}$*/Flt3-ITD*$^{+/-}$*/MxCre*$^{+/-}$ LT-HSCs, taking advantage of the PicoPureTM RNA Isolation Kit (ThermoFisher) optimized for small number of cells, according to the manufacturer's instructions. DNAse (QIAGEN) digestion step was added before elution to ensure the complete elimination of contaminant DNA. The integrity of RNA was analyzed by Bioanalyzer (Agilent). Sequencing libraries were generated using the SMARTseq protocol based on polyA-enrichment (Picelli et al. 2014). Briefly, for cDNA library production Reverse Transcription reaction has been performed on oligo-dT hybridized mRNA molecules (0.5ng total) using the SuperScript II reverse transcriptase (Thermo Fisher) followed by PCR pre-amplification reaction with KAPA HiFi HotStart ReadyMix (Kapa Biosystem). PCR product has been purified by adding 25µl of Ampure XP beads (1:1 ratio, Beckman Coulter) on a magnetic support and quality of the cDNA library has been checked by Bioanalyzer. Then tagmentation reaction has been performed on 1.5ng of cDNA library by incubation with the home-made Tn5 enzyme (working temperature 55°C) for 5min, followed by 5min incubation RT with 0.2% SDS to inhibit the Tn5 activity. Lastly, the PCR based amplification of the adapter-ligated fragments was completed, then followed by the final PCR purification and Bioanalyzer quality check. 50bp single-end sequencing was performed with a HiSeq2000 device (Illumina), five barcoded cDNA libraries per lane, which yielded ~3.0x10^{7}reads/sample.

2.5.3 Bioinformatic analysis

2.5.3.1 Micro-array analysis

Microarray data were normalized by RMA using Partek Genomic Suite 6.6. To normalize the signal intensity obtained from three independent experiments the "remove batch effect" option was applied to the analysis. Then, a set of differentially expressed

genes between pre-leukemic NPMc+ and WT LT-HSC samples was identified by applying a threshold of FC>|1.5| and p<0.05.

2.5.3.2 RNAseq analysis

Sequences were aligned to the mouse reference genome (NCBI37/mm9) using TopHat2 (Kim et al. 2013). After alignment, raw gene expression values were obtained with HTseq (Anders, Pyl, and Huber 2015). Differential gene expression was then estimated using the edgeR R package, using a TMM normalization (Robinson, McCarthy, and Smyth 2010).

2.5.3.3 Gene set enrichment analysis (GSEA)

GSEA (v2.14 software Broad Institute) (Subramanian et al. 2005) was used to investigate whether a gene set was significantly over-represented in the transcriptome of the pre-leukemic cells. The curated gene set collection (c2.all.v2.1.symbols.gmt) was downloaded from MSigDB (http://www.broad.mit.edu/gsea/). Moreover, custom gene sets related to quiescence, self-renewal and cell cycle, together with gene set available in the literature, have been tested for enrichment. A gene set was identified as significantly enriched when associated with FDR<0.1. A detailed description of the GSEA methodology and interpretation is provided at broadinstitute.org/gsea/doc/GSEAUserGuideFrame.html.

2.6 Statistical analysis

All analyses were performed using two-tailed t-test assuming equal variance. Statistical significance is indicated by *p<0.05. Results from survival experiments was analyzed with a log-rank non-parametric test and expressed as Kaplan-Meier survival curve.

3 Background, rationale and aim

AML evolution is largely accepted as a long, stepwise process, and HSCs are assumed to be the target of early transforming events since they are long-lived cells with self-renewal ability and they can potentially fix and propagate mutations. Such mutated HSCs, known as pre-leukemic HSCs, accumulate in the normal BM, and are phenotypically indistinguishable from their normal counterpart. Both the mechanisms involved in the transition from normal to malignant HSC and the pathways leading to the malignant clone dominance are still poorly understood and hence they represent an open research challenge.

Recent functional and genetic studies on AML genome and its sub-clonal organization shed light on the understanding of mutation contribution to disease clonal selection. These studies have confirmed NPMc+ as a critical driver oncogene, that is highly conserved at relapse, and characterizes the leukemic phenotype (Papaemmanuil et al. 2016; Krönke et al. 2013). Likely, NPMc+ has a pivotal role in the selection of the main leukemic clone, and in the maintenance of the clone that leads to disease relapse.

In order to elucidate leukemogenic mechanism triggered by NPMc+, we took advantage of our mouse model in which the expression of NPMc+ can be induced in the hematopoietic system through a classical Cre-Lox DNA recombination approach (Mallardo et al. 2013). This model is characterized by a prolonged leukemia-free phase that allows to study how the expression of NPMc+ modifies the hematopoietic compartment prior to the onset of the disease. In particular, our experimental approach is originally based on *ex vivo* treatment of BM-MNCs with TAT-CRE recombinant protein, followed by transplantation in lethally irradiated recipient animals. In order to study the pre-leukemic phase, we crossed our NPMc+ mice with the conditional *Rosa26-eYFP* reporter strain (Srinivas et al. 2001), obtaining the *NPM1c+*$^{fl/fl}$*/YFP*$^{fl/-}$ (thereafter NPMc+/YFP) or *YFP*$^{fl/-}$ control mice (thereafter YFP). In these animals, upon TAT-CRE

treatment, the BM-MNCs express both NPMc+ and YFP, therefore, they can be easily isolated and/or transplanted and are detectable in the PB of transplanted animal months after injection (schematic representation in Fig12A). By using this model, a former member of our group showed a higher repopulating capacity of NPMc+ BM compared to control. This result strongly suggested a role of NPMc+ in modifying the biology of the HSCs. Accordingly, she showed that NPMc+ expression leads to a significant *in vivo* expansion of the HSC pool and an increased proliferative rate (data not shown).

Based on these preliminary data, the general aim of this study is to further characterize how NPMc+ modifies the homeostasis of the hematopoietic system, eventually leading to LIC selection and leukemia expansion.

In this view, our attention is mainly dedicated to the study of the hematopoietic stem and progenitor cell compartment. Moreover, considering the strong co-occurrence of NPMc+ with mutations in the *FLT3* locus (*FLT3-ITD*), we investigate the mechanisms that underlie this cooperation.

Understanding the cellular mechanisms through which NPMc+ and FLT3-ITD elicit LIC selection and sustain AML development might point out new pharmacological targets in a wide group of patients with poor prognosis.

4 Results

4.1 NPMc+ expression increases the HSCs self-renewal rate of division

Based on the observation that the expression of NPMc+ leads to an expanded number of HSCs in the BM, we tested if this phenotype reflected an increased HSC self-renewal rate of division. To assess the HSC self-renewal rate, we measured the number of HSCs at the time of transplantation and four months later, and then calculated the so called "self-renewal quotient" (Fig13) (Challen et al. 2012).

HSC number was determined through immune-phenotyping analysis using the Weissman method (Spangrude, Heimfeld, and Weissman 1988; Morrison and Weissman 1994). This method defines the long-term reconstituting HSCs (LT-HSCs) as Lin-, Sca-1+, cKit+, CD34-, Flk2- BM cells. A representative graph of the analysis performed on NPMc+ expressing BM-MNCs and control WT cells is depicted in Fig10.

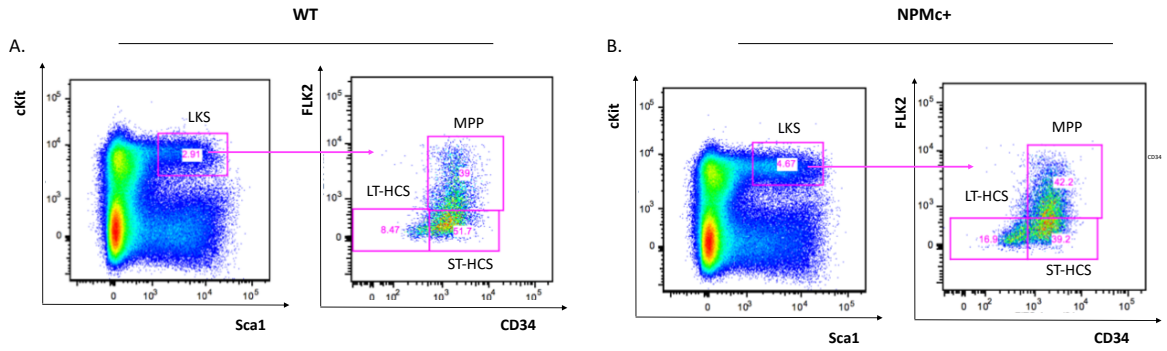

Figure 10 BM-MNC subpopulation analysis based on the expression of lineage-specific Abs.
Gating strategy of the LSK (c-Kit+, Sca-1+, Lin-) population within lineage negative cells and for LT-HSCs (Lin-, Sca-1+, cKit+, CD34-, Flk2-), ST-HSCs (Lin-, Sca-1+, cKit+, CD34+, Flk2-), and MPPs (Lin-, Sca-1+, cKit+, CD34+, Flk2+) within LKS cells.
A) Representative BM-MNC subpopulation analysis for WT sample. B) Representative BM-MNC subpopulation analysis for NPMc+ sample.

We further analyzed the HSC compartment using the SLAM strategy combined with the CD34 staining. As reported (Wilson et al. 2008), This assay consists in exploiting CD34 expression to discriminate, within the CD150+ and CD48- SLAM pool, between MPP1 (CD34+) and *bona fide* HSCs (CD34-). The latter ones are, consistently, expanded by NPMc+ (Fig11).

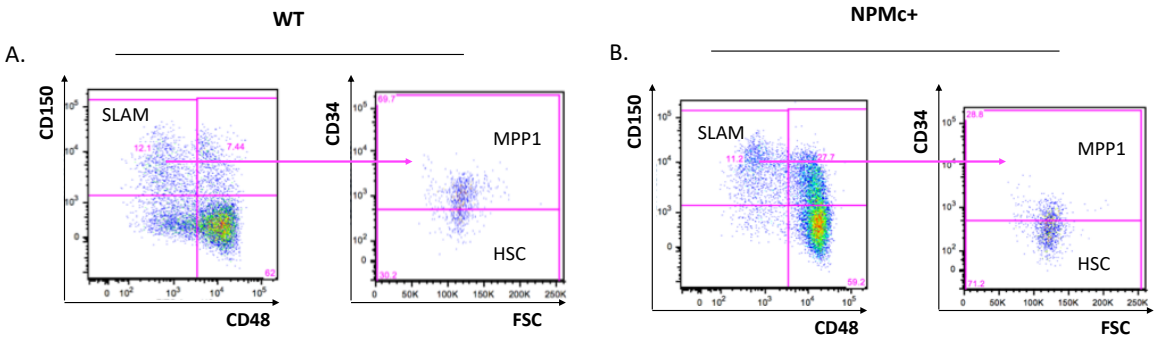

Figure 11 BM-MNC subpopulation analysis based on the expression of SLAM and CD34 markers
Gating strategy of the SLAM population (CD150+, CD48-) within LKS cells. Then, SLAM cells are analyzed according to the CD34 expression and separated in HSCs (CD34-) and MPP1(CD34+).
A) Representative BM-MNC subpopulation analysis for WT sample. B) Representative BM-MNC subpopulation analysis for NPMc+ sample.

Upon *in vitro* TAT-CRE treatment, BM-MNCs cells lose the expression of their surface markers, thus preventing the evaluation of HSC number by immune-phenotyping analysis. To overcome this problem we crossed the NPMc+/YFP and YFP animals with the 4-OHT inducible *CMV-CreER^{T} strain* (Feil et al. 1996) (thereafter CRE), obtaining a triple mutant model *NPM1c+$^{fl/fl}$/YFP$^{fl/-}$/Cre$^{+/-}$* (thereafter NPMc+/YFP/CRE) or *YFP$^{fl/-}$/Cre$^{+/-}$*(thereafter YFP/CRE). NPMc+/YFP/CRE model allows the *in vivo* NPMc+ recombination (upon two weeks of 4-OHT administration) and the possibility to sort NPMc+ expressing cells thanks to the concurrent YFP expression, as illustrated in Fig12B. We performed FACS immune-phenotype analysis of the *in vivo* inducible NPMc+/YFP/CRE mouse model, 4 months after transplantation. Noteworthy, we observed that NPMc+ expression leads to the same expansion of the HSC pool as in the *ex vivo* inducible system (data not shown).

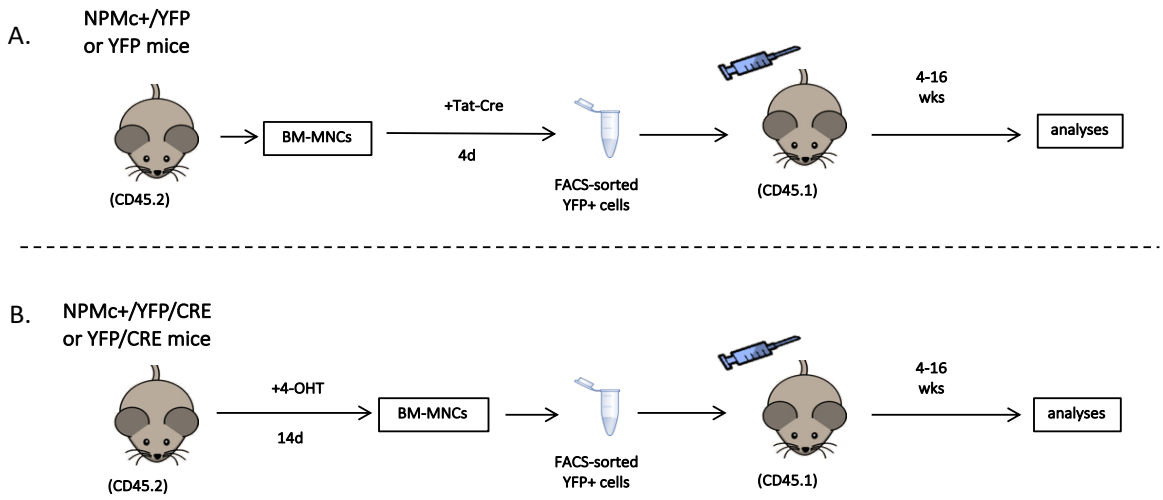

Figure 12 *In vitro* and *in vivo* inducible NPMc+ Cre recombinase model system.
Schematic representation of the experimental approach to induce NPMc+ expression.
A) BM-MNCs collected from NPMc+/YFP and YFP were TAT-CRE treated *in vitro* for 4 days. Recombined cells were FACS-sorted according to YFP expression and transplanted in lethally irradiated recipient animals. Reconstituted animals were analyzed 4 months later.
B) NPMc+/YFP/CRE and YFP/CRE animals were *in vivo* treated with 4-OHT for 14 days. Recombined BM-MNCs were collected and sorted according to YFP expression. As in approach A, cells were transplanted in lethally irradiated recipient animals and analyzed 4 months later.

To perform the self-renewal assay, as depicted in Fig13, we treated YFP/CRE and NPMc+/CRE/YFP animals for two weeks with 4-OHT. At the end of the treatment, we sacrificed the animals and we used FACS-sorted YFP+ positive BM cells to reconstitute lethally irradiated syngeneic mice expressing the CD45.1 surface marker (CD45.2 antigen is expressed on donor cells) (Fig 13(a)).

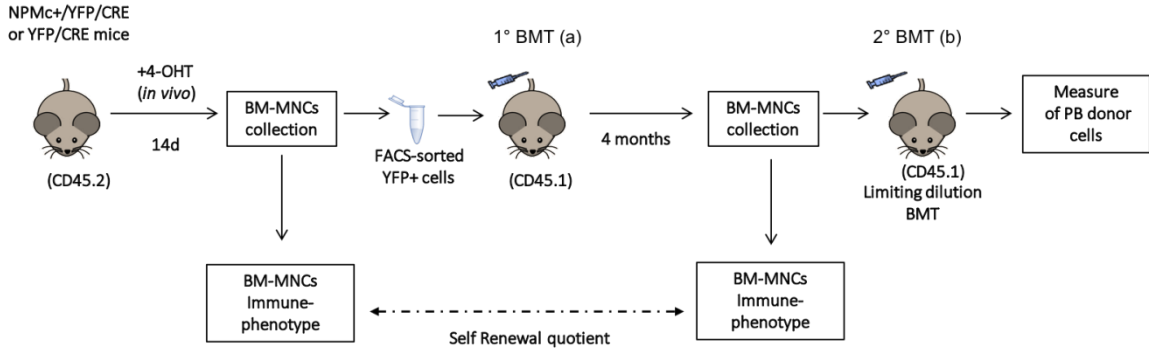

Figure 13 Self-Renewal assay and limiting number BMT experimental scheme. YFP/CRE and NPMc+/YFP/CRE donor animals (CD45.2+) have been administered *in vivo* for 14 days with 4-OHT. (a) YFP/CRE and NPMc+/CRE/YFP recombined BM-MNCs have been FACS-analyzed/sorted and transplanted in recipient mice (CD45.1+). (b) After 4 months, the BM has been collected, FACS-analyzed and transplanted in limiting condition (10.000 BM-MNCs) in recipient mice. Percentage of donor cells in recipient PB has been weekly monitored. The ratio between the number of HSCs transplanted in BMT 1(a) and recovered in BMT 2(b) provided the self-renewal quotient.

The HSC number in donor BM was determined both at the time of transplantation and four months later. Representative FACS plots of the immune-phenotype analyses are reported in Fig14A. At the time of transplantation, the HSC number in the donor BM was comparable in NPMc+/YFP/CRE and YFP/CRE samples (Fig14B). Four months later, the number of LT-HSCs was significantly higher in mice transplanted with NPMc+/YFP/CRE cells and, accordingly, the calculated self-renewal quotient (Challen et al. 2012) was significantly increased in NPMc+ transplanted animals (Fig14C).

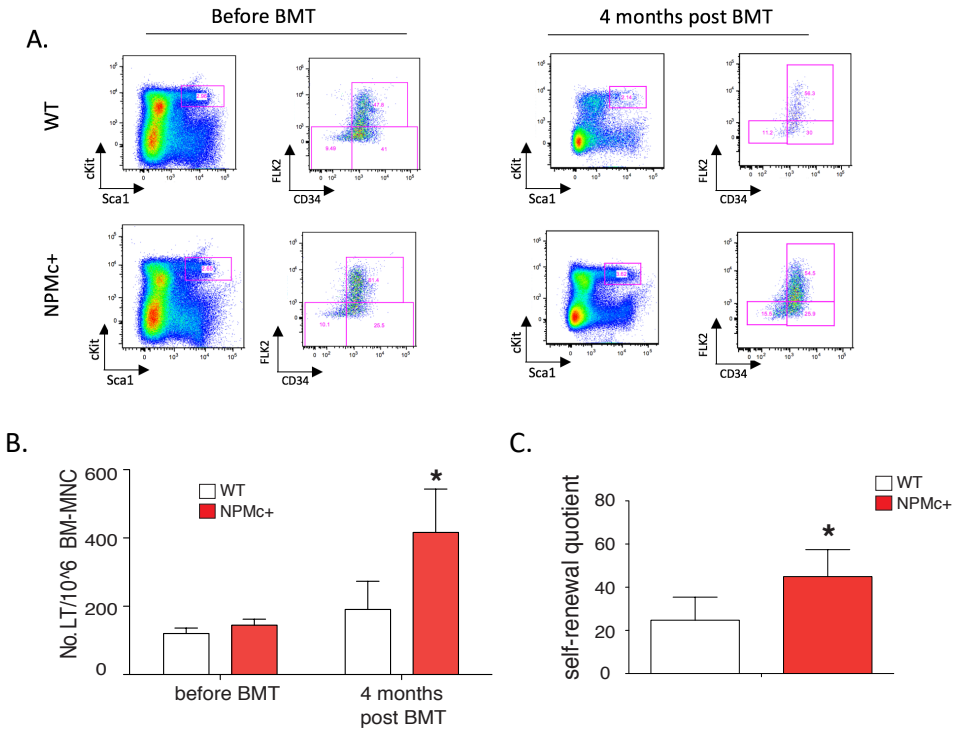

Figure 14 NPMc expression increases self-renewal rate of HSCs.
A) Representative FACS plots of the immune-phenotype analysis performed on NPMc+ and control BM-MNCs before (left panels) and 4 months after BMT (right panels). B) YFP+ BM purified from 4-OH-T NPMc+/YFP/CRE and YFP/CRE mice were used to reconstitute CD45.1 mice. LT-HSC number was determined, both at the time of BMT (inputs) and 4 months after BMT. (N=5; graph representative of 1 of 2 independent experiments; *p<0.05). C) Self-renewal quotient as the ratio between the donor LT-HSCs calculated in the whole BM of recipient mice at 4 months post BMT and the numbers of transplanted LT-HSCs (*p<0.05).

To confirm these data at functional level, we re-transplanted secondary recipient mice with a limiting number of LT-HSCs isolated from the animals reconstituted with the BM-MNCs of YFP/CRE and NPMc+/YFP/ CRE mice (as depicted in Fig13(b)). Based on the results of the immune-phenotypic analysis, we injected decreasing amount of total BM cells up to 10,000 BM-MNCs, corresponding to a calculated LT-HSC frequency of ~1:5,000 in the YFP/CRE sample or ~1:2,500 in the NPMc+/YFP/CRE sample.

As shown in Table7, the BM-MNCs derived from animals reconstituted with 10,000 NPMc+/YFP/CRE cells showed a higher engraftment rate compared to control 10,000 YFP/CRE cells. Therefore, the frequency of Competitive Repopulating Units (CRUs), calculated by ELDA web tool (Hu and Smyth 2009), is higher (1:8676 compared to 1:21762 of controls mice), in good agreement with the expected CRU frequency in the

LT-HSCs compartment (~1:4) (Osawa et al. 1996). Consistently, NPMc+/YFP/CRE recipients showed significantly higher percentage of donor derived PB cells, indicating the HSCs ability to terminally differentiate (Table7).

	Cell Number	No engrafted mice	CRU frequency	% donor cells (PB)
WT	500.000	4/4	1:21762	17 ±5.04
WT	100.000	5/5		3.48 ±0.75
WT	10.000	7/19		0.97 ±0.42
NPMc+	500.000	4/4	1:8676 *	18.27 ±5.07
NPMc+	100.000	5/5		4.1 ±0.27
NPMc+	10.000	13/19		1.43 ±063 **

Table 7 NPMc+ expressing BM-MNCs show a higher engraftment rate in limiting number BMT condition.
BMT under limiting numbers of HSCs. Engrafted animals are defined as recipients with >0.1% donor-derived PB cells, 4mo post BMT. The frequency of functional HSCs (CRUs) was calculated with the ELDA software. (*p<0.05, **p<0.01).

In summary these data demonstrate that NPMc+ expression increases the self-renewing division rate of HSCs while maintaining their repopulating ability.

4.2 NPMc+ preserves the quiescent potential of the HSC pool

At steady state, HSCs are largely in a dormant state, which is thought to be critical for the maintenance of lifelong self-renewal potential (Pietras, Warr, and Passegué 2011). Indeed, stimuli that promote HSCs proliferation are usually associated with decreased quiescence, leading to the exhaustion of the compartment (Wilson et al. 2008; Pietras et al. 2014). Our data revealed the NPMc+ ability to expand the HSC pool by increasing the HSCs self-renewal rate. Therefore, we aimed to investigate whether NPMc+ expression correlated to a concomitant reduced quiescence.

To address this point, we analyzed the cell cycle of LT-HSCs in mice transplanted with NPMc+/YFP+ or YFP+ BM-MNCs, four months after transplantation. In particular, we analyzed by FACS the LT-HSCs stained with Hoechst and anti-Ki67 antibody. Hoechst staining allows to define the DNA content of the cells (2n or 4n), while the nuclear protein Ki67 is expressed in all the cell-cycle phases, except for quiescent cells (Gerdes et al. 1984, 67). Therefore, as represented by the plot in Fig15A, the cell cycle phases are defined as G0: 2n, Ki67-; G1: 2n, Ki67+ and S-G2-M: 4n, Ki67+.

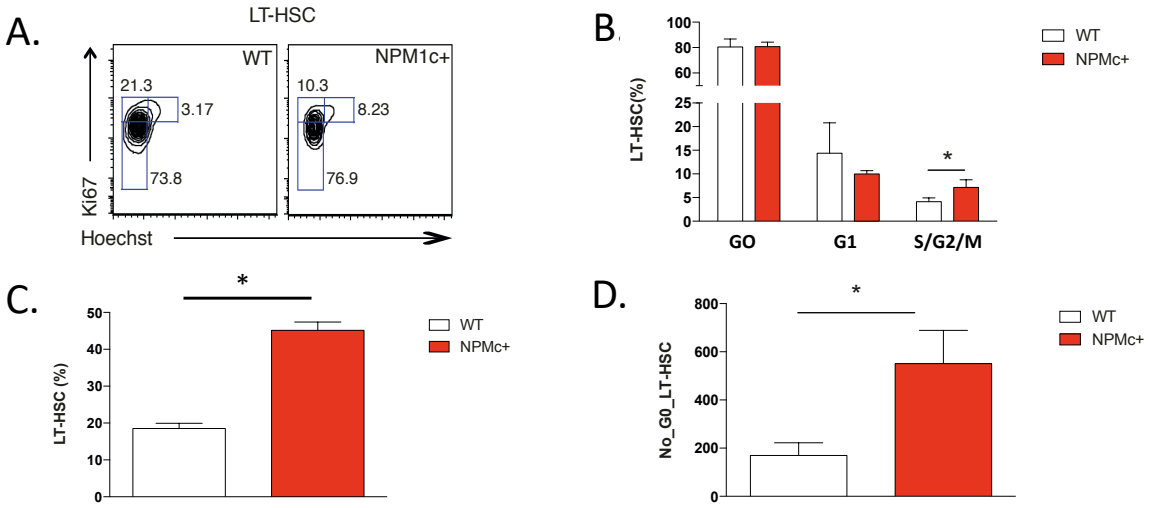

Figure 15 NPMc+ LT-HSCs show increased proliferation with no variation in the quiescent fraction.
A) Representative FACS plots showing the gate strategy for the cell cycle analysis of the LT-HSC population based on the Hoechst/Ki67 staining. B) Histograms indicate the percentage of LT-HSCs in the different cell cycle states. C) Percentage of LT-HSCs in the BM of NPM/YFP and YFP mice 4 months after transplantation, evaluated by immune phenotype FACS analysis. D) Histograms indicate the absolute number of the G0 LT-HSCs per million of BM, in the same cohort of animals as in panel B (N=4; *p<0.05).

We observed a decreased percentage of cells in G1 and a significant increase of cells in the S/G2/M, confirming the expansion of NPMc+ cycling LT-HSCs. However, we did not observe any variation in the percentage of G0/quiescent LT-HSCs (Fig15B). Moreover, since the whole LT-HSC compartment is expanded in the NPMc+/YFP transplanted animals (Fig15C), the evaluation of the absolute number of quiescent LT-HSCs showed a significant increment as compared to control cells (Fig15D).

In order to confirm the expanded number of quiescent NPMc+ expressing LT-HSCs, we performed a pulse-chasing Labeling Retaining Assay, which allows to measure the number of quiescent cells *in vivo,* over an extended timeframe (Wilson et al. 2008). As depicted in Fig16A, two months after transplantation, reconstituted recipient mice were pulsed with BrdU in drinking water for 13 days. Homogenous labeling of the whole BM compartment has been verified by FACS at the end of the pulsing time (data not shown). After three months of chasing, we quantified Long Term BrdU Retaining (LTR) cells as *bona fide,* slow cycling/quiescent cells over the chasing time. As shown in Fig16B, the number of quiescent LTR LT-HSCs was significantly higher in NPMc+ expressing cells, as compared to control, further supporting the ability of NPMc+ to expand the LT-HSCs without compromising their quiescence status.

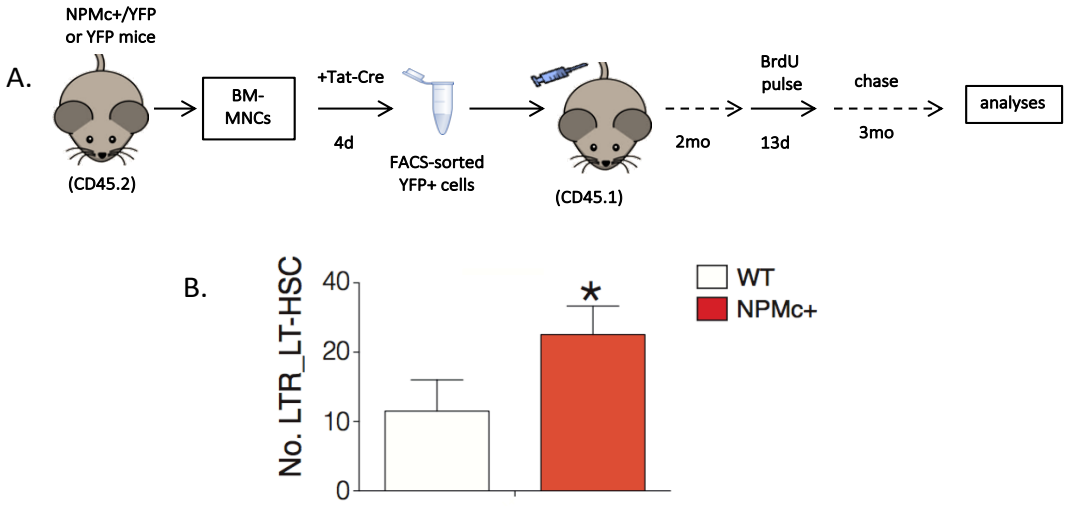

Figure 16 NPMc+ expression in LT-HSCs expands the number of quiescent LT-HSCs.
A) Experimental scheme for the pulse-chasing Labeling Retaining Assay. B) Histograms indicate the number of LTR BrdU+ LT-HSCs per million of BM cells at the end of the chasing period (N=4; *p<0.02. Data are representative of two independent experiments).

According to their definition, adult stem cells have the ability to self-renew and generate multiple mature cell types. Once the physiological homeostasis is altered by any stress factor (e.g. wounds, infections), quiescent cells act as a reservoir, re-enter the cell

cycle, and reconstitute the damaged system. Consequently, this process is intrinsically limited by the amount of available quiescent stem cells and by their functionality.

To validate whether NPMc+ quiescent LT-HSCs were fully competent in sustaining hematopoiesis in stress conditions, we took advantage of the 5-FU serial treatment stress assay. As known, 5-FU is a chemotherapeutic agent that kills the hematopoietic cycling cells and thus challenges the activation of quiescent HSCs in order to repopulate the damaged BM. Therefore, by weekly 5-FU injections of NPMc+/YFP and YFP reconstituted recipients, we monitored the mouse ability to recover from the continuous depletion of their proliferating progenitor population, which is mirror of the regenerating potential of the HSCs pool.

Notably, we observed that NPMc+ mice were more resistant to 5-FU treatments than controls, further supporting the expansion of a functional quiescent stem cell reservoir in these mice (Fig17).

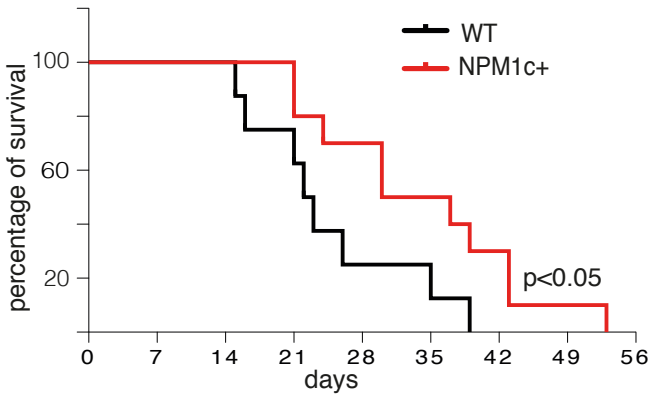

Figure 17 NPMc+ expressing mice have an extended survival rate upon serial 5-FU administrations
Kaplan Meyer curve of YFP and NPMc+/YFP mice weekly treated with 5-FU (N=8; graph representative of 1 of 2 independent experiments)

In summary, these data strongly suggest that, during the pre-leukemic phase, NPMc+ expression leads to the expansion of the LT-HSC pool, though maintaining its reconstituting potential and preserving quiescence.

4.3 NPMc+ enforces a stem cell transcriptional program promoting quiescence

Following the data on NPMc+ HSCs self-renewal and quiescence previously reported, we investigated the transcriptional changes imposed by NPMc+ expression on HSCs.

To this aim, we performed an Affymetrix microarray global gene-expression analysis on LT-HSCs sorted from NPMc+/YFP+ and YFP+ reconstituted mice, 4 months after transplantation. RNA was extracted just after sorting and hybridized on Mouse Gene ST 2.0 Arrays. NPMc+ expression resulted in a total of 562 significantly deregulated genes; among these, 322 were up-regulated (Fold Change [FC]≥ 1.5, False Discovery Rate [FDR]≤ 0.1) and 240 were down- regulated (FC ≤ -1.5, FDR≤ 0.1).

We ran a number of Gene Set Enrichment Analyses (GSEA) (Subramanian et al. 2005) on the HSCs pre-leukemic expression profile in different relevant datasets. These analyses showed that NPMc+ presence in LT-HSCs enforced the expression of genes up-regulated in human normal HSCs (Fig18A) (Jaatinen et al. 2006; Ivanova 2002). Moreover, NPMc+ LT-HSCs gene expression profile showed a marked correlation with the expression profile of human AMLs with mutated *NPM1* (Alcalay 2005; Mullighan et al. 2007) (Fig18B) and, notably, with the expression profile of acute myeloid LSCs (Gal et al. 2006) (Fig18C).

A. Hematopoietic Stem Cell Program

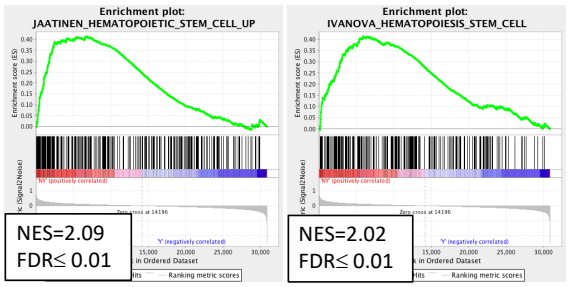

B. NPMc human AML

C. Leukemia Stem Cell

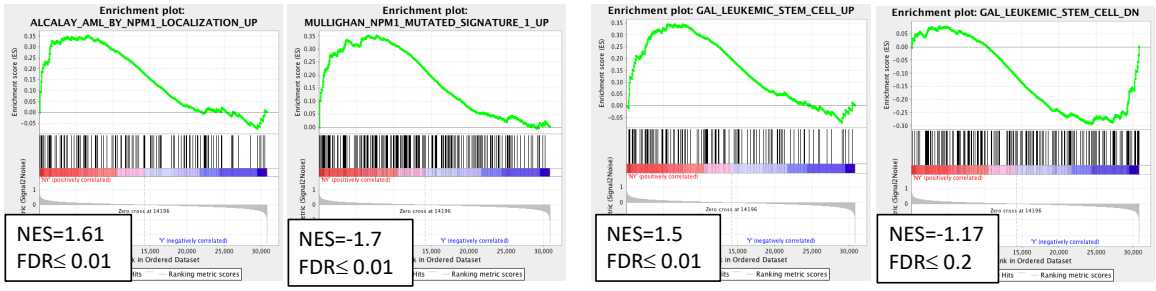

Figure 18 NPMc+ induces the expression of genes upregulated in both normal HSCs and acute myeloid LSCs.
Gene expression microarray data were used to identify enriched gene sets in NPMc+/YFP LT-HSCs compared to YFP LT-HSCs. GSEA enrichment plots correlate the NPMc+ LT-HSCs gene expression profile with:
(A) genes up-regulated in two different human HSCs data sets;
(B) genes up-regulated in two independent data sets of *NPM1* mutated human AMLs;
(C) genes up- and down-regulated in leukemic stem cells (LSCs).
Normalized enrichment score (NES) and false discovery rate (FDR) are indicated.

Among the up-regulated genes, we found clustered *Hoxa* genes and *Meis1* (Fig19). The overexpression of this set of genes has been previously correlated with the expression profile of AML patients, including NPMc+ AML (Alcalay 2005). Moreover, *HOXA* genes showed higher expression in HSCs, they are required to maintain and promote HSC self-renewal, and are widely involved in leukemia development (Argiropoulos and Humphries 2007). Moreover, *HOXA* genes are targeted by signals that maintain the HSC self-renewal by promoting quiescence (e.g., *Ash1l* gene (Jones et al. 2015) and MPL/THPO pathway (de Graaf and Metcalf 2011)).

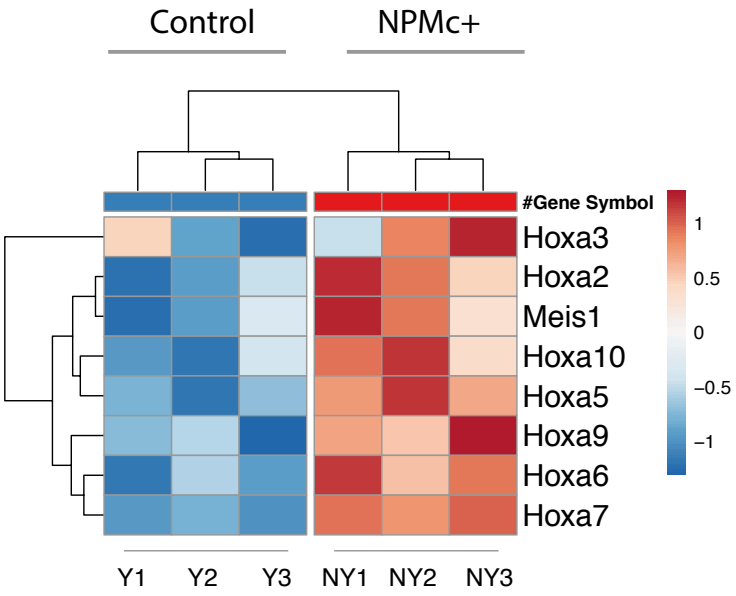

Figure 19 NPMc+ expression in LT-HSCs induces the expression of *Hoxa* cluster genes and *Meis1* gene.
The heatmap shows the Z scores of normalized Affymetrix expression values of each replicate for selected marker genes. Both rows and columns are clustered using Euclidean distance and average linkage. Decreased gene expression is indicated by shades of blue, increased gene expression is indicated by shades of red. All the selected genes show a statistically significant difference between the two conditions. (3 independent experiments).

Next, we directly addressed whether the NPMc+ LT-HSCs expression profile is enriched in genes that are specifically regulated in quiescent HSCs. We performed GSEA comparing the NPMc+ LT-HSCs gene expression profile with both the quiescence and the proliferative signature generated by Goodell's group (Venezia et al. 2004). These signatures have been generated comparing adult quiescent HSCs gene expression profiles to more proliferating HSCs (e.g. fetal-liver HSCs and HSCs mobilized with 5-FU treatment) or ST-HSCs. As depicted in Fig20, we found that genes up-regulated in NPMc+ LT-HSCs were significantly enriched in the quiescent HSCs signature (Fig20A), while the HSC-proliferation signature did not show any significant enrichment (Fig20B).

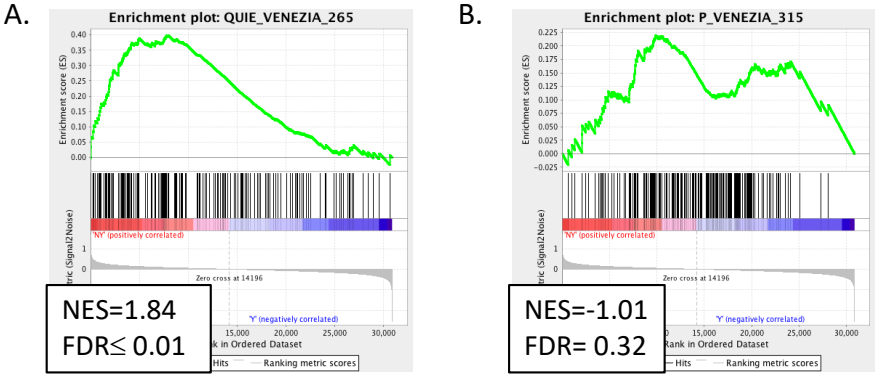

Figure 20 NPMc+ promotes the expression of genes associated with the control of HSCs quiescence.
GSEA enrichment plots correlate NPMc+ LT-HSCs gene expression profile with:
(A) genes known to be upregulated in quiescent murine HSCs;
(B) genes known to be upregulated in proliferating murine HSCs.
Normalized enrichment score (NES) and false discovery rate (FDR) are indicated.

We further considered a manually curated list of genes that have been reported in the literature as required for the maintenance of HSC self-renewal potential, favoring quiescence. According to previous data, in the list of genes up-regulated by NPMc+ expression in LT-HSCs, we found a number of these manually curated quiescence genes (e.g., *Gfi1*, *p21* [*Cdkn1a*], *Tgfb1*, *Tgfbr2*, *Smad3*, *Egr1*, *Angpt1*) (Yamada, Park, and Lacorazza 2013; Min et al. 2008; Hock et al. 2004; Yamazaki et al. 2009; Cheng et al. 2000; Arai et al. 2004) (Fig.21). On the other hand, we did not observe a coherent up-regulation of genes that induce cell-cycle entry and progression (data not shown).

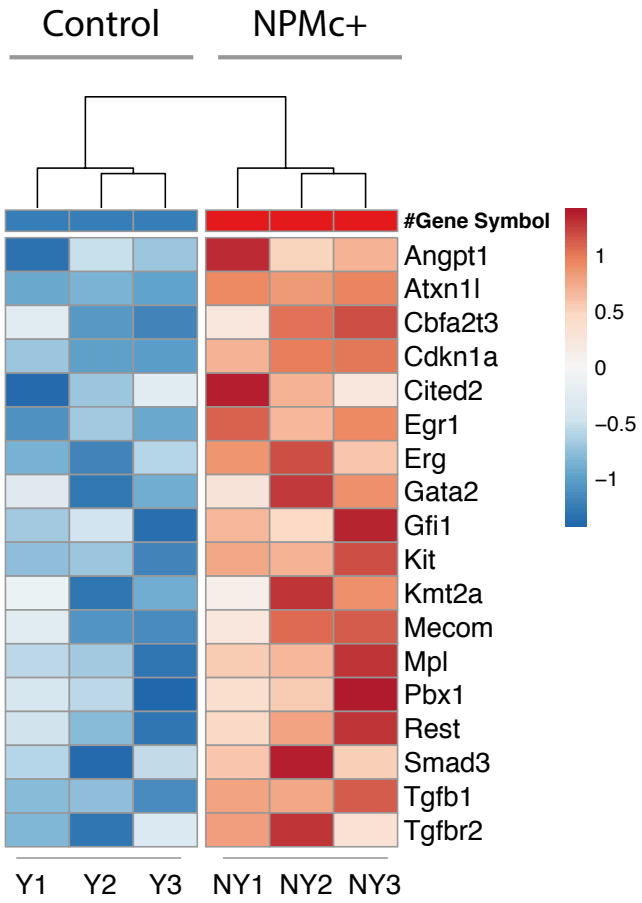

Figure 21 NPMc+ expression in LT-HSCs induces the expression of genes required to maintain HSCs quiescence.
The heatmap shows the Z scores of normalized Affymetrix expression values of each replicate for selected marker genes. Both rows and columns are clustered using Euclidean distance and average linkage. Decreased gene expression is indicated by shades of blue, increased gene expression is indicated by shades of red. All the selected genes show a statistically significant difference between the two conditions. (3 independent experiments).

In conclusion, our transcriptional data provide evidence that NPMc+ enforces, in HSCs, a transcriptional program that characterizes NPMc+ AMLs and is enriched in LSCs. Furthermore, consistent with the observed effect on HSC amount and fitness in the BM, we showed that NPMc+ regulates the expression of both quiescence and self-renewal essential genes, thus imposing a "stem cell program".

4.4 NPMc+ prevents the exhaustion of FLT3-ITD HSCs

Recent studies on a large cohort of patients showed that nearly 40% of *NPM1* mutated AML have *FLT3-ITD* as associated alteration worsening NPMc+-related favorable outcome (Papaemmanuil et al. 2016). This cooperative effect is well recapitulated by our NPMc+ mouse model, which develops a rapid and fully penetrant AML upon FLT3-ITD expression (Mallardo et al. 2013). Noteworthy, FLT3-ITD mutated HSCs have an increased proliferative rate. However, their contribution to the BM population is reduced and the BM displays impaired repopulating abilities, suggesting that they progressively exhaust due to the constitutive over-proliferative signals delivered by FLT3-ITD (Lee et al. 2007; Chu et al. 2012). Interestingly, these animals develop a myeloproliferative disease but not AML. Bearing all this in mind, we investigated the impact of NPMc+ on the HSPCs preleukemic compartment in the presence of the FLT3 mutations.

4.4.1 Generation of an *in vivo* inducible NPMc+/FLT3-ITD model system

We aimed to generate a model to study the cooperation of the two mutations during the initial phase of the disease. For this purpose, we crossed our NPMc+ model with the *Mx-Cre* strain, where the Cre is expressed under the control of the Mx dynamin-like GTPase1 (Mx1) promoter. The *Mx1* gene is part of the response to virus attack and its expression is mainly restricted to the hematopoietic system. Since the IFN system is the first line of defense against viral infection in mammals, Mx1 promoter can be transiently activated by the polyinosinic:polycytidylic acid (pIpC), which is structurally similar to the double strand RNA present in some viruses (Kuhn et al. 2016).

We have generated a cohort of mice sharing the same MxCRE genetic background, by crossing Mx-Cre$^{-/+}$ mice with both NPMc+ and *Flt3-ITD* single mutant animals, to get the definitive experimental cohort composed by *Mx-Cre*$^{-/+}$, *NPM1c+*$^{fl/fl}$*/Mx-Cre*$^{-/+}$, *Flt3-*

ITD/Mx-Cre$^{-/+}$ and *NPM1c+*$^{fl/fl}$*/Flt3-ITD*$^{-/+}$*/Mx-Cre*$^{-/+}$ strains (thereafter Mx, NPMc+, FLT3-ITD and NPMc+/FLT3-ITD) (Fig22).

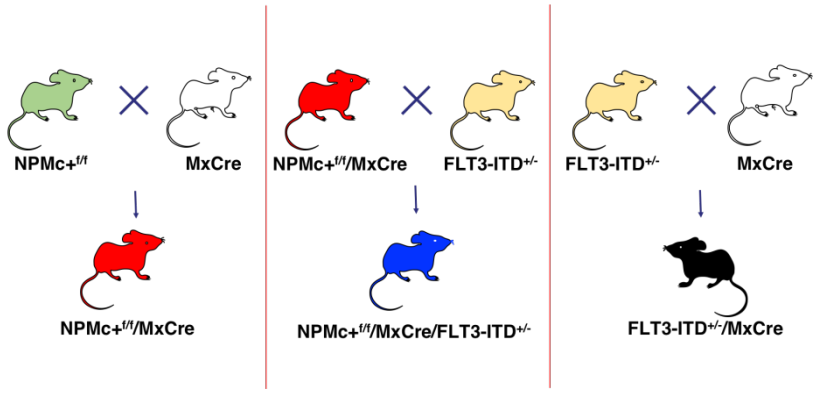

Figure 22 Breeding scheme to generate the experimental cohort in the MxCRE background.
Both *NPMc+*$^{fl/fl}$, *Flt3-ITD*$^{-/+}$ and *NPMc+*$^{fl/fl}$*/Flt3-ITD*$^{-/+}$ have been mated with the *MxCre*$^{-/+}$ strain obtaining a cohort of mice with the same MxCre background.

According to published protocols, we injected mice with pIpC for 10 days, every other day. At the end of the treatment, the efficiency of NPMc+ recombination was assessed by immunofluorescence on WBCs from the PB, using a homemade antibody that specifically recognizes only the mutated portion of the NPM protein. As depicted in Fig23A, we confirmed the accumulation of NPMc+ mutated protein in the cytoplasm. In both NPMc+ and NPMc+/FLT3-ITD PB samples analyzed, the percentage of NPMc+ expressing WBCs was around 80% (Fig23B). Since we aimed to investigate NPMc+ and FLT3-ITD molecular cooperation in the HSPCs, we checked NPMc+ expression also in the FACS sorted LKS population. Widefield images of stained LKSs have been collected and the quantitative analysis of the NPMc+ signal has been carried out by the Automated Microscopy for Image-Cytometry (A.M.I.CO.) computational platform developed by our group (Furia, Pelicci, and Faretta 2013). As reported in Fig23C, the number of NPMc+ expressing LKS was 98% ± 0.42.

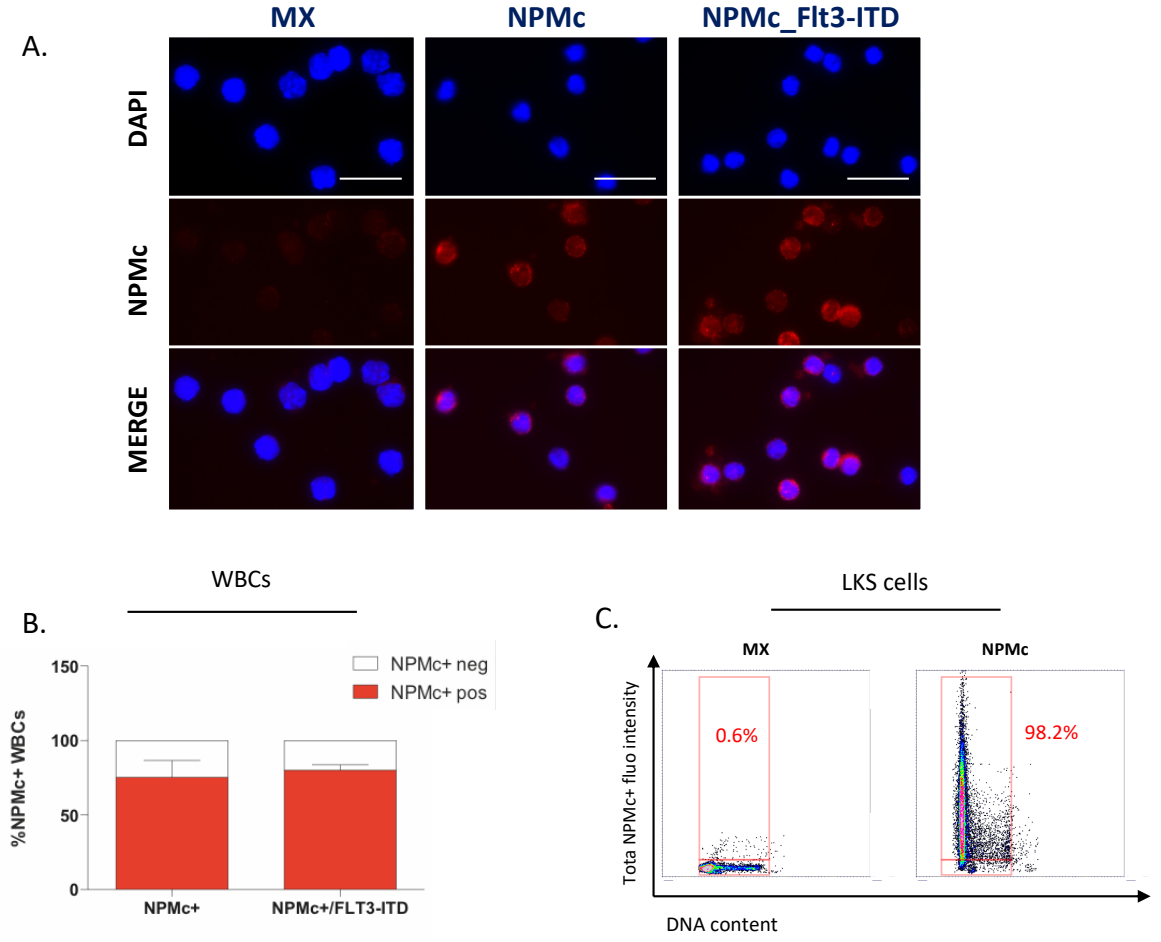

Figure 23 Mx-CRE mediated NPMc+ expression in the PB and in the LKS compartment.
A) Representative images of the immunofluorescence analysis performed on Cytospin® preparations of WBCs derived from pIpC treated Mx, NPMc+ and NPMc+/FLT3-ITD mice. In red, rabbit polyclonal antibody against NPMc+; in blue, DAPI staining of nuclei. NPMc+ cytoplasmic localization is confirmed by merging red and blue staining. Scale bar 100 um B) Histograms represent the percentage of NPMc+ positive WBCs in the total WBCs population (data represent the pool of four independent experiments). C) Plots represent NPMc+ fluorescence signal intensity quantified by the A.M.I.CO. computational platform in LKS samples (data represent the pool of two independent experiments).

We next confirmed the cooperation between NPMc+ and FLT3-ITD mutation in inducing AML in our new Mx-based model. As shown in Fig24A, in line with ours and others previous work (Mallardo et al. 2013; Vassiliou et al. 2011; Mupo et al. 2013), our NPMc+/FLT3-ITD mice developed a fully penetrant AML with a median latency of 69 days after pIpC treatment, while FLT3-ITD single mutant mice did not develop the disease within the same time frame. The Giemsa staining of BM and spleen of leukemic animals in

Fig 23B show how leukemic cells diffusely effaced splenic and BM structure, and the occurrence of a high number of blasts in the PB smears.

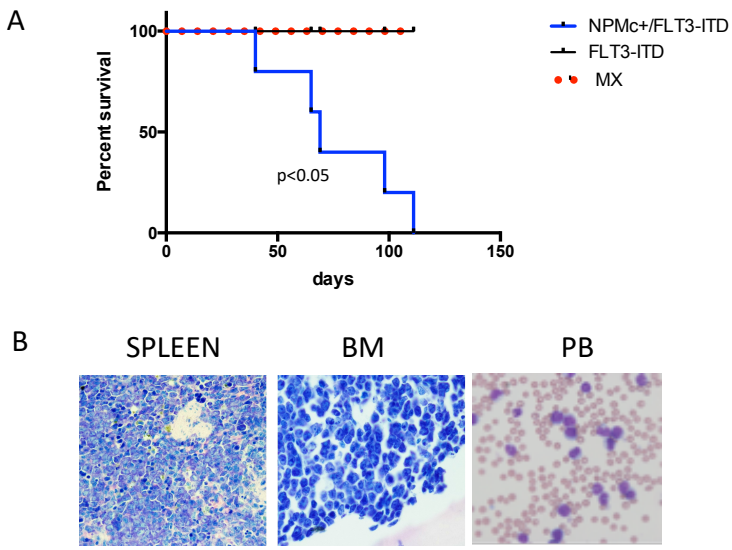

Figure 24 pIpC induced NPMc+/FLT3-ITD mice develop AML.
A) Kaplan Meier survival curve of FLT3-ITD, NPMc+/FLT3-ITD and control mice (n=5, Log Rank ≤ 0.05). B) Representative images of Giemsa-stained BM/spleen and May-Grumwald stained peripheral blood smear from NPMc+/FLT3-ITD mice at the time of AML development.

4.4.2 Characterization of the NPMc+/FLT3-ITD pre-leukemic phase.

The main issue to consider in defining a pre-leukemic phase in the NPMc+/FLT3-ITD model is the early onset of the disease in some animals (about 70 days post pIpC injection, Fig24A). We therefore estimated three weeks after pIpC treatment as suitable time point for the pre-leukemia analysis, as confirmed by the analysis of the BM morphology evaluating the presence of any sign of overt leukemia in the double mutant model.

Ineffective thrombopoiesis was the most outstanding feature of NPMc+ mice, since their BM displays a striking expansion of dystrophic megakaryocytes bearing “cloud-like” nuclei and abundant cytoplasm (Fig25, panels c/d), accompanied by a reduced platelet amount in the blood (Table8). Notably, the NPMc+ alteration on megakaryocytic

development has been already reported by Falini's group (Sportoletti et al. 2013). The FLT3-ITD mice showed a mildly expanded myelopoiesis with an increase in neutrophil and monocyte blood count and reduced lymphocytes (Fig25, panels e/f, and Table8). The NPMc+/FLT3-ITD mice recapitulated the alterations observed both in NPMc+ and FLT3-ITD mice, sharing many features with human myeloproliferative/myelodysplastic syndromes (MPN/MDSs). In particular, NPMc+/FLT3-ITD mice showed thrombocytopenia and dysplasia involving one or more of the myeloid lineages, and myeloproliferative changes as neutrophilia and mono-cytosis (Fig25, panels g/f, and Table8).

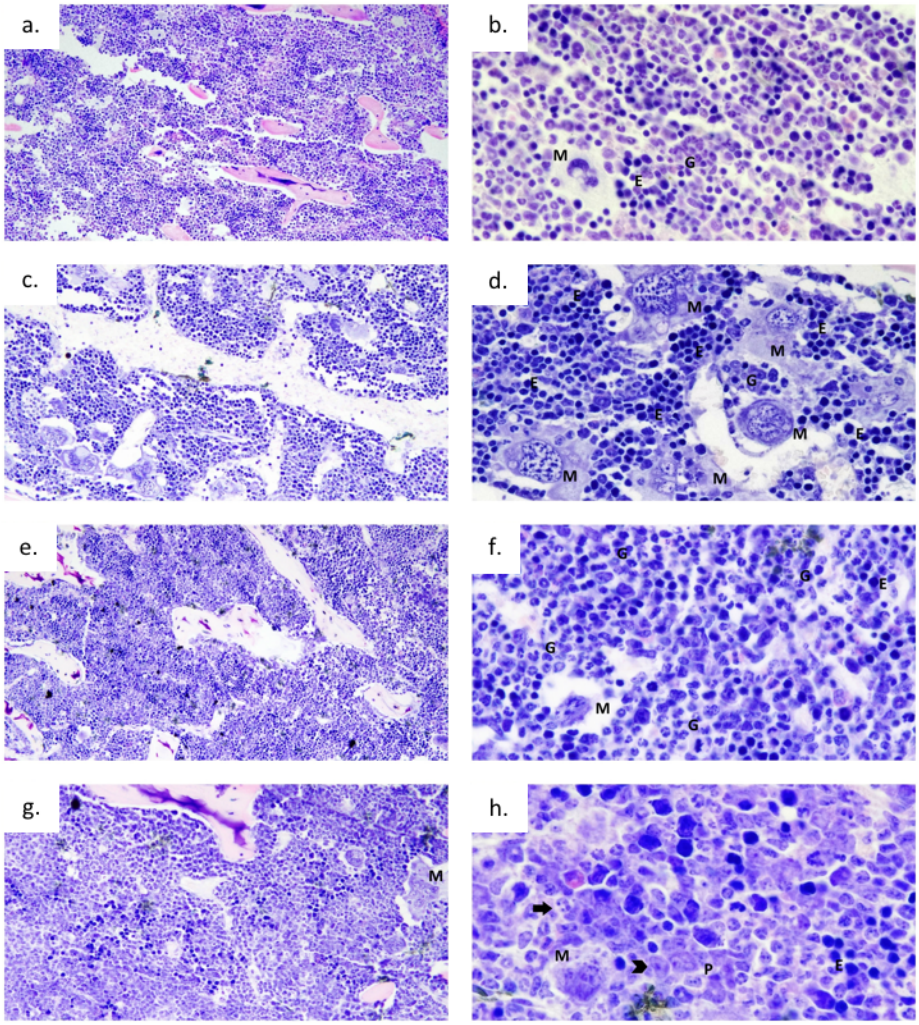

Figure 25 Histological characterization of the hematopoietic compartment of Mx, NPMc+, FLT3-ITD and NPMc+/FLT3-ITD mice.
Giemsa stains of Mx (a, b), NPMc+ (c, d), FLT3-ITD (e, f) and NPMc+/FLT3-ITD (g, h) murine BM sections, at 200x (left panels) and 600x magnification (right panels). G: granulocytes; E: erythroid islands; M: megakaryocytes**.** Arrowheads indicate the precursors and arrows indicate band-like elements.

	WT	NPMc+	FLT3-ITD	NPMc+/FLT3-ITD
WBC x 10^3/uL	8,35 ±2,92	7,1 ±3,20	7,18 ±2,45	15,27 ±7,67 *
RBC x 10^6/uL	6,854 ±1,03	5,99 ±1,61	6,54 ±1,41	5,94 ±1,70
HGB g/dL	18,61 ±8,99	16,98 ±9,67	18,1 ±9,44	17,74 ±8,26
PLTs x 10^3/uL	601 ±222,26	158,4 ±74,46 *	659,1 ±343,29	166,6 ±90,1 *
% Neutrophils	2,21 ±1,45	4,97 ±8,54	6,01 ±3,01 *	3,03 ±2,21 *
% Lymphocytes	90,59 ±4,12	86,32 ±14,52	78,99 ±8,37 *	88,36 ±3,27
% Monocytes	5,92 ±2,49	5,39 ±2,16	12,57 ±5,4 *	7,45 ±2,67

Table 8 PB analysis of Mx, NPMc+, FLT3-ITD and NPMc+/FLT3-ITD mice.
Complete PB cell counting and WBC differential counting (in percentage). Values are presented as mean ± SD (n=10, *$p<0.05$, data represent the pool of three independent experiments).

Therefore, the histological evaluation indicated that, although in our NPMc+/FLT3-ITD mice at 21 days post induction a general alteration of the BM morphology had occurred, these animals still displayed a leukemia-free BM that can be analyzed with the same parameters viable for normal BM.

We then proceeded with the characterization of the HSPCs composition in our experimental cohort of mice, by immune-phenotype FACS analysis 3 weeks after NPMc+ induction. We confirmed, in the NPMc+/MxCRE model, the BM phenotype observed in NPMc+/YFP mice, namely the expansion of both the percentage of LKS cells within the Lin- compartment (Fig26A) and the increase of LT-HSC percentage within the LKS compartment (with a corresponding slight decrease in the percentage of MPPs) (Fig25B-D). Moreover, FLT3-ITD mice showed no difference in the LKS cell number (Fig26A), but a marked reduction of the percentage of the LT-HSCs with the concomitant increase of the MPP fraction (Fig26B-D). Notably, the expression of NPMc+ in the FLT3-ITD context significantly expanded the percentage of LKS within the Lin- compartment, compared to both control and FLT3-ITD mice (Fig26A), and significantly increased the percentage of LT-HSCs compared to the FLT3-ITD mice (Fig26B).

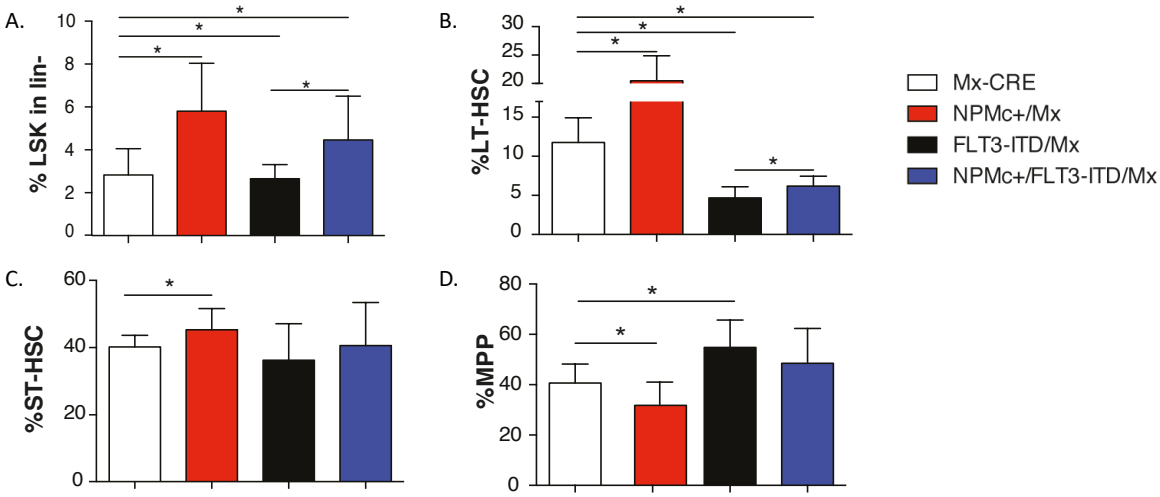

Figure 26 NPMc+ expression increases the percentage of LT-HSCs in the BM of FLT3-ITD mice.
BM immune-phenotype FACS analysis of Mx, NPMc+, FLT3-ITD and NPMc+/FLT3-ITD animals upon pIpC treatment. Histograms indicate the percentage of the specified cell types (A: LKS cells B: LT-HSCs C: ST-HSCs D: MPPs) in the BM (LKS) or in LKS compartment (N=10, *=$p<0.05$, data represent the pool of three independent experiments).

Representation of these data as number of cells per million of vital BM-MNCs showed that, due to the expansion of the LKS compartment (Fig27A), the co-expression of NPMc+ and FLT3-ITD completely rescued (compared to control mice) the LT-HSCs number (Fig27B) and significantly increased the number of ST-HSCs and MPPs compared to both the FLT3-ITD and control mice (Fig27C-D).

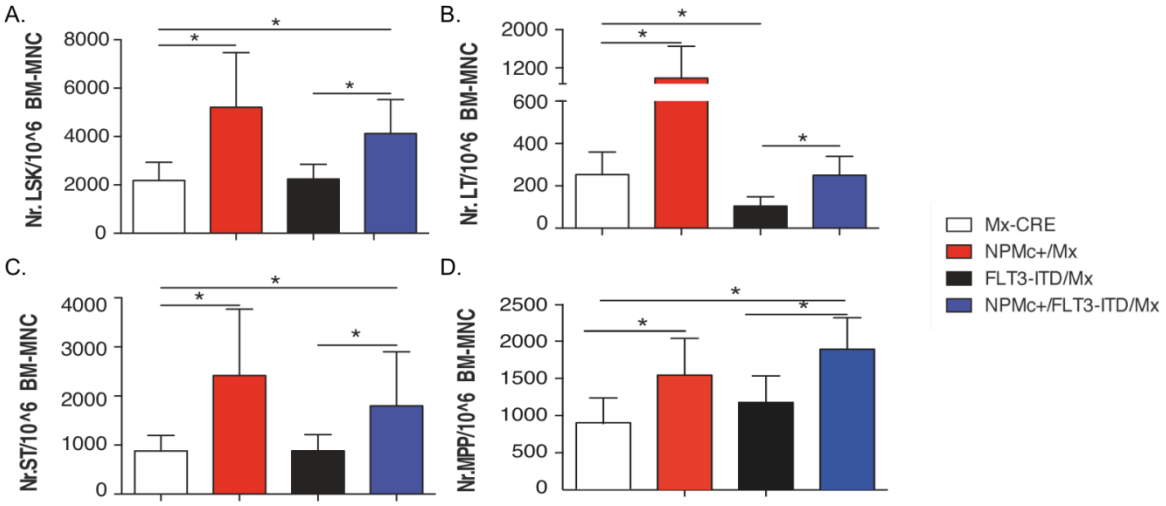

Figure 27 NPMc+ expression rescues the number of LT-HSCs in the bone marrow of FLT3-ITD mice.
BM immune-phenotype FACS analysis of Mx, NPMc+, FLT3-ITD and NPMc+/FLT3-ITD upon pIpC treatment. Histograms indicate the absolute number per million of BM of the specified cell types (A: LKS cells B: LT-HSCs C: ST-HSCs D: MPPs) in the BM (LKS) or in LKS compartment (N=10, *=$p<0.05$, data represent the pool of three independent experiments).

We have previously shown that NPMc+ total BM has a higher repopulating capacity compared to controls (data not shown), while FLT3-ITD total BM has impaired repopulating abilities (Chu et al. 2012). Therefore, to further validate our results at functional level, we performed a competitive BMT assay. We co-transplanted CD45.2 Mx (or Flt3-ITD or NPMc+/FLT3-ITD) BM-MNCs in irradiated congenic mice (CD45.1) along with CD45.1 BM-MNCs (1:1 ratio). The repopulating ability of donor cells was evaluated at different time points after transplantation, by analyzing the percentage of CD45.2 WBCs in PB of the recipient mice. As indicated in Fig28, mice transplanted with FLT3-ITD cells showed a significantly lower proportion of CD45.2 WBCs in the PB, while the proportion of NPMc+/FLT3-ITD CD45.2 WBCs was similar to the control up to 16 weeks, thus indicating the ability of NPMc+ expression to rescue the FLT3-ITD long term HSC repopulating deficiency.

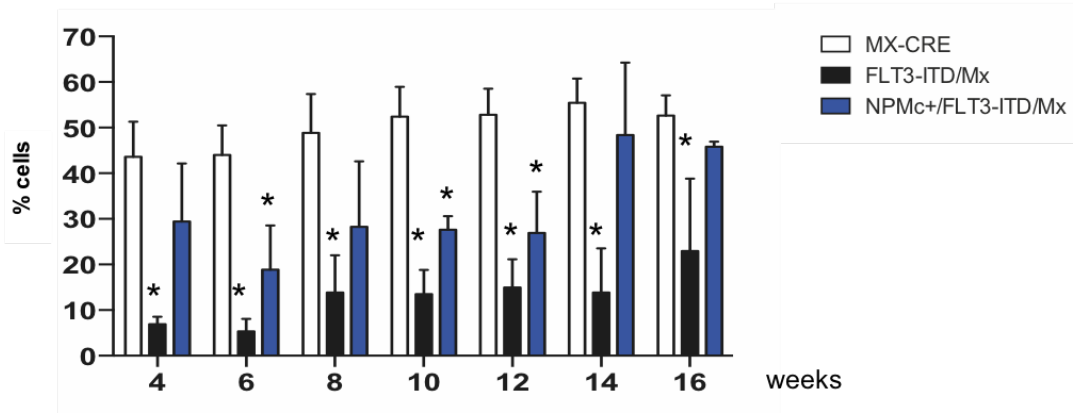

Figure 28 NPMc+ expression rescues the FLT3-ITD defective hematopoietic reconstitution ability.
FACS analysis of the percentage of donor derived (CD45.2) cells in the peripheral blood of transplanted mice at different time points (N=3, *=p<0.05).

In conclusion, our data demonstrate that NPMc+ expression is able to prevent the exhaustion of FLT3-ITD HSCs and favor the expansion of the entire HPSC compartment, thus confirming an NPMc+ dependent program aimed to maintain a functional HSC reservoir in the pre-leukemic phase.

4.5 Expression of NPMc+ in FLT3-ITD HSCs restores quiescence and prevents excessive proliferation.

Our data on the pre-leukemic NPMc+/YFP BM have shown the peculiar ability of NPMc+ to expand the HSC compartment, though preventing its exhaustion through the promotion of quiescence. Therefore, we aimed to investigate how NPMc+ expression impacts the HSCs balance between quiescence and proliferation in the FLT3-ITD background. In order to evaluate the quiescence, the G0 cell population in the LT-HSC pool has been quantified using the Ki67 marker (Gerdes et al. 1984). As depicted in Fig 28A, NPMc+ and Mx samples showed a comparable percentage of G0 LT-HSCs, confirming our previous data in NPMc+/YFP model (Fig14B). On the contrary, FLT3-ITD

LT-HSCs showed a significant lower percentage of cells in the G0 phase. Interestingly enough, the NPMc+/FLT3-ITD G0 LT-HSC fraction was comparable with the control, thus demonstrating the ability of NPMc+ to restore a normal quiescent pool of HSCs in the FLT3-ITD background (Fig29A). We then evaluated the absolute number of quiescent/G0 LT-HSCs per million of vital BM-MNCs. Since NPMc+ expanded the whole LT-HSC compartment (Fig29B), the number of cells in G0 phase in this compartment resulted greatly augmented compared to Mx sample (Fig29C). Coherently, since NPMc+ increased the LT-HSCs number also in the FLT3-ITD background (Fig28B), the number of NPMc+/FLT3-ITD G0 LT-HSCs was significantly expanded compared to FLT3-ITD (Fig29C), thus emphasizing the NPMc+ ability to promote quiescence in the presence of FLT3-ITD.

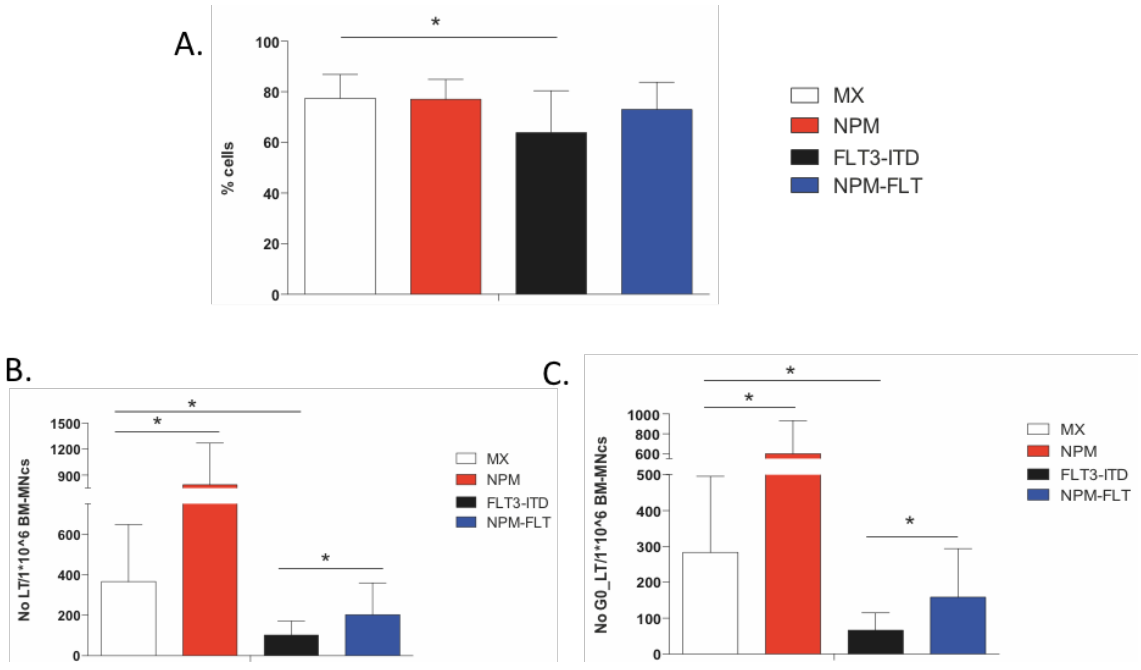

Figure 29 NPMc+ expression rescues the FLT3-ITD dependent loss of quiescence in the LT-HSCs
A) Histograms indicate the percentage of LT-HSCs in the G0 phase of the cell cycle. B) Histograms report the absolute number of LT-HSCs per million of vital BM-MNCs evaluated by Immune-phenotype FACS analysis. C) Histograms depict the absolute number of the G0 LT-HSC per million of BM-MNCs (N=12; *=p<0.05, data represent the pool of four independent experiments).

The *in vivo* BrdU labeling retaining assay has been performed to further investigate the quiescent versus proliferative behavior in our model system. Notably, because of the rapid AML onset in NPMc+/FLT3-ITD mice, we were forced to change the previous pulse-chase protocol, combining the pIpC injections with the BrdU feeding, then shortening the chasing time and quantifying the retained BrdU population at 26 days post induction (Fig30A).

As depicted in Fig30C, the number of BrdU retaining LT-HSCs in FLT3-ITD BM was significantly lower than controls both in percentage and in number, coherently with the strong proliferation signal provided in the hematopoietic system by FLT3-ITD (Chu et al. 2012; Lee et al. 2007). NPMc+ did not affect the percentage of BrdU retaining LT-HSCs, whilst, due to the expansion of the compartment (not shown), the number of BrdU retaining LT-HSCs was twice compared to controls. Strikingly, the presence of NPMc+ in the FLT3-ITD context increased the percentage and the number of LT-HSCs retaining BrdU compared to FLT3-ITD BM condition, thus restoring both the same percentage and the number as in controls animals.

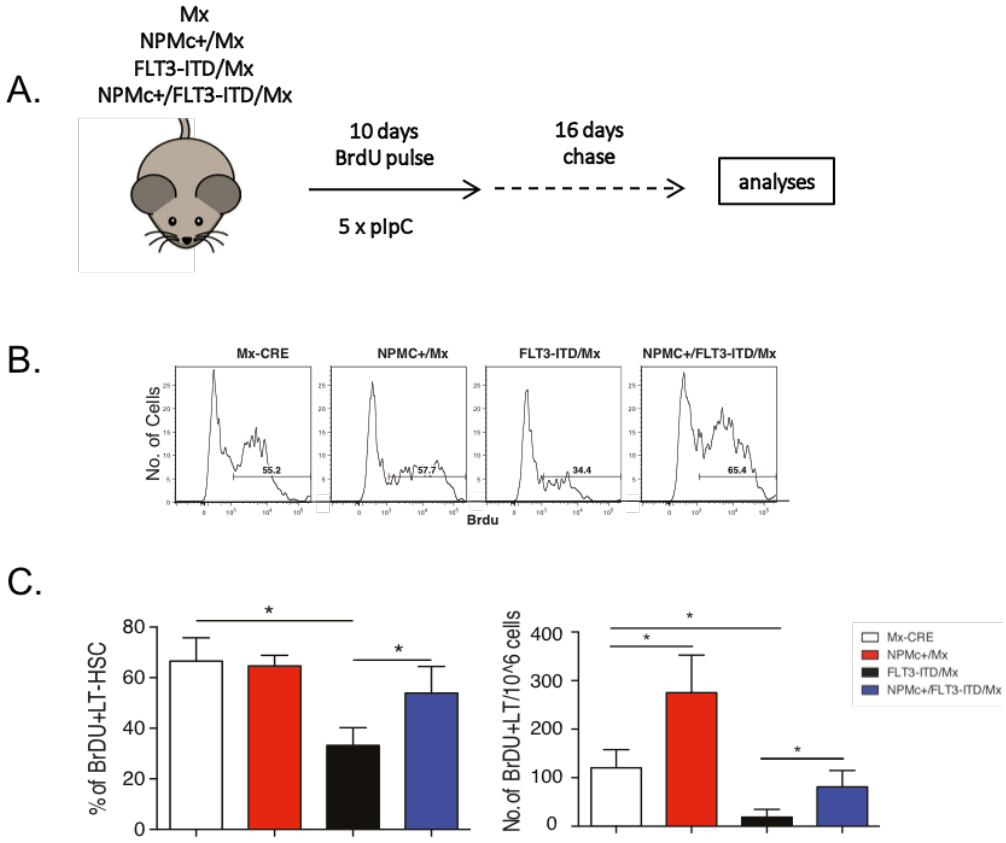

Figure 30 NPMc+ mutation prevents the FLT3-ITD-dependent hyper-proliferative phenotype in the LT-HSCs.
A) BrdU "short" retaining assay experimental scheme. Animals have been pIpC injected and BrdU fed for 10 days, followed by 16 days of chase. B) Representative plots showing the gate strategy for the analysis of BrdU retaining LT-HSC after 16 days of chase. C) Histograms represent the percentage (right panels) and number (left panels) of BrdU retaining LT-HSC in NPMc+, FLT3-ITD, NPMc+/FLT3-ITD and control Mx-CRE mice. (N=6, $p<0.05$, data represent the pool of two independent experiments).

In summary, our data further support the ability of NPMc+ expression in the FLT3-ITD background to restore the self-renewal potential of the hyper-proliferative FLT3-ITD HSCs, by limiting proliferation and enforcing quiescence.

4.6 NPMc+ promotes a stem-related transcriptional program in FLT3-ITD HSCs

At this point, we were intrigued to establish the transcriptional profile of FLT3-ITD HSCs and the impact of the concomitant NPMc+ expression. To this aim, we analyzed the transcriptome of FLT3-ITD and NPMc+/FLT3-ITD HSCs, three weeks after pIpC treatment, using high-throughput RNA sequencing (RNA-seq). Briefly, we FACS-sorted LT-HSCs from two independent cohorts of Mx, FLT3-ITD and NPMc+/FLT3-ITD mice and we generated two independent RNA-seq libraries. High quality data, as assessed from standard quality control analyses, were produced for all samples and the R package edgeR22 was used to test differential expression at gene level.

In the FLT3-ITD HSCs we found 500 deregulated genes (190 up regulated [FC≥ 1.5, FDR≤ 0.1] and 310 down regulated [FC≤ -1.5, FDR≤ 0.1]), while in NPMc+/FLT3-ITD HSCs we found 472 deregulated gene, 170 of which were up-regulated and 302 were down-regulated. Since we are mainly interested in the impact of NPMc+ expression on the FLT3-ITD background, we also evaluated the genes regulated in the NPMc+/FLT3-ITD HSCs compared to FLT3-ITD HSCs, and we found 183 deregulated genes, including 60 up-regulations and 123 down-regulations.

We next used these three data sets to run some GSEA (Subramanian et al. 2005). In particular, we started to investigate the same data set we have found significantly regulated in HSCs expressing NPMc+ (see section 4.3, Fig20).

These analyses showed that FLT3-ITD expression dramatically reduces the expression of the quiescence gene set (Fig31A) while it promotes the expression of proliferating genes (Fig31D). A similar trend was still evident, although attenuated, when we analyzed the genes regulated in NPMc+/FLT3-ITD HSCs compared to controls (Fig31B-E).

Strikingly, when we analyzed the genes that are regulated in the NPMc+/FLT3-ITD HSCs compared to the FLT3-ITD HSCs, we appreciated a complete reversion of the regulation both in terms of quiescence and proliferation (Fig31C-F). These data mirrored the results shown in Fig26, where we evidenced a significant increase in the percentage of LT-HSC in NPMc+/FLT3-ITD samples compared to FLT3-ITD, however we did not see a complete rescue compared to controls.

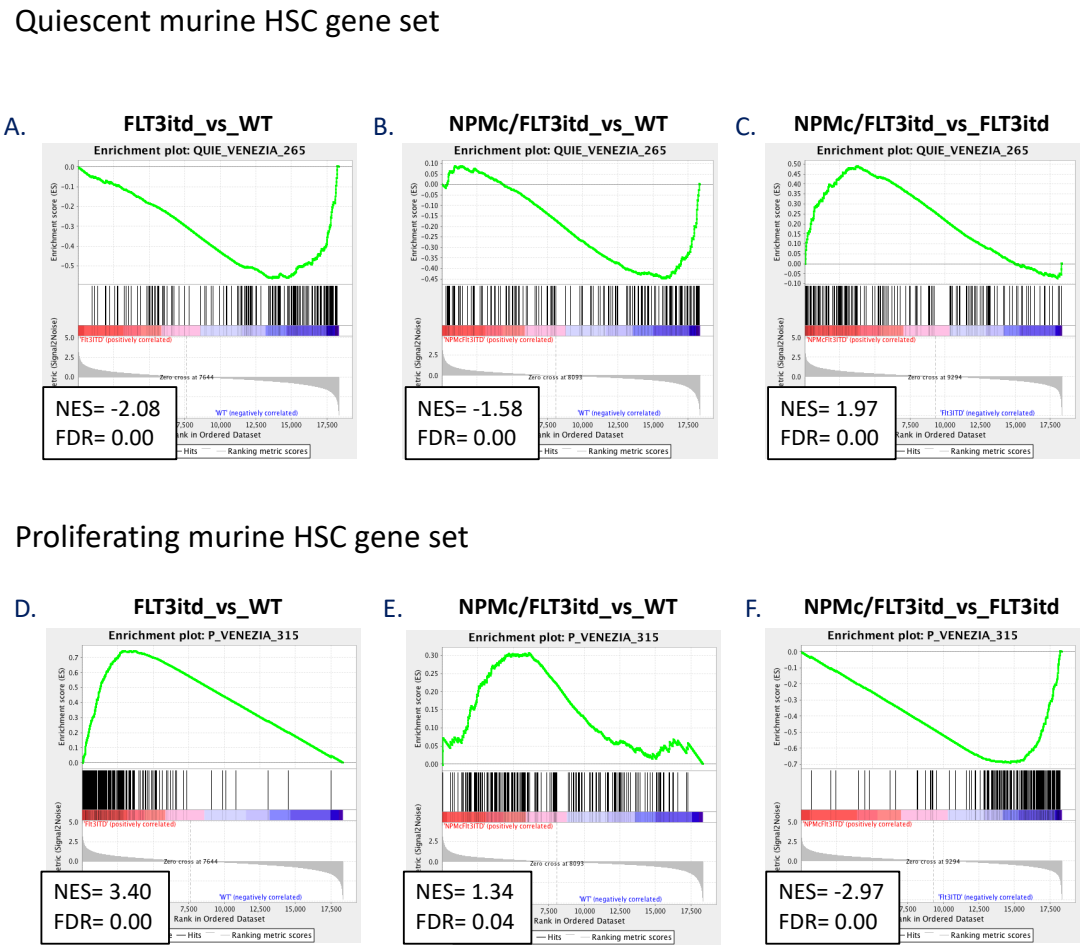

Figure 31 NPMc+ promotes a significant reversion of FLT3-ITD HSC transcriptional regulation both in terms of quiescence and proliferation.
RNAseq data were used to identify enriched gene sets in FLT3-ITD and NPMc+/FLT3-ITD LT-HSCs compared to MxCRE LT-HSCs (A-B; D-E) or NPMc+/FLT3-ITD LT-HSCs compared to FLT3-ITD LT-HSCs (C-F). GSEA enrichment plots correlating FLT3-ITD and NPMc+/FLT3-ITD LT-HSCs gene expression profile with genes known to be upregulated in quiescent (upper panels) or in proliferating (lower panels) murine HSCs.
Normalized enrichment score (NES) and false discovery rate (FDR) are indicated.

A similar trend was also evident when we analyzed the hematopoietic stem cell gene set (Fig32, upper panels) and the leukemia stem cell program gene set (Fig32, lower panels) that we previously reported as being regulated by NPMc+ in HSCs (see section 4.3, Fig17).

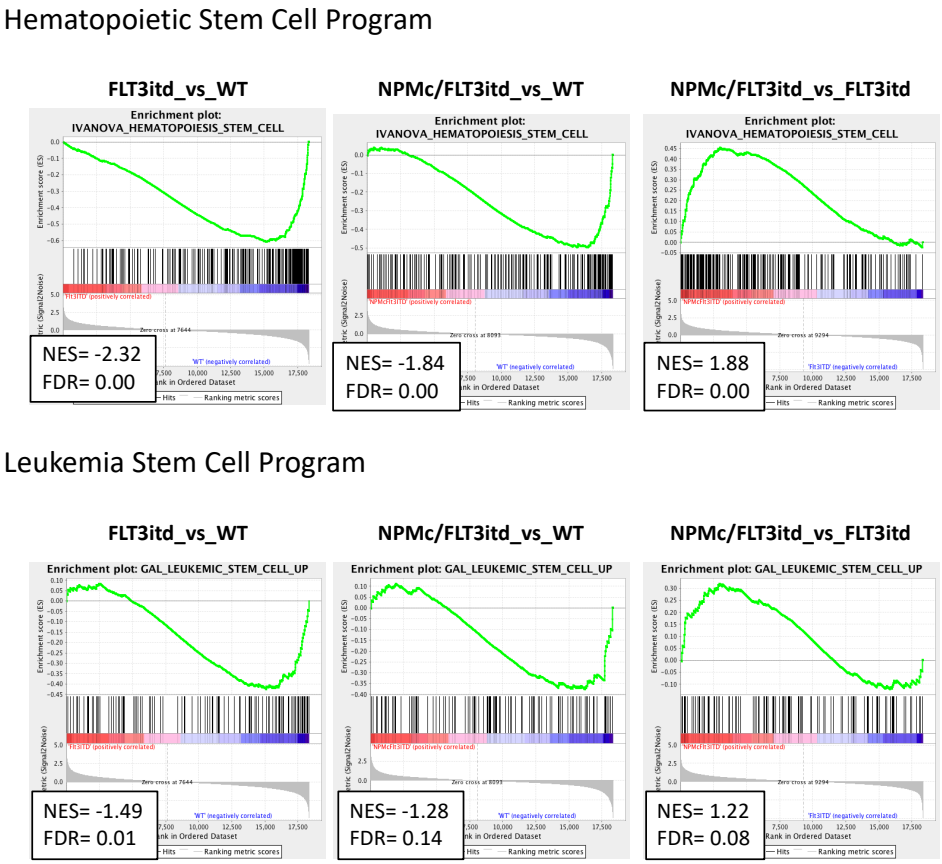

Figure 32 NPMc+ promotes the expression of human HSCs and LSCs genes otherwise prevented by FLT3-ITD.
RNAseq data were used to identify enriched gene sets in FLT3-ITD and NPMc+/FLT3-ITD LT-HSCs compared to MxCRE LT-HSCs (left and middle panels) or NPMc+/FLT3-ITD LT-HSCs compared to FLT3-ITD LT-HSCs (right panel). GSEA enrichment plots correlate FLT3-ITD and NPMc+/FLT3-ITD LT-HSCs gene expression profile with genes up-regulated in human HSCs (upper panel) and genes up-regulated in leukemic stem cells (LSCs) (lower panel). Normalized enrichment score (NES) and false discovery rate (FDR) are indicated.

In addition, we evaluated the level of the expression of *Hox* genes that are positively regulated by NPMc+ both in pre-leukemic (Fig19) and leukemic cells (Alcalay 2005). As shown in Fig33, FLT3-ITD expression led to a general downregulation of *Hoxa* gene family in LT-HSCs, while the NPMc+/FLT3-ITD samples showed, once again, a general reversion of the FLT3-ITD phenotype. Interestingly, in some cases, as for *Hoxa7* and *Hoxa9*, we could appreciate a significantly higher level of expression also compared to the control sample, suggesting that NPMc+ and FLT3-ITD may cooperate in the upregulation of some genes.

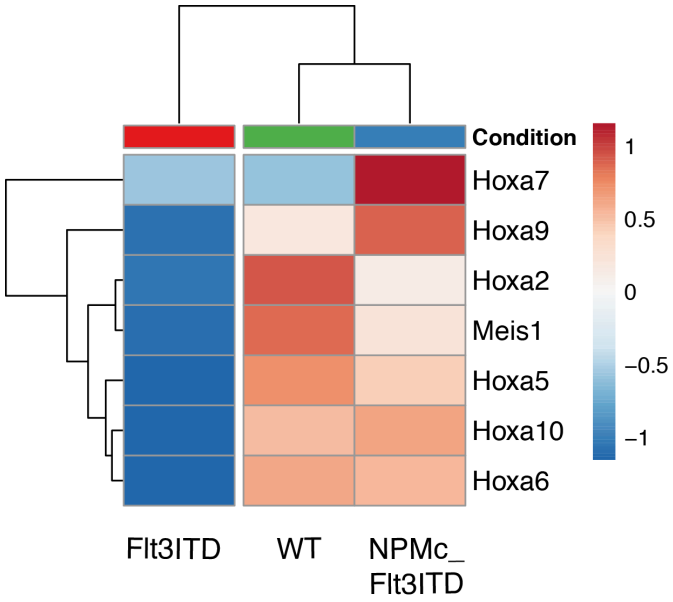

Figure 33 NPMc+ expression in FLT3-ITD LT-HSCs induces the expression of *Hoxa* cluster genes and *Meis1* gene.
The heatmap shows the Z scores of averaged RNA-seq normalized expression values across replicates for selected marker genes. Both rows and columns are clustered using Euclidean distance and average linkage. Decreased gene expression is indicated by shades of blue, increased gene expression is indicated by shades of red. (2 independent experiments).

To gain further insights into the putative NPMc+ and FLT3-ITD synergic transcriptional effect, we focused on the genes that significantly contributed to the GSEA enrichment score in the quiescence signature, the so-called leading-edge genes (LE-genes).

In particular, we compared the LE-genes that contributed to the negative enrichment in FLT3-ITD HSC (86 genes) with the LE-genes that contributed to the positive enrichment in NPMc+/FLT3-ITD HSC when compared to FLT3-ITD (73 genes). As depicted in Fig34A, these two lists overlapped in 53 genes and we could appreciate three behaviors (Fig34B): *i)* genes upregulated in NPMc+/FLT3-ITD compared to FLT3-ITD, yet less expressed compared to controls (n=17), *ii)* genes with a similar expression in NPMc+/FLT3-ITD samples and controls (n=27) and *iii)* genes upregulated in

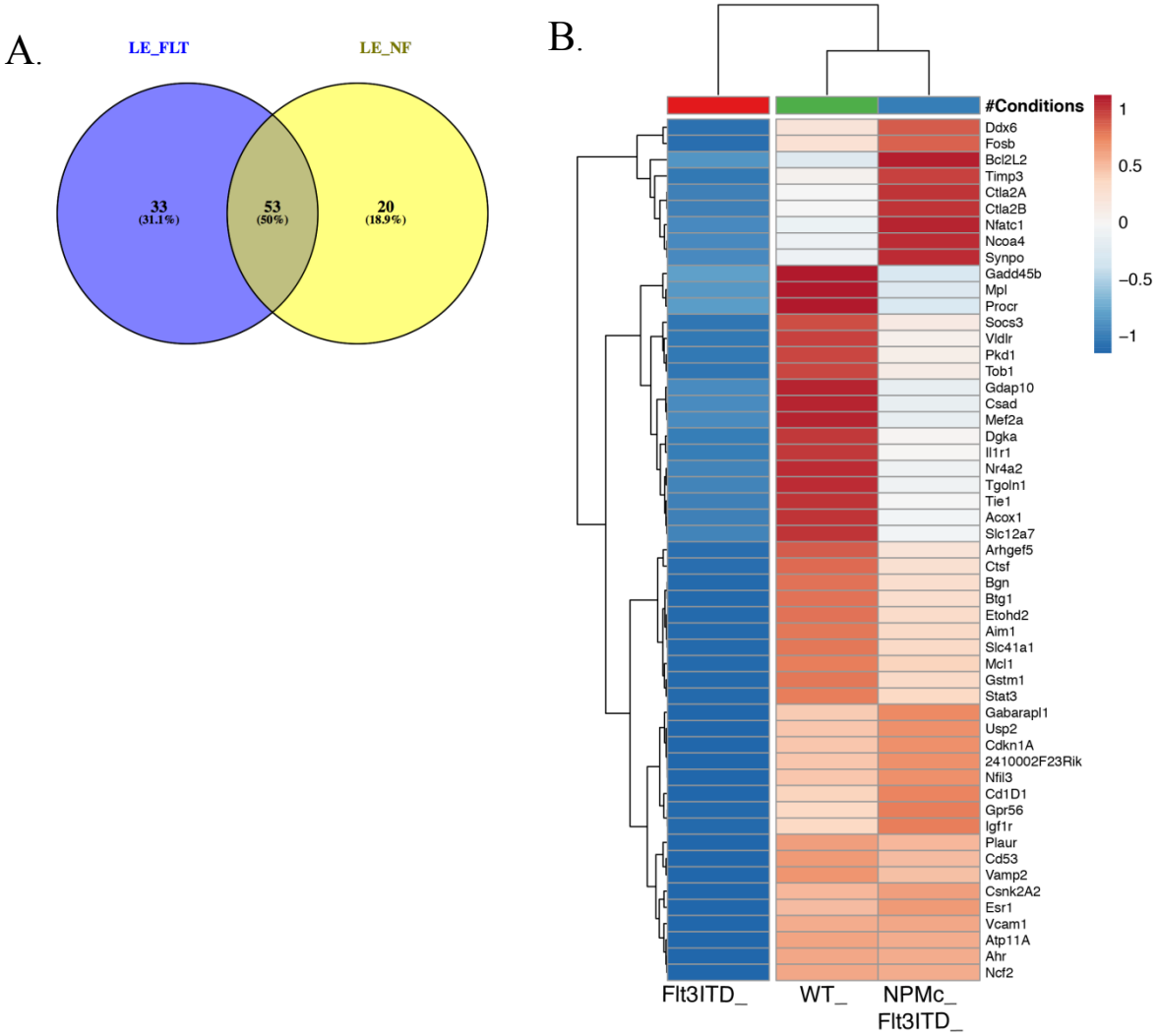

Figure 34 NPMc+ transcriptional effect onto quiescence genes downregulated in FLT3-ITD LT-HSCs.
A) Overlap between the LE quiescence genes downregulated in FLT3-ITD_vs_WT (purple circle) and the LE quiescence genes upregulated in NPMc+/FLT-ITD_vs_FLT3-ITD (yellow circle). B) The heatmap shows the Z scores of averaged RNA-seq normalized expression values across replicates for the 53 overlapping genes in panel A. Both rows and columns are clustered using Euclidean distance and average linkage. Decreased gene expression is indicated by shades of blue, increased gene expression is indicated by shades of red. (2 independent experiments).

NPMc+/FLT3-ITD both compared to FLT3-ITD and controls (n=9), suggesting again a possible cooperative effort between NPMc+ and FLT3-ITD.

Intriguingly, among the latter genes (synergic regulation by NPMc+ and FLT3-ITD) we noticed the nuclear factor of activated T cells c1 (*Nfatc1*) gene. Nfatc1 has been found highly expressed in niche Hair Follicle Stem Cells and required to maintain their quiescence (Horsley et al. 2008). Moreover, NFATC1 has been found frequently overexpressed in human FLT3-ITD AML and its inhibition sensitizes FLT3-ITD primary AML blasts to the treatment with FLT3-ITD inhibitors, suggesting that the impaired quiescence might be the mechanism that sensitizes the AML to the treatment (Metzelder et al. 2015).

In conclusion, we described that NPMc+ expression in the FLT3-ITD HSCs reverts the transcriptional regulation of three categories of genes crucial for HSCs fitness maintenance: quiescence, self-renewal and proliferation. Moreover, we uncovered the existence of a proportion of quiescence genes strongly up-regulated by NPMC+ in the presence of FLT3-ITD, which might be mediators with a critical role in the maintenance of the pre-leukemic HSCs reservoir, in the further selection of the LIC, and possibly in leukemia growth.

4.6.1 Pharmacological inhibition of TGFβ pathway impacts NPMc+/Flt3-ITD AML growth *in vivo.*

Previous transcriptional data reinforced our hypothesis that quiescence might sustain tumor development and growth and therefore it could represent a pharmacological target. In this view, we further investigated quiescence pathways bolstered by NPMc+ and conserved in the FLT3-ITD background. Our Affymetrix expression data revealed the

upregulation in NPMc+ LT-HSCs of a TGFβ pathway gene signature derived from murine HSCs stimulated with TGFβ (Fig35) (Billing et al. 2016).

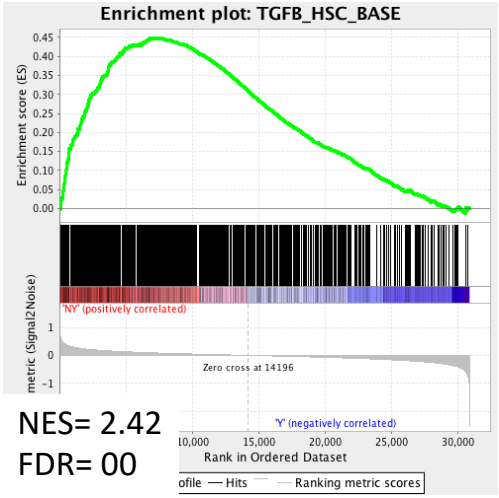

Figure 35 NPMc+ promotes in LT-HSCs the expression of genes associated with the control of the TGFβ pathway.
GSEA plot correlates NPMc+ LT-HSCs gene expression profile with a TGFβ pathway gene set derived from murine HSCs stimulated with TGFβ. Normalized enrichment score (NES) and false discovery rate (FDR) are indicated.

We next evaluated the level of expression of the TGFβ regulated HSC gene set in the NPMc+/FLT3-ITD and FLT3-ITD HSCs transcriptional profiles. The GSEA showed that FLT3-ITD expression strongly reduced the expression of the TGFβ pathway gene set (Fig36A), while a positive enrichment was evident, although not significant, when we analyzed the genes regulated in NPMc+/FLT3-ITD HSCs compared to controls (Fig36B). Interestingly, we appreciated a complete reversion of the TGFβ pathway regulation when we analyzed genes that are regulated in the NPMc+/FLT3-ITD HSCs compared to the FLT3-ITD ones (Fig36C).

TGFb_pathway_murine_HSC

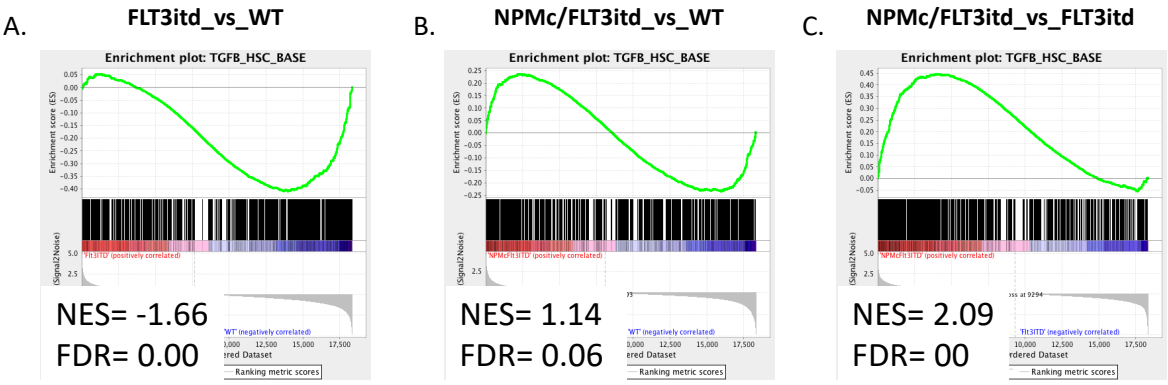

Figure 36 The NPMc+ expression reverts the FLT3-ITD dependent transcriptional regulation of the TGFβ pathway in HSCs.
RNAseq data were used to identify enriched gene sets in FLT3-ITD and NPMc+/FLT3-ITD LT-HSCs compared to Mx LT-HSCs (A-B) or NPMc+/FLT3-ITD LT-HSCs compared to FLT3-ITD LT-HSCs. (C) GSEA enrichment plots correlate FLT3-ITD and NPMc+/FLT3-ITD LT-HSCs gene expression profile with genes activated in murine HSCs upon TGFβ stimulation. Normalized enrichment score (NES) and false discovery rate (FDR) are indicated.

Several studies support TGFβ as master regulators of quiescence in the HSC system (Blank and Karlsson 2015). TGFβ is mainly secreted by megakaryocytes, which are physically associated with HSCs, and it has been involved both in maintaining HSCs quiescence during homeostasis and promoting HSCs regeneration after chemotherapeutic stress (Zhao et al. 2014; Brenet et al. 2013). Notably, the TGFβ pathway has been shown to be necessary for the maintenance of tumor initiating cells in Chronic Myeloid Leukemia (CML) and in squamous carcinoma (Naka et al. 2010; J. A. Brown et al. 2017). Moreover, based on TCGA data set, AML patients overexpressing TGFβ1, or TGFβ receptor II (Wu et al. 2017), exhibit a poorer overall survival (Fig37).

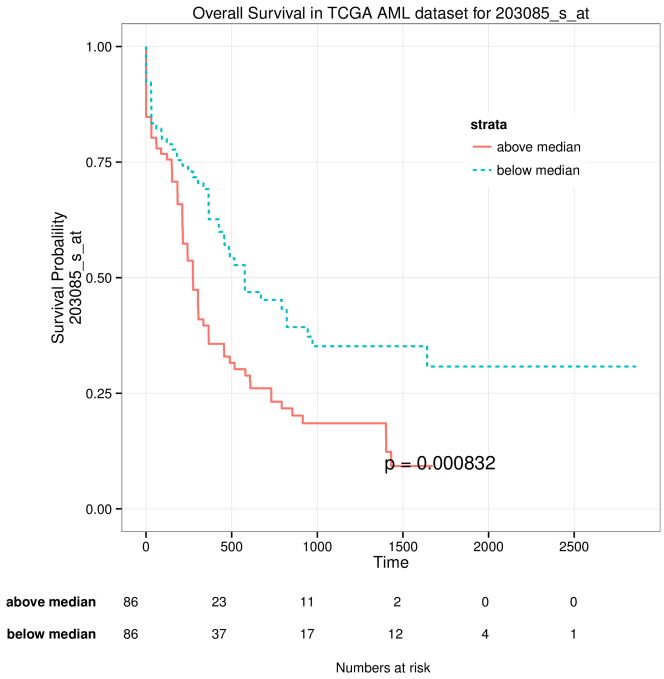

Figure 37 High level of TGFβ expression in AML correlates with poorer overall survival
Survival plot based on TCGA dataset that displays the Kaplan-Meier analysis based on gene expression above or below median for TGFb1 query. (source: BloodSpot (Bagger et al. 2016))

This evidence prompted us to investigate the possibility that interfering the TGFβ pathway in murine NPMc+/FLT3-ITD AML might limit leukemia growth in mice, either alone or in combination with the standard chemotherapy protocol.

To this purpose, as depicted in Fig38A, we injected the NPMc+/FLT3-ITD AML blasts in recipient mice, followed by 10 days of TGFβ inhibitor (LY364947) treatment either alone or in combination with the chemotherapy (3 days Doxorubicin and Ara-C + 2 days Ara-C) (Zuber et al. 2009). In the two groups of mice receiving the TGFb inhibitor, the treatment has been interrupted at day 25 due to the development of toxicity in mice that had received chemotherapy. As depicted in Fig38B, in the group of mice treated with TGFβ inhibitor alone the median survival was significantly prolonged compared to untreated ones (35 days vs 52 days). In the group of mice receiving both chemotherapy and TGFβ inhibitor, even the animals that eventually died showed a clear trend towards an extended survival, although not statistically significant, compared to the ones treated with

the chemotherapy only. Overall, this preliminary result supports our hypothesis of a functional role of TGFβ pathway in the NPMc+/FLT3-ITD AML growth *in vivo* and provides the rationale for further investigation.

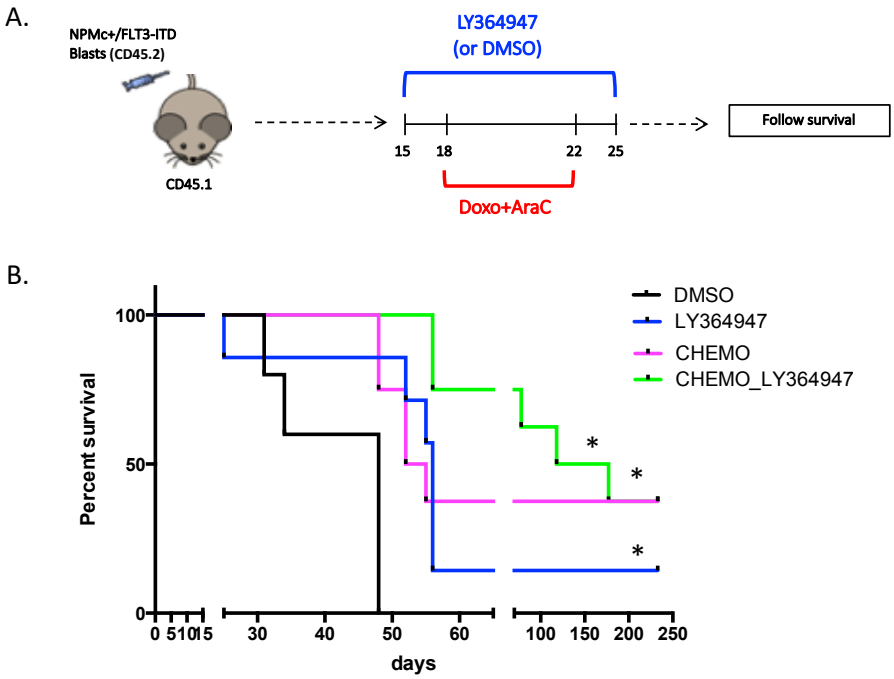

Figure 38 TGFβ inhibition prolongs survival in AML transplanted animal.
A) Experimental Design: AML transplanted mice have been treated with TGFβ inhibitor LY364947 (or vehicle) for 10days, with or without Doxorubicin and Ara-C for 5 days. B) Kaplan Meier survival curve of mice treated with LY364947(n=6), Chemotherapy (n=8), Chemotherapy and LY364947 (n=8) or vehicle (n=5). Log Rank test (compared to control group) ≤0.02.

Since we hypothesized that TGFβ pathway may play a role in LSCs maintenance, we set up an assay to directly address this point. LSCs are a very rare population of blasts capable to perpetuate the growth of AML thanks to their infinite self-renewal ability, and the only ones able to re-form the tumor upon transplantation (Lapidot et al. 1994; Bonnet and Dick 1997). To understand if TGFβ is a critical factor, as depicted in Fig39A, we treated the animals transplanted with the murine NPMc+/FLT3-ITD AML for 16 days with the TGFβ inhibitor (or DMSO as control). Then, we have sacrificed the mice and we have re-transplanted 500,000 blasts derived either from TGFβ treated or control mice in new

recipients and we have evaluated both their survival and, weekly, the percentage of blasts in the PB. Interestingly, in mice transplanted with the TGFβ inhibitor treated blasts, we saw a progressive decrease in the number of blasts in the PB that led to the long-term survival of 4 out of 5 mice (Fig39B-C). In the control cohort, only 1 out of 5 animals showed the same behavior, while the other 4 died due to AML outgrowth.

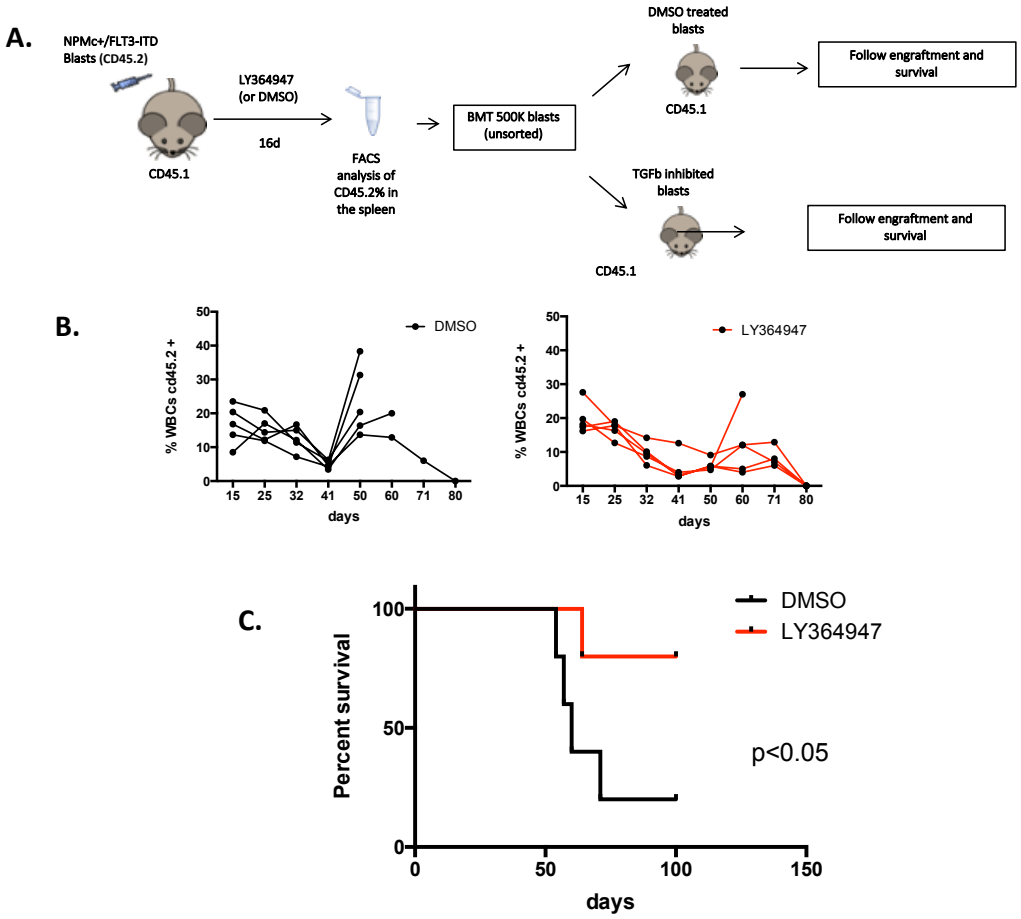

Figure 39 TGFβ inhibition impairs the engraftment capability of NPMc+/FLT3-ITD blasts, preventing the disease onset in secondary recipients.
A) Experimental design: mice have been sacrificed at the end of the treatment with the TGFβ inhibitor and 500,000 blasts have been transplanted in secondary sub-lethally irradiated recipient mice. B) Graphs represent the percentage of control (left panel) or TGFβ inhibited (right panel) blasts (CD45.2+) in the PB of secondary transplanted mice. C) Kaplan Meier survival curve of mice transplanted with LY364947 blasts (n=5) or control blasts (n=5). Log Rank ≤0.05.

Since the transplantation procedure challenges the LSCs to exit their quiescent state and reform the tumor in recipient mice, our finding suggests that treating the tumor with

the TGFβ inhibitor may have modified the functionality and/or the number of LSCs, possibly by impairing the balance between quiescence and proliferation.

In summary, these data, although preliminary, support a putative role of the TGFβ pathway in maintaining the growth potential of NPMc+/FLT3-ITD AMLs. Additional studies are needed to exploit these findings in future therapeutic applications, as discussed in the paragraph 5.3 of the Discussion section.

5 Discussion

Recent studies disclosed some critical aspects about the process of clonal evolution in AML. In particular, mutated pre-leukemic HSCs (preL-HSCs) harboring some, but not all, AML mutations have been isolated from human AMLs, with critical clinical implications. The proportion of preL-HSCs in the residual HSC compartment, at the time of diagnosis, is associated with poor clinical outcome (Corces et al. 2016). Indeed, given their quiescence state, preL-HSCs tend to resist to chemotherapy, are present during remission and might contribute to relapse. However, the oncogenic mechanism behind preL-HSCs progression into LICs still needs to be elucidated, in order to prevent tumor and/or relapse formation.

Collectively, here we provided an extensive study investigating the impact of NPMc+ expression on normal HSCs, in order to define the early mechanisms of NPMc+ induced leukemogenesis and to identify oncogenic pathways that may cooperate with other co-recurrent mutations in patients, such as FLT3-ITD.

5.1 NPMc+ enhances both the self-renewing and the quiescent potential of preL-HSCs

We have shown that NPMc+ expression impacts the hematopoietic homeostasis increasing the rate of HSC self-renewal division and leading to a significant expansion of the HSC pool. As a consequence, NPMc+ BM cells show higher reconstitution potential under limiting number BMT condition. This phenotype is likely related to the NPMc+ ability to enforce the expression of the *Hoxa* gene cluster. Indeed, *Hox* genes have been found preferentially expressed in immature hematopoietic cell population and a number of studies reported their role in the control of the HSCs division outcome (self-renewal vs differentiation). However, their precise mechanism of action remains unclear

(Argiropoulos and Humphries 2007). Consistently, the overexpression of several *Hox* genes (e.g. *Hoxb4*) has been linked to HSC pool expansion, likely reflecting their ability to promote symmetrical self-renewing divisions (Antonchuk, Sauvageau, and Humphries 2002; Thorsteinsdottir, Sauvageau, and Humphries 1999). Similarly, the expanded number of HSCs in mice transplanted with NPMc+ expressing BM-MNCs (Fig15C) strongly suggest that NPMc+ enforces symmetrical self-renewing divisions in these cells. However, a direct experimental evidence has not been provided yet. In parallel with the higher self-renewing symmetric division rate, we have shown that NPMc+ LT-HSCs display a higher proportion of cells in the S-G2-M cell-cycle phase compared to control, indicating an overall increased proliferation of the compartment, and confirming previous BrdU *in vivo* experiments (not shown).

On the other hand, we have shown that NPMc+ LT-HSCs have the same proportion of quiescent (Ki67-) cells compared to controls, yet expanded in number. Accordingly, we revealed a NPMc+ dependent transcriptional program that supports this phenotype. Quiescence is an intrinsic property of normal HSCs and is required to balance their self-renewal/differentiation potential allowing the preservation of a lifelong functional HSC reservoir. Hence, the NPMc+ enforced quiescence in LT-HSCs may be required to enable a higher self-renewing symmetric division rate. It is known that functional quiescent HSCs have the capacity to rapidly enter the cell cycle in response to physiological stimuli and then they rapidly return to quiescence, therefore preventing the exhaustion of their self-renewal potential (Wilson et al. 2008; Pietras et al. 2014). Interestingly, we have shown that NPMc+ quiescent HSCs are able to sustain the prolonged survival of 5-FU treated animals, suggesting that this feature is maintained and possibly enhanced in NPMc+ expressing HSCs.

At first glance, the co-existence of higher proliferative rate with increased quiescence potential might represent a conundrum. However, several studies pointed out a high degree of heterogeneity among HSCs with the existence of “active” HSCs and

"dormant" HSCs (Wilson et al. 2008). Thus, the bimodal cell cycle regulation imposed by NPMc+ in HSCs may reflect the NPMc+ ability to act on different pools of HSCs, enhancing the individual features of each subpopulation, such as self-renewal and quiescence. Our forthcoming analysis at single cell level, will help us in deciphering this aspect.

5.2 NPMc+ induced quiescence as a leukemogenic mechanism

The preleukemic NPMc+ phenotype closely resembles the one reported by Li and colleagues for mutated *NRAS* (*NRAS*^{G12D}). Indeed, this AML-related oncogene enforces quiescence in a specific subset of HSCs, while it increases proliferation in another subset, leading to increased self-renewal (Li et al. 2013). In their proposed model, short lived but rapidly dividing *Nras*^{G12D} HSCs outcompete WT HSCs, and are replenished over time by quiescent *Nras*^{G12D} HSCs slowly recruited into the cycle. These data suggest the possibility that different AML associated mutations may have evolved the ability to preserve HSC/LSC self-renewal, promoting a quiescence program. Accordingly, our group has shown that the expression of the AML specific PML/RAR fusion protein leads to p21 overexpression, which in turn induces a reversible HSC cell cycle arrest, indispensable to prevent DNA-damage accumulation and LSC functional exhaustion (Viale et al. 2009). Moreover, we observed that PML/RAR, as well as AML1/ETO and MLL-AF9 oncogenes, are able to enforce, in the pre-leukemic HSCs, the same HSC quiescent gene signature upregulated by NPMc+ (unpublished).

To further address the significance of this phenotype in the initiation of leukemogenesis, we have investigated it in the context of mutated *FLT3* (FLT3-ITD). These two mutations are frequently associated in AML and their co-occurrence in animal models contributes to a rapid disease development, supporting a strong cooperation of the two mutations in selecting the LIC (Papaemmanuil et al. 2016; Mupo et al. 2013; Mallardo

et al. 2013). A previous study has shown that FLT3-ITD significantly increases the proliferative rate of HSCs, resulting in the progressive depletion of the HSC compartment. As a consequence, FLT3-ITD KI animals do not develop AML, but a myeloproliferative disease (Chu et al. 2012). We have shown that FLT3-ITD significantly decreases the number of both total and quiescent HSCs resulting in a defective hematopoietic reconstitution ability of the FLT3-ITD BM. Coherently, FLT3-ITD downregulates the quiescent HSC gene signature, while promotes the proliferating HSC one. Strikingly, co-expression of FLT3-ITD and NPMc+ prevents the HSCs exhaustion imposed by FLT3-ITD and favors the expansion of the entire HPSC compartment, re-establishing the normal BM reconstitution ability and limiting the FLT3-ITD imposed hyperproliferation. Accordingly, the expression of NPMc+, in presence of FLT3-ITD, restores the wild type-like expression of both quiescence and cell cycle HSC genes. We further evidenced a number of genes upregulated in NPMc+/FLT3-ITD HSCs, both compared to FLT3-ITD and controls, that might represent a signature enforced by the synergy of the two oncogenes, as previously reported for other cooperating mutations (Liubin Yang et al. 2016; Shih et al. 2015). Noteworthy, among these genes we detected *Hoxa9*, known to be highly expressed in the most aggressive AMLs (Collins and Hess 2016). It has been recently reported that HOXA9-induced leukemic transformation of normal BM-MNCs involves the alteration of the enhancer landscape, with the formation of *de novo* enhancers that activate an ectopic embryonic gene program (Sun et al. 2018, 9). Further investigations are needed in order to dissect the impact of NPMc+ expression on the enhancer landscape of HSC cells, either alone or in cooperation with FLT3-ITD, in order to gain information about the NPMc+/FLT3-ITD cooperation at genomic level.

Based on these considerations, we propose a model where NPMc+ and FLT3-ITD mutations cooperate in inducing AML, thanks to the NPMc+ ability to limit LT-HSC exhaustion and reconstitute a fully competent LT-HSC population in which the oncogenic activities of FLT3-ITD are exerted (possibly enhanced by a suitable epigenetic

environment favored by NPMc+) leading to a rapid selection of the leukemia initiating cells.

It is generally accepted that LIC selection is the result of the cooperation between type-1 mutations, which provide a proliferative advantage, and type-2 mutations, which impact on normal hematopoietic differentiation process. However, the molecular mechanisms underlying this complex process are poorly understood. Our data indicate that NPMc+, similarly to $NRAS^{G12D}$, has evolved a distinguishing function that may represent a critical clock in the preL-HSCs (a sort of bridge between a typical type I (e.g. *FLT3-ITD*) and type II (e.g. *DNMT3a*) mutations). Such acquired function envisions a higher level of heterogeneity at molecular level in the oncogenic mechanisms triggered by different AML associated mutations. As consequence, how different mutations synergize and cooperate with each other in the course of AML development may differ, also in relation to their order of appearance in the preL-HSC.

DNMT3A is mutated (*DNMT3A_mut*) in over half of the NPMc+ AMLs (Papaemmanuil et al. 2016), counting as the most frequent co-occurrent mutation in NPMc+ AMLs. Conditional deletion of the *Dnmt3a* gene in mouse models leads to the expansion of the HSC pool, which is, however, not due to increased proliferation. On the contrary, *Dnmt3a*-null HSCs proliferate rather less than control and the expansion is mainly due to impaired differentiation (Challen et al. 2012). If *DNMT3A* ablation, or the expression of DNMT3a_mut, affects HSC quiescence, remains to be addressed.

Mutations in the *DNMT3A* locus are largely the most frequent in the preL-HSCs isolated from AML patients, both at diagnosis and at relapse, when all the other AML specific mutations are lost (Shlush et al. 2014; Corces-Zimmerman et al. 2014). Accordingly, *DNMT3A_mut* shows the highest persistence between AMLs at diagnosis and at relapse (97%) (Shlush et al. 2014; Krönke et al. 2013). These findings support a model where *DNMT3A_mut* arises very early in AML evolution and creates an expanded pre-

leukemic HSC pool from which AML evolves. Consistently, NGS analysis of thousands of individuals with no history of hematologic disease revealed an extremely high incidence of *DNMT3A* mutation driving the clonal outgrowth of hematopoietic cells, known as clonal hematopoiesis (CH) (Jaiswal et al. 2014; Genovese et al. 2014). CH is age-related and associated with an increased risk of hematologic cancer. Nonetheless, a large portion of CH patients do not experience overt leukemia, indicating that *DNMT3A_mut* can persist for years in a subclinical state. It is interesting to note that *DNMT3A* mutations are found only in adult AML and they are absent in pediatric AML (Bolouri et al. 2017), further confirming that this mutation accumulates over the years in old BM where it creates a suitable epigenetic status that favors accumulation of other mutations, supporting and enhancing their oncogenic potential. *NPM1* mutations are still present in pediatric AMLs, still at much lower frequency, thus suggesting that *DNMT3A* mutations (or others preL-HSC associated mutations) strongly support NPMc+ occurrence even though they are not absolutely required.

A recent study on pre-clinical models of AML has contributed to gain insight into the role of *DNMT3A*, *NPM1* and *FLT3* mutations in AML onset. Guryanova and colleagues reported that *Npmc+/Dnmt3a_mut* mice do not develop leukemia up to 45 weeks of observation, while both *Dnmt3a_mut/Flt3-ITD* and *Npmc+/Flt3-ITD* do, with the latter showing a higher penetrance and shorter latency. Moreover, the co-occurrence of all three mutations significantly accelerates the disease onset (Guryanova et al. 2016). Hence, NPMc+ and DNMT3A_mut seem to perturb similar pathways on which they act in an additive way, in cooperation with FLT3-ITD. In support, we have found a significant overlap among genes regulated by NPMc+ in the LT-HSC compartment and genes regulated by DNMT3A_mut (Lu et al. 2016) (data not shown). Nonetheless, both of them need the cooperation of FLT3-ITD to develop leukemia, indicating the proliferative oncogenic stimulus as a crucial trigger for transformation.

Collectively, these evidences support our preleukemic HSCs expressing NPMc+, both alone and in combination with FLT3-ITD, as a suitable model to highlight critical mechanisms for LIC evolution. In particular, the novel finding regarding the quiescent phenotype, if maintained by NPMc+ LSC, could be critical for therapy resistance, and the selective targeting of this feature could improve definitive AML eradication.

5.3 NPMc+-induced quiescence as therapeutic target

The origin and function of LICs is closely linked to their enhanced self-renewal, which is a characteristic of the HOX proteins activity. Some oncogenes (e.g. MLL-AF9) re-program normal progenitors into LSCs by aberrant induction of *Hox* genes (Krivtsov et al. 2006), further indicating that it is a critical step in leukemic transformation. Both NPMc+ and MLL1-rearranged AMLs have been found to aberrantly upregulate *HOXA* and *HOXB* cluster genes and they play a critical role in the maintenance of the disease (Alcalay 2005; Armstrong et al. 2001). Indeed, *in vitro* Crisp-Cas9 mediated disruption of *Hoxa* genes or their co-factors (e.g. *Meis1*, *Pbx*, *Bcl2*, *Lmo2*) reveals that *Hox* genes, and *Hoxa10* in particular, are required for the survival of NPMc+ AML blasts (Dovey et al. 2017). Accordingly, it has been recently shown that the re-localization of NPMc+ into the nucleus, in an AML NPMc+ expressing cell line (by selective inhibition of the Exportin1 by Selinexor), leads to a massive downregulation of *HOXA* and *HOXB* genes with a consequent cell differentiation. Moreover Selinexor *in vivo* administration prolongs the survival of NPMc+/FLT3-ITD mice (Brunetti et al. 2018). From a therapeutic point of view, effective indirect HOX inhibitory strategies have been proposed. In particular, Kuhn and colleagues recently demonstrate that the pharmacologic inhibition of both MLL1 and DOTL1 histone modifiers reduces the HOX gene expression in NPMc+ blasts, thus inducing their differentiation *in vitro*. Moreover, MLL and DOLT1 inhibitors diminished the leukemia initiation potential of NPMc+ blasts, upon transplantation in recipient mice (Kuhn et al. 2016).

Considering that LSCs represent the aberrant counterpart of normal HSCs, it is conceivable to hypothesize that increased self-renewal can be sustained by a concomitant strengthening of the quiescence potential. Indeed, our data support the hypothesis that NPMc+ (and possibly other AML mutations) sustains the preL-HSCs transformation by enforcing, at the same extent, both self-renewal and quiescence. Therefore, we are proposing the NPMc+-induced quiescence as an additional level of LSC regulation that might be interfered with in order to prevent LSC development and maintenance. Several pathways have been reported to regulate quiescence both in LSCs and in HSCs. For some of them effective therapeutic strategies have been exploited. This is the case of a novel inhibitor of EZH1/2 (two catalytic sub-units of the Polycomb repressive complex 2 involved in HSCs maintenance and mutated in many cancer types) that has been shown to reduce the number of LSCs and impair leukemia progression in preclinical models (Fujita et al. 2018). Among the pathways that regulate HSCs quiescence, TGFβ signaling has been identified as one of the most critical (Zhao et al. 2014; Yamazaki et al. 2009), and its role in LIC maintenance has been demonstrated in a model of CML (Naka et al. 2010). Moreover, Brown and colleagues further demonstrated that the TGFβ pathway is upregulated in quiescent squamous carcinoma propagating cells, and that TGFβ signaling abrogation increases the susceptibility of these cells to chemotherapy, by preventing their entry into a quiescence state (J. A. Brown et al. 2017).

In our model, the TGFβ pathway is upregulated by NPMc+ either alone or in combination with FLT3-ITD. Therefore, we hypothesize that it might be a suitable target to interfere with NPMc+-dependent quiescence in HSCs. We have shown that in transplanted animals pharmacological inhibition of the TGFβ pathway significantly delayed NPMc+/FLT3-ITD AML onset. Moreover, we observed a clear trend towards a prolonged survival in animals receiving both chemotherapy and TGFβ inhibitor compared to those treated with the chemotherapy alone. These data are in line with previous results by Tabe and colleagues reporting that the TGFβ inhibition, both alone and in combination

with Ara-C, reduces leukemia burden in a preclinical model of FLT3-ITD AML (Tabe et al. 2013).

These findings indicate a functional role of TGFβ in maintaining the growth potential of NPMc+/FLT3-ITD AML, however, they do not provide clear insight about the mechanism of action. Moreover, the effect is rather modest and is far from inducing AML eradication, facing the possibility that this treatment schedule may not fully exploit the TGFβ inhibitor therapeutic potential.

Interestingly, in mice transplanted with TGFβ inhibited blasts we observed, after an initial engraftment, a progressive decrease in the number of circulating blasts, resulting in long-term survival. Since LSCs are the only cells able to re-form the tumor in secondary recipients, this result suggests that treating the tumor with the TGFβ inhibitor might have modified the fitness and/or the number of LSCs, perhaps by impairing the balance between quiescence and proliferation. To which extent this effect is cell autonomous or is linked to the complex interaction between the LSC and its proper niche has to be established. Indeed, it has been shown that *in vitro* TGFβ inhibitor treatment of AML blasts co-cultured with stromal cells reduces the homing of blasts once transplanted *in vivo* (Hamilton, Foster, and Bonnet 2104). This suggests the possibility that treated blasts, after being re-transplanted, fail to connect to their niche and, as consequence, after an initial burden, they are unable to enter quiescence and they progressively exhaust. Alternatively, the exhaustion might occur already in primary recipient animals during the treatment, even though the fact that a 2week-treatment is unable to eradicate disease progression (Fig38) would argue against this hypothesis. Nonetheless, it may be worth to investigate if an extended administration of the TGFβ inhibitor alone to the NPMc+/FLT3-ITD AML transplanted mice could result in a more effective LSC exhaustion and possibly AML eradication.

At this stage, the question is how to translate this information into a therapeutic approach that could be suitable for AML patients. In this regard, an interesting paper

recently showed that in AML patient-derived xenograft models, Ara-C treatment induces, during the remission phase, a transient state of LSC, defined as leukemic regenerating cells (LRCs) that can be targeted to block accelerated regrowth and relapse (Boyd et al. 2018). It is possible that treating the animals with the TGFβ inhibitor at the end of the chemotherapy cycle, when LRCs are established, will prevent the ability of LRCs to re-enter quiescence and induce their exhaustion. Moreover, we would like to investigate if this protocol allows the usage of a milder chemotherapy treatment followed by TGFβ inhibitor to induce AML eradication. If effective, this approach will allow the treatment of old patients that cannot support a strong remission induction therapy (Walter and Estey 2015). Last but not least, since anti-TGFβ drugs for solid tumors are already in phase III clinical trials, TGFβ inhibitor-based protocol could rapidly enter the clinic.

References

Adolfsson, J., O. J. Borge, D. Bryder, K. Theilgaard-Mönch, I. Astrand-Grundström, E. Sitnicka, Y. Sasaki, and S. E. Jacobsen. 2001. "Upregulation of Flt3 Expression within the Bone Marrow Lin(-)Sca1(+)c-Kit(+) Stem Cell Compartment Is Accompanied by Loss of Self-Renewal Capacity." *Immunity* 15 (4): 659–69.

Agathocleous, Michalis, Corbin E. Meacham, Rebecca J. Burgess, Elena Piskounova, Zhiyu Zhao, Genevieve M. Crane, Brianna L. Cowin, et al. 2017. "Ascorbate Regulates Haematopoietic Stem Cell Function and Leukaemogenesis." *Nature*, August. https://doi.org/10.1038/nature23876.

Alcalay, M. 2005. "Acute Myeloid Leukemia Bearing Cytoplasmic Nucleophosmin (NPMc+ AML) Shows a Distinct Gene Expression Profile Characterized by up-Regulation of Genes Involved in Stem-Cell Maintenance." *Blood* 106 (3): 899–902. https://doi.org/10.1182/blood-2005-02-0560.

Alibhai, Shabbir M. H., Marc Leach, Mark D. Minden, and Joseph Brandwein. 2009. "Outcomes and Quality of Care in Acute Myeloid Leukemia over 40 Years." *Cancer* 115 (13): 2903–11. https://doi.org/10.1002/cncr.24373.

Almeida, Antonio M., and Fernando Ramos. 2016. "Acute Myeloid Leukemia in the Older Adults." *Leukemia Research Reports* 6: 1–7. https://doi.org/10.1016/j.lrr.2016.06.001.

Anders, S., P. T. Pyl, and W. Huber. 2015. "HTSeq--a Python Framework to Work with High-Throughput Sequencing Data." *Bioinformatics* 31 (2): 166–69. https://doi.org/10.1093/bioinformatics/btu638.

Antonchuk, Jennifer, Guy Sauvageau, and R. Keith Humphries. 2002. "HOXB4-Induced Expansion of Adult Hematopoietic Stem Cells Ex Vivo." *Cell* 109 (1): 39–45.

Arai, Fumio, Atsushi Hirao, Masako Ohmura, Hidetaka Sato, Sahoko Matsuoka, Keiyo Takubo, Keisuke Ito, Gou Young Koh, and Toshio Suda. 2004. "Tie2/Angiopoietin-1 Signaling Regulates Hematopoietic Stem Cell Quiescence in the Bone Marrow Niche." *Cell* 118 (2): 149–61. https://doi.org/10.1016/j.cell.2004.07.004.

Araten, David J., David W. Golde, Rong H. Zhang, Howard T. Thaler, Lucia Gargiulo, Rosario Notaro, and Lucio Luzzatto. 2005. "A Quantitative Measurement of the Human Somatic Mutation Rate." *Cancer Research* 65 (18): 8111–17. https://doi.org/10.1158/0008-5472.CAN-04-1198.

Arber, D. A., A. Orazi, R. Hasserjian, J. Thiele, M. J. Borowitz, M. M. Le Beau, C. D. Bloomfield, M. Cazzola, and J. W. Vardiman. 2016. "The 2016 Revision to the World Health Organization Classification of Myeloid Neoplasms and Acute Leukemia." *Blood* 127 (20): 2391–2405. https://doi.org/10.1182/blood-2016-03-643544.

Arber, Daniel A., Karen L. Chang, Mark H. Lyda, Victoria Bedell, Ricardo Spielberger, and Marilyn L. Slovak. 2003. "Detection of NPM/MLF1 Fusion in t(3;5)-Positive Acute Myeloid Leukemia and Myelodysplasia." *Human Pathology* 34 (8): 809–13.

Argiropoulos, B, and R K Humphries. 2007. "Hox Genes in Hematopoiesis and Leukemogenesis." *Oncogene* 26 (47): 6766–76. https://doi.org/10.1038/sj.onc.1210760.

Armstrong, Scott A., Jane E. Staunton, Lewis B. Silverman, Rob Pieters, Monique L. den Boer, Mark D. Minden, Stephen E. Sallan, Eric S. Lander, Todd R. Golub, and Stanley J. Korsmeyer. 2001. "MLL Translocations Specify a Distinct Gene Expression

Profile That Distinguishes a Unique Leukemia." *Nature Genetics* 30 (1): 41–47. https://doi.org/10.1038/ng765.

Baum, C. M., I. L. Weissman, A. S. Tsukamoto, A. M. Buckle, and B. Peault. 1992. "Isolation of a Candidate Human Hematopoietic Stem-Cell Population." *Proceedings of the National Academy of Sciences* 89 (7): 2804–8. https://doi.org/10.1073/pnas.89.7.2804.

Becker, A. J., E. A. McCulloch, and J. E. Till. 1963. "Cytological Demonstration of the Clonal Nature of Spleen Colonies Derived from Transplanted Mouse Marrow Cells." *Nature* 197: 452–54.

Bennett, J. M., D. Catovsky, M. T. Daniel, G. Flandrin, D. A. Galton, H. R. Gralnick, and C. Sultan. 1976. "Proposals for the Classification of the Acute Leukaemias. French-American-British (FAB) Co-Operative Group." *British Journal of Haematology* 33 (4): 451–58.

Billing, Matilda, Emma Rörby, Gillian May, Alex J. Tipping, Shamit Soneji, John Brown, Marjo Salminen, Göran Karlsson, Tariq Enver, and Stefan Karlsson. 2016. "A Network Including TGFβ/Smad4, Gata2, and P57 Regulates Proliferation of Mouse Hematopoietic Progenitor Cells." *Experimental Hematology* 44 (5): 399-409.e5. https://doi.org/10.1016/j.exphem.2016.02.001.

Blank, U., and S. Karlsson. 2015. "TGF- Signaling in the Control of Hematopoietic Stem Cells." *Blood* 125 (23): 3542–50. https://doi.org/10.1182/blood-2014-12-618090.

Bolouri, Hamid, Jason E Farrar, Timothy Triche, Rhonda E Ries, Emilia L Lim, Todd A Alonzo, Yussanne Ma, et al. 2017. "The Molecular Landscape of Pediatric Acute Myeloid Leukemia Reveals Recurrent Structural Alterations and Age-Specific Mutational Interactions." *Nature Medicine* 24 (1): 103–12. https://doi.org/10.1038/nm.4439.

Bonetti, Paola, Teresa Davoli, Cristina Sironi, Bruno Amati, Pier Giuseppe Pelicci, and Emanuela Colombo. 2008. "Nucleophosmin and Its AML-Associated Mutant Regulate c-Myc Turnover through Fbw7γ." *The Journal of Cell Biology* 182 (1): 19–26. https://doi.org/10.1083/jcb.200711040.

Bonnet, D., and J. E. Dick. 1997. "Human Acute Myeloid Leukemia Is Organized as a Hierarchy That Originates from a Primitive Hematopoietic Cell." *Nature Medicine* 3 (7): 730–37.

Boyd, Allison L., Lili Aslostovar, Jennifer Reid, Wendy Ye, Borko Tanasijevic, Deanna P. Porras, Zoya Shapovalova, et al. 2018. "Identification of Chemotherapy-Induced Leukemic-Regenerating Cells Reveals a Transient Vulnerability of Human AML Recurrence." *Cancer Cell* 34 (3): 483-498.e5. https://doi.org/10.1016/j.ccell.2018.08.007.

Brenet, Fabienne, Pouneh Kermani, Roman Spektor, Shahin Rafii, and Joseph M. Scandura. 2013. "TGFβ Restores Hematopoietic Homeostasis after Myelosuppressive Chemotherapy." *The Journal of Experimental Medicine* 210 (3): 623–39. https://doi.org/10.1084/jem.20121610.

Brown, Jessie A., Yoshiya Yonekubo, Nicole Hanson, Ana Sastre-Perona, Alice Basin, Julie A. Rytlewski, Igor Dolgalev, et al. 2017. "TGF-β-Induced Quiescence Mediates Chemoresistance of Tumor-Propagating Cells in Squamous Cell Carcinoma." *Cell Stem Cell* 21 (5): 650-664.e8. https://doi.org/10.1016/j.stem.2017.10.001.

Brown, P., E. McIntyre, R. Rau, S. Meshinchi, N. Lacayo, G. Dahl, T. A. Alonzo, M. Chang, R. J. Arceci, and D. Small. 2007. "The Incidence and Clinical Significance of Nucleophosmin Mutations in Childhood AML." *Blood* 110 (3): 979–85. https://doi.org/10.1182/blood-2007-02-076604.

Brunetti, Lorenzo, Michael C. Gundry, Daniele Sorcini, Anna G. Guzman, Yung-Hsin Huang, Raghav Ramabadran, Ilaria Gionfriddo, et al. 2018. "Mutant NPM1 Maintains the Leukemic State through HOX Expression." *Cancer Cell* 34 (3): 499-512.e9. https://doi.org/10.1016/j.ccell.2018.08.005.

Cabezas-Wallscheid, Nina, Florian Buettner, Pia Sommerkamp, Daniel Klimmeck, Luisa Ladel, Frederic B. Thalheimer, Daniel Pastor-Flores, et al. 2017. "Vitamin A-Retinoic Acid Signaling Regulates Hematopoietic Stem Cell Dormancy." *Cell* 169 (5): 807-823.e19. https://doi.org/10.1016/j.cell.2017.04.018.

Cabezas-Wallscheid, Nina, Daniel Klimmeck, Jenny Hansson, Daniel B. Lipka, Alejandro Reyes, Qi Wang, Dieter Weichenhan, et al. 2014. "Identification of Regulatory Networks in HSCs and Their Immediate Progeny via Integrated Proteome, Transcriptome, and DNA Methylome Analysis." *Cell Stem Cell* 15 (4): 507–22. https://doi.org/10.1016/j.stem.2014.07.005.

Calvi, L. M., G. B. Adams, K. W. Weibrecht, J. M. Weber, D. P. Olson, M. C. Knight, R. P. Martin, et al. 2003. "Osteoblastic Cells Regulate the Haematopoietic Stem Cell Niche." *Nature* 425 (6960): 841–46. https://doi.org/10.1038/nature02040.

Cazzaniga, G. 2005. "Nucleophosmin Mutations in Childhood Acute Myelogenous Leukemia with Normal Karyotype." *Blood* 106 (4): 1419–22. https://doi.org/10.1182/blood-2005-03-0899.

Challen, Grant A, Deqiang Sun, Mira Jeong, Min Luo, Jaroslav Jelinek, Jonathan S Berg, Christoph Bock, et al. 2012. "Dnmt3a Is Essential for Hematopoietic Stem Cell Differentiation." *Nature Genetics* 44 (1): 23–31. https://doi.org/10.1038/ng.1009.

Cheng, T., N. Rodrigues, H. Shen, Y. Yang, D. Dombkowski, M. Sykes, and D. T. Scadden. 2000. "Hematopoietic Stem Cell Quiescence Maintained by P21cip1/Waf1." *Science (New York, N.Y.)* 287 (5459): 1804–8.

Cheshier, S. H., S. J. Morrison, X. Liao, and I. L. Weissman. 1999. "In Vivo Proliferation and Cell Cycle Kinetics of Long-Term Self-Renewing Hematopoietic Stem Cells." *Proceedings of the National Academy of Sciences of the United States of America* 96 (6): 3120–25.

Chou, Wen-Chien, Jih-Luh Tang, Liang-In Lin, Ming Yao, Woei Tsay, Chien-Yuan Chen, Shang-Ju Wu, et al. 2006. "Nucleophosmin Mutations in de Novo Acute Myeloid Leukemia: The Age-Dependent Incidences and the Stability during Disease Evolution." *Cancer Research* 66 (6): 3310–16. https://doi.org/10.1158/0008-5472.CAN-05-4316.

Chu, S. Haihua, Diane Heiser, Li Li, Ian Kaplan, Michael Collector, David Huso, Saul J. Sharkis, Curt Civin, and Don Small. 2012. "FLT3-ITD Knockin Impairs Hematopoietic Stem Cell Quiescence/Homeostasis, Leading to Myeloproliferative Neoplasm." *Cell Stem Cell* 11 (3): 346–58. https://doi.org/10.1016/j.stem.2012.05.027.

Collins, C T, and J L Hess. 2016. "Role of HOXA9 in Leukemia: Dysregulation, Cofactors and Essential Targets." *Oncogene* 35 (9): 1090–98. https://doi.org/10.1038/onc.2015.174.

Colombo, E, M Alcalay, and P G Pelicci. 2011. "Nucleophosmin and Its Complex Network: A Possible Therapeutic Target in Hematological Diseases." *Oncogene* 30 (23): 2595–2609. https://doi.org/10.1038/onc.2010.646.

Colombo, E., P. Bonetti, E. Lazzerini Denchi, P. Martinelli, R. Zamponi, J.-C. Marine, K. Helin, B. Falini, and P. G. Pelicci. 2005. "Nucleophosmin Is Required for DNA Integrity and P19Arf Protein Stability." *Molecular and Cellular Biology* 25 (20): 8874–86. https://doi.org/10.1128/MCB.25.20.8874-8886.2005.

Corces, M Ryan, Jason D Buenrostro, Beijing Wu, Peyton G Greenside, Steven M Chan, Julie L Koenig, Michael P Snyder, et al. 2016. "Lineage-Specific and Single-Cell Chromatin Accessibility Charts Human Hematopoiesis and Leukemia Evolution." *Nature Genetics* 48 (10): 1193–1203. https://doi.org/10.1038/ng.3646.

Corces-Zimmerman, M. R., W.-J. Hong, I. L. Weissman, B. C. Medeiros, and R. Majeti. 2014. "Preleukemic Mutations in Human Acute Myeloid Leukemia Affect Epigenetic Regulators and Persist in Remission." *Proceedings of the National Academy of Sciences* 111 (7): 2548–53. https://doi.org/10.1073/pnas.1324297111.

Corces-Zimmerman, M R, and R Majeti. 2014. "Pre-Leukemic Evolution of Hematopoietic Stem Cells: The Importance of Early Mutations in Leukemogenesis." *Leukemia* 28 (12): 2276–82. https://doi.org/10.1038/leu.2014.211.

De Kouchkovsky, I, and M Abdul-Hay. 2016. "'Acute Myeloid Leukemia: A Comprehensive Review and 2016 Update.'" *Blood Cancer Journal* 6 (7): e441–e441. https://doi.org/10.1038/bcj.2016.50.

Delhommeau, François, Sabrina Dupont, Véronique Della Valle, Chloé James, Severine Trannoy, Aline Massé, Olivier Kosmider, et al. 2009. "Mutation in TET2 in Myeloid Cancers." *New England Journal of Medicine* 360 (22): 2289–2301. https://doi.org/10.1056/NEJMoa0810069.

Dohner, H., E. H. Estey, S. Amadori, F. R. Appelbaum, T. Buchner, A. K. Burnett, H. Dombret, et al. 2010. "Diagnosis and Management of Acute Myeloid Leukemia in Adults: Recommendations from an International Expert Panel, on Behalf of the European LeukemiaNet." *Blood* 115 (3): 453–74. https://doi.org/10.1182/blood-2009-07-235358.

Dohner, Konstanze, and Lars Bullinger. 2017. "Clonal Evolution of AML." presented at the ESH 4th international conference on Acute Myeloid Leukemia, Estoril, Portugal, October 5.

Dovey, Oliver M., Jonathan L. Cooper, Annalisa Mupo, Carolyn S. Grove, Claire Lynn, Nathalie Conte, Robert M. Andrews, et al. 2017. "Molecular Synergy Underlies the Co-Occurrence Patterns and Phenotype of *NPM1* -Mutant Acute Myeloid Leukemia." *Blood* 130 (17): 1911–22. https://doi.org/10.1182/blood-2017-01-760595.

Falini, B., M. P. Martelli, C. Mecucci, A. Liso, N. Bolli, B. Bigerna, A. Pucciarini, et al. 2008. "Cytoplasmic Mutated Nucleophosmin Is Stable in Primary Leukemic Cells and in a Xenotransplant Model of NPMc+ Acute Myeloid Leukemia in SCID Mice." *Haematologica* 93 (5): 775–79. https://doi.org/10.3324/haematol.12225.

Falini, B., C. Mecucci, G. Saglio, F. L. Coco, D. Diverio, P. Brown, F. Pane, et al. 2008. "NPM1 Mutations and Cytoplasmic Nucleophosmin Are Mutually Exclusive of Recurrent Genetic Abnormalities: A Comparative Analysis of 2562 Patients with Acute Myeloid Leukemia." *Haematologica* 93 (3): 439–42. https://doi.org/10.3324/haematol.12153.

Falini, B., C. Mecucci, Enrico Tiacci, Myriam Alcalay, Roberto Rosati, Laura Pasqualucci, Roberta La Starza, et al. 2005. "Cytoplasmic Nucleophosmin in Acute Myelogenous Leukemia with a Normal Karyotype." *New England Journal of Medicine* 352 (3): 254–66. https://doi.org/10.1056/NEJMoa041974.

Feil, R., J. Brocard, B. Mascrez, M. LeMeur, D. Metzger, and P. Chambon. 1996. "Ligand-Activated Site-Specific Recombination in Mice." *Proceedings of the National Academy of Sciences of the United States of America* 93 (20): 10887–90.

Figueroa, Maria E., Omar Abdel-Wahab, Chao Lu, Patrick S. Ward, Jay Patel, Alan Shih, Yushan Li, et al. 2010. "Leukemic IDH1 and IDH2 Mutations Result in a Hypermethylation Phenotype, Disrupt TET2 Function, and Impair Hematopoietic

Differentiation." *Cancer Cell* 18 (6): 553–67. https://doi.org/10.1016/j.ccr.2010.11.015.

Forghieri, Fabio, Ambra Paolini, Monica Morselli, Sara Bigliardi, Goretta Bonacorsi, Giovanna Leonardi, Valeria Coluccio, et al. 2015. "NPM1 Mutations May Reveal Acute Myeloid Leukemia in Cases Otherwise Morphologically Diagnosed as Myelodysplastic Syndromes or Myelodysplastic/Myeloproliferative Neoplasms." *Leukemia & Lymphoma* 56 (11): 3222–26. https://doi.org/10.3109/10428194.2015.1026900.

Foudi, Adlen, Konrad Hochedlinger, Denille Van Buren, Jeffrey W. Schindler, Rudolf Jaenisch, Vincent Carey, and Hanno Hock. 2009. "Analysis of Histone 2B-GFP Retention Reveals Slowly Cycling Hematopoietic Stem Cells." *Nature Biotechnology* 27 (1): 84–90. https://doi.org/10.1038/nbt.1517.

Frehlick, Lindsay J., José María Eirín-López, and Juan Ausió. 2007. "New Insights into the Nucleophosmin/Nucleoplasmin Family of Nuclear Chaperones." *BioEssays* 29 (1): 49–59. https://doi.org/10.1002/bies.20512.

Fujita, S, D Honma, N Adachi, K Araki, E Takamatsu, T Katsumoto, K Yamagata, et al. 2018. "Dual Inhibition of EZH1/2 Breaks the Quiescence of Leukemia Stem Cells in Acute Myeloid Leukemia." *Leukemia* 32 (4): 855–64. https://doi.org/10.1038/leu.2017.300.

Furia, Laura, Pier Giuseppe Pelicci, and Mario Faretta. 2013. "A Computational Platform for Robotized Fluorescence Microscopy (I): High-Content Image-Based Cell-Cycle Analysis." *Cytometry Part A* 83A (4): 333–43. https://doi.org/10.1002/cyto.a.22266.

Gal, H, N Amariglio, L Trakhtenbrot, J Jacob-Hirsh, O Margalit, A Avigdor, A Nagler, et al. 2006. "Gene Expression Profiles of AML Derived Stem Cells; Similarity to Hematopoietic Stem Cells." *Leukemia* 20 (12): 2147–54. https://doi.org/10.1038/sj.leu.2404401.

Gallogly, Molly M., Hillard M. Lazarus, and Brenda W. Cooper. 2017. "Midostaurin: A Novel Therapeutic Agent for Patients with FLT3-Mutated Acute Myeloid Leukemia and Systemic Mastocytosis." *Therapeutic Advances in Hematology* 8 (9): 245–61. https://doi.org/10.1177/2040620717721459.

Genovese, Giulio, Anna K. Kähler, Robert E. Handsaker, Johan Lindberg, Samuel A. Rose, Samuel F. Bakhoum, Kimberly Chambert, et al. 2014. "Clonal Hematopoiesis and Blood-Cancer Risk Inferred from Blood DNA Sequence." *New England Journal of Medicine* 371 (26): 2477–87. https://doi.org/10.1056/NEJMoa1409405.

Gerdes, J., H. Lemke, H. Baisch, H. H. Wacker, U. Schwab, and H. Stein. 1984. "Cell Cycle Analysis of a Cell Proliferation-Associated Human Nuclear Antigen Defined by the Monoclonal Antibody Ki-67." *Journal of Immunology (Baltimore, Md.: 1950)* 133 (4): 1710–15.

Gilliland, D. G., and J. D. Griffin. 2002. "The Roles of FLT3 in Hematopoiesis and Leukemia." *Blood* 100 (5): 1532–42. https://doi.org/10.1182/blood-2002-02-0492.

Goodell, M. A., K. Brose, G. Paradis, A. S. Conner, and R. C. Mulligan. 1996. "Isolation and Functional Properties of Murine Hematopoietic Stem Cells That Are Replicating in Vivo." *The Journal of Experimental Medicine* 183 (4): 1797–1806.

Graaf, Carolyn A. de, and Donald Metcalf. 2011. "Thrombopoietin and Hematopoietic Stem Cells." *Cell Cycle* 10 (10): 1582–89. https://doi.org/10.4161/cc.10.10.15619.

Grimwade, D., A. Ivey, and B. J. P. Huntly. 2016. "Molecular Landscape of Acute Myeloid Leukemia in Younger Adults and Its Clinical Relevance." *Blood* 127 (1): 29–41.

https://doi.org/10.1182/blood-2015-07-604496.

Grisendi, Silvia, Rosa Bernardi, Marco Rossi, Ke Cheng, Luipa Khandker, Katia Manova, and Pier Paolo Pandolfi. 2005. "Role of Nucleophosmin in Embryonic Development and Tumorigenesis." *Nature* 437 (7055): 147–53. https://doi.org/10.1038/nature03915.

Grisendi, Silvia, Cristina Mecucci, Brunangelo Falini, and Pier Paolo Pandolfi. 2006. "Nucleophosmin and Cancer." *Nature Reviews Cancer* 6 (7): 493–505. https://doi.org/10.1038/nrc1885.

Grove, C. S., and G. S. Vassiliou. 2014. "Acute Myeloid Leukaemia: A Paradigm for the Clonal Evolution of Cancer?" *Disease Models & Mechanisms* 7 (8): 941–51. https://doi.org/10.1242/dmm.015974.

Guryanova, Olga A, Kaitlyn Shank, Barbara Spitzer, Luisa Luciani, Richard P Koche, Francine E Garrett-Bakelman, Chezi Ganzel, et al. 2016. "DNMT3A Mutations Promote Anthracycline Resistance in Acute Myeloid Leukemia via Impaired Nucleosome Remodeling." *Nature Medicine* 22 (12): 1488–95. https://doi.org/10.1038/nm.4210.

Hamilton, A., K. Foster, and D. Bonnet. 2104. "Impairment of AML Engraftment to the Bone Marrow Niche Following Inhibition of TGF-Beta Signaling." *Blood* 121 (21): 4372.

Hock, Hanno, Melanie J. Hamblen, Heather M. Rooke, Jeffrey W. Schindler, Shireen Saleque, Yuko Fujiwara, and Stuart H. Orkin. 2004. "Gfi-1 Restricts Proliferation and Preserves Functional Integrity of Haematopoietic Stem Cells." *Nature* 431 (7011): 1002–7. https://doi.org/10.1038/nature02994.

Horsley, Valerie, Antonios O. Aliprantis, Lisa Polak, Laurie H. Glimcher, and Elaine Fuchs. 2008. "NFATc1 Balances Quiescence and Proliferation of Skin Stem Cells." *Cell* 132 (2): 299–310. https://doi.org/10.1016/j.cell.2007.11.047.

Hu, Yifang, and Gordon K. Smyth. 2009. "ELDA: Extreme Limiting Dilution Analysis for Comparing Depleted and Enriched Populations in Stem Cell and Other Assays." *Journal of Immunological Methods* 347 (1–2): 70–78. https://doi.org/10.1016/j.jim.2009.06.008.

Ivanova, N. B. 2002. "A Stem Cell Molecular Signature." *Science* 298 (5593): 601–4. https://doi.org/10.1126/science.1073823.

Jaatinen, Taina, Heidi Hemmoranta, Sampsa Hautaniemi, Jari Niemi, Daniel Nicorici, Jarmo Laine, Olli Yli-Harja, and Jukka Partanen. 2006. "Global Gene Expression Profile of Human Cord Blood-Derived CD133+Cells." *Stem Cells* 24 (3): 631–41. https://doi.org/10.1634/stemcells.2005-0185.

Jaiswal, Siddhartha, Pierre Fontanillas, Jason Flannick, Alisa Manning, Peter V. Grauman, Brenton G. Mar, R. Coleman Lindsley, et al. 2014. "Age-Related Clonal Hematopoiesis Associated with Adverse Outcomes." *New England Journal of Medicine* 371 (26): 2488–98. https://doi.org/10.1056/NEJMoa1408617.

Jan, M., M. P. Chao, A. C. Cha, A. A. Alizadeh, A. J. Gentles, I. L. Weissman, and R. Majeti. 2011. "Prospective Separation of Normal and Leukemic Stem Cells Based on Differential Expression of TIM3, a Human Acute Myeloid Leukemia Stem Cell Marker." *Proceedings of the National Academy of Sciences* 108 (12): 5009–14. https://doi.org/10.1073/pnas.1100551108.

Jan, M., T. M. Snyder, M. R. Corces-Zimmerman, P. Vyas, I. L. Weissman, S. R. Quake, and R. Majeti. 2012. "Clonal Evolution of Preleukemic Hematopoietic Stem Cells Precedes Human Acute Myeloid Leukemia." *Science Translational Medicine* 4 (149):

149ra118-149ra118. https://doi.org/10.1126/scitranslmed.3004315.

Jones, Morgan, Jennifer Chase, Michelle Brinkmeier, Jing Xu, Daniel N. Weinberg, Julien Schira, Ann Friedman, et al. 2015. "Ash1l Controls Quiescence and Self-Renewal Potential in Hematopoietic Stem Cells." *Journal of Clinical Investigation* 125 (5): 2007–20. https://doi.org/10.1172/JCI78124.

Juntilla, M. M., V. D. Patil, M. Calamito, R. P. Joshi, M. J. Birnbaum, and G. A. Koretzky. 2010. "AKT1 and AKT2 Maintain Hematopoietic Stem Cell Function by Regulating Reactive Oxygen Species." *Blood* 115 (20): 4030–38. https://doi.org/10.1182/blood-2009-09-241000.

Kang, Y. J., M. O. Olson, and H. Busch. 1974. "Phosphorylation of Acid-Soluble Proteins in Isolated Nucleoli of Novikoff Hepatoma Ascites Cells. Effects of Divalent Cations." *The Journal of Biological Chemistry* 249 (17): 5580–85.

Kiel, Mark J., Ömer H. Yilmaz, Toshihide Iwashita, Osman H. Yilmaz, Cox Terhorst, and Sean J. Morrison. 2005. "SLAM Family Receptors Distinguish Hematopoietic Stem and Progenitor Cells and Reveal Endothelial Niches for Stem Cells." *Cell* 121 (7): 1109–21. https://doi.org/10.1016/j.cell.2005.05.026.

Kim, Daehwan, Geo Pertea, Cole Trapnell, Harold Pimentel, Ryan Kelley, and Steven L Salzberg. 2013. "TopHat2: Accurate Alignment of Transcriptomes in the Presence of Insertions, Deletions and Gene Fusions." *Genome Biology* 14 (4): R36. https://doi.org/10.1186/gb-2013-14-4-r36.

Kozar, Katarzyna, Maria A. Ciemerych, Vivienne I. Rebel, Hirokazu Shigematsu, Agnieszka Zagozdzon, Ewa Sicinska, Yan Geng, et al. 2004. "Mouse Development and Cell Proliferation in the Absence of D-Cyclins." *Cell* 118 (4): 477–91. https://doi.org/10.1016/j.cell.2004.07.025.

Krivtsov, Andrei V., David Twomey, Zhaohui Feng, Matthew C. Stubbs, Yingzi Wang, Joerg Faber, Jason E. Levine, et al. 2006. "Transformation from Committed Progenitor to Leukaemia Stem Cell Initiated by MLL–AF9." *Nature* 442 (7104): 818–22. https://doi.org/10.1038/nature04980.

Krönke, Jan, Lars Bullinger, Veronica Teleanu, Florian Tschürtz, Verena I. Gaidzik, Michael W. M. Kühn, Frank G. Rücker, et al. 2013. "Clonal Evolution in Relapsed NPM1-Mutated Acute Myeloid Leukemia." *Blood* 122 (1): 100–108. https://doi.org/10.1182/blood-2013-01-479188.

Kuhn, M. W. M., E. Song, Z. Feng, A. Sinha, C.-W. Chen, A. J. Deshpande, M. Cusan, et al. 2016. "Targeting Chromatin Regulators Inhibits Leukemogenic Gene Expression in NPM1 Mutant Leukemia." *Cancer Discovery* 6 (10): 1166–81. https://doi.org/10.1158/2159-8290.CD-16-0237.

Kühn, R., F. Schwenk, M. Aguet, and K. Rajewsky. 1995. "Inducible Gene Targeting in Mice." *Science (New York, N.Y.)* 269 (5229): 1427–29.

Lapidot, Tsvee, Christian Sirard, Josef Vormoor, Barbara Murdoch, Trang Hoang, Julio Caceres-Cortes, Mark Minden, Bruce Paterson, Michael A. Caligiuri, and John E. Dick. 1994. "A Cell Initiating Human Acute Myeloid Leukaemia after Transplantation into SCID Mice." *Nature* 367 (6464): 645–48. https://doi.org/10.1038/367645a0.

Laurenti, Elisa, and Berthold Göttgens. 2018. "From Haematopoietic Stem Cells to Complex Differentiation Landscapes." *Nature* 553 (7689): 418–26. https://doi.org/10.1038/nature25022.

Lee, Benjamin H., Zuzana Tothova, Ross L. Levine, Kristina Anderson, Natalija Buza-Vidas, Dana E. Cullen, Elizabeth P. McDowell, et al. 2007. "FLT3 Mutations Confer

Enhanced Proliferation and Survival Properties to Multipotent Progenitors in a Murine Model of Chronic Myelomonocytic Leukemia." *Cancer Cell* 12 (4): 367–80. https://doi.org/10.1016/j.ccr.2007.08.031.

Levis, Mark. 2017. "Midostaurin Approved for FLT3-Mutated AML." *Blood* 129 (26): 3403–6. https://doi.org/10.1182/blood-2017-05-782292.

Li, Qing, Natacha Bohin, Tiffany Wen, Victor Ng, Jeffrey Magee, Shann-Ching Chen, Kevin Shannon, and Sean J. Morrison. 2013. "Oncogenic Nras Has Bimodal Effects on Stem Cells That Sustainably Increase Competitiveness." *Nature* 504 (7478): 143–47. https://doi.org/10.1038/nature12830.

Liso, A, A Bogliolo, V Freschi, M P Martelli, S A Pileri, M Santodirocco, N Bolli, M F Martelli, and B Falini. 2008. "In Human Genome, Generation of a Nuclear Export Signal through Duplication Appears Unique to Nucleophosmin (NPM1) Mutations and Is Restricted to AML." *Leukemia* 22 (6): 1285–89. https://doi.org/10.1038/sj.leu.2405045.

Longley, Daniel B., D. Paul Harkin, and Patrick G. Johnston. 2003. "5-Fluorouracil: Mechanisms of Action and Clinical Strategies." *Nature Reviews Cancer* 3 (5): 330–38. https://doi.org/10.1038/nrc1074.

Lu, Rui, Ping Wang, Trevor Parton, Yang Zhou, Kaliopi Chrysovergis, Shira Rockowitz, Wei-Yi Chen, et al. 2016. "Epigenetic Perturbations by Arg882-Mutated DNMT3A Potentiate Aberrant Stem Cell Gene-Expression Program and Acute Leukemia Development." *Cancer Cell* 30 (1): 92–107. https://doi.org/10.1016/j.ccell.2016.05.008.

Majeti, Ravindra, Mark P. Chao, Ash A. Alizadeh, Wendy W. Pang, Siddhartha Jaiswal, Kenneth D. Gibbs, Nico van Rooijen, and Irving L. Weissman. 2009. "CD47 Is an Adverse Prognostic Factor and Therapeutic Antibody Target on Human Acute Myeloid Leukemia Stem Cells." *Cell* 138 (2): 286–99. https://doi.org/10.1016/j.cell.2009.05.045.

Mallardo, M, A Caronno, G Pruneri, P R Raviele, A Viale, P G Pelicci, and E Colombo. 2013. "NPMc+ and FLT3_ITD Mutations Cooperate in Inducing Acute Leukaemia in a Novel Mouse Model." *Leukemia* 27 (11): 2248–51. https://doi.org/10.1038/leu.2013.114.

Malumbres, Marcos, Rocío Sotillo, David Santamaría, Javier Galán, Ana Cerezo, Sagrario Ortega, Pierre Dubus, and Mariano Barbacid. 2004. "Mammalian Cells Cycle without the D-Type Cyclin-Dependent Kinases Cdk4 and Cdk6." *Cell* 118 (4): 493–504. https://doi.org/10.1016/j.cell.2004.08.002.

Massagué, Joan. 2004. "G1 Cell-Cycle Control and Cancer." *Nature* 432 (7015): 298–306. https://doi.org/10.1038/nature03094.

Matsumoto, Akinobu, Shoichiro Takeishi, Tomoharu Kanie, Etsuo Susaki, Ichiro Onoyama, Yuki Tateishi, Keiko Nakayama, and Keiichi I. Nakayama. 2011. "P57 Is Required for Quiescence and Maintenance of Adult Hematopoietic Stem Cells." *Cell Stem Cell* 9 (3): 262–71. https://doi.org/10.1016/j.stem.2011.06.014.

Mead, A. J., D. C. Linch, R. K. Hills, K. Wheatley, A. K. Burnett, and R. E. Gale. 2007. "FLT3 Tyrosine Kinase Domain Mutations Are Biologically Distinct from and Have a Significantly More Favorable Prognosis than FLT3 Internal Tandem Duplications in Patients with Acute Myeloid Leukemia." *Blood* 110 (4): 1262–70. https://doi.org/10.1182/blood-2006-04-015826.

Meloni, G., M. Mancini, V. Gianfelici, M. P. Martelli, R. Foa, and B. Falini. 2009. "Late Relapse of Acute Myeloid Leukemia with Mutated NPM1 after Eight Years: Evidence of NPM1 Mutation Stability." *Haematologica* 94 (2): 298–300. https://doi.org/10.3324/haematol.2008.000059.

Metzelder, S K, C Michel, M von Bonin, M Rehberger, E Hessmann, S Inselmann, M Solovey, et al. 2015. “NFATc1 as a Therapeutic Target in FLT3-ITD-Positive AML.” *Leukemia* 29 (7): 1470–77. https://doi.org/10.1038/leu.2015.95.

Min, Irene M., Giorgio Pietramaggiori, Francis S. Kim, Emmanuelle Passegué, Kristen E. Stevenson, and Amy J. Wagers. 2008. “The Transcription Factor EGR1 Controls Both the Proliferation and Localization of Hematopoietic Stem Cells.” *Cell Stem Cell* 2 (4): 380–91. https://doi.org/10.1016/j.stem.2008.01.015.

Miyamoto, Kana, Kiyomi Y. Araki, Kazuhito Naka, Fumio Arai, Keiyo Takubo, Satoshi Yamazaki, Sahoko Matsuoka, et al. 2007. “Foxo3a Is Essential for Maintenance of the Hematopoietic Stem Cell Pool.” *Cell Stem Cell* 1 (1): 101–12. https://doi.org/10.1016/j.stem.2007.02.001.

Miyamoto, T., K. Nagafuji, K. Akashi, M. Harada, T. Kyo, T. Akashi, K. Takenaka, et al. 1996. “Persistence of Multipotent Progenitors Expressing AML1/ETO Transcripts in Long-Term Remission Patients with t(8;21) Acute Myelogenous Leukemia.” *Blood* 87 (11): 4789–96.

Miyamoto, T., I. L. Weissman, and K. Akashi. 2000. “AML1/ETO-Expressing Nonleukemic Stem Cells in Acute Myelogenous Leukemia with 8;21 Chromosomal Translocation.” *Proceedings of the National Academy of Sciences of the United States of America* 97 (13): 7521–26.

Morris, S. W., M. N. Kirstein, M. B. Valentine, K. G. Dittmer, D. N. Shapiro, D. L. Saltman, and A. T. Look. 1994. “Fusion of a Kinase Gene, ALK, to a Nucleolar Protein Gene, NPM, in Non-Hodgkin’s Lymphoma.” *Science (New York, N.Y.)* 263 (5151): 1281–84.

Morrison, S. J., and I. L. Weissman. 1994. “The Long-Term Repopulating Subset of Hematopoietic Stem Cells Is Deterministic and Isolatable by Phenotype.” *Immunity* 1 (8): 661–73.

Mullighan, C G, A Kennedy, X Zhou, I Radtke, L A Phillips, S A Shurtleff, and J R Downing. 2007. “Pediatric Acute Myeloid Leukemia with NPM1 Mutations Is Characterized by a Gene Expression Profile with Dysregulated HOX Gene Expression Distinct from MLL-Rearranged Leukemias.” *Leukemia* 21 (9): 2000–2009. https://doi.org/10.1038/sj.leu.2404808.

Mupo, A, L Celani, O Dovey, J L Cooper, C Grove, R Rad, P Sportoletti, B Falini, A Bradley, and G S Vassiliou. 2013. “A Powerful Molecular Synergy between Mutant Nucleophosmin and Flt3-ITD Drives Acute Myeloid Leukemia in Mice.” *Leukemia* 27 (9): 1917–20. https://doi.org/10.1038/leu.2013.77.

Nagasawa, T., H. Kikutani, and T. Kishimoto. 1994. “Molecular Cloning and Structure of a Pre-B-Cell Growth-Stimulating Factor.” *Proceedings of the National Academy of Sciences of the United States of America* 91 (6): 2305–9.

Naka, Kazuhito, Takayuki Hoshii, Teruyuki Muraguchi, Yuko Tadokoro, Takako Ooshio, Yukio Kondo, Shinji Nakao, Noboru Motoyama, and Atsushi Hirao. 2010. “TGF-β–FOXO Signalling Maintains Leukaemia-Initiating Cells in Chronic Myeloid Leukaemia.” *Nature* 463 (7281): 676–80. https://doi.org/10.1038/nature08734.

Nakao, M., S. Yokota, T. Iwai, H. Kaneko, S. Horiike, K. Kashima, Y. Sonoda, T. Fujimoto, and S. Misawa. 1996. “Internal Tandem Duplication of the Flt3 Gene Found in Acute Myeloid Leukemia.” *Leukemia* 10 (12): 1911–18.

Ogawa, M., Y. Matsuzaki, S. Nishikawa, S. Hayashi, T. Kunisada, T. Sudo, T. Kina, H. Nakauchi, and S. Nishikawa. 1991. “Expression and Function of C-Kit in Hemopoietic Progenitor Cells.” *The Journal of Experimental Medicine* 174 (1): 63–71.

Okada, S., H. Nakauchi, K. Nagayoshi, S. Nishikawa, Y. Miura, and T. Suda. 1992. "In Vivo and in Vitro Stem Cell Function of C-Kit- and Sca-1-Positive Murine Hematopoietic Cells." *Blood* 80 (12): 3044–50.

Orford, Keith W., and David T. Scadden. 2008. "Deconstructing Stem Cell Self-Renewal: Genetic Insights into Cell-Cycle Regulation." *Nature Reviews Genetics* 9 (2): 115–28. https://doi.org/10.1038/nrg2269.

Osawa, M., K. Hanada, H. Hamada, and H. Nakauchi. 1996. "Long-Term Lymphohematopoietic Reconstitution by a Single CD34-Low/Negative Hematopoietic Stem Cell." *Science (New York, N.Y.)* 273 (5272): 242–45.

Pabst, Thomas, Beatrice U. Mueller, Pu Zhang, Hanna S. Radomska, Sailaja Narravula, Susanne Schnittger, Gerhard Behre, Wolfgang Hiddemann, and Daniel G. Tenen. 2001. "Dominant-Negative Mutations of CEBPA, Encoding CCAAT/Enhancer Binding Protein-α (C/EBPα), in Acute Myeloid Leukemia." *Nature Genetics* 27 (3): 263–70. https://doi.org/10.1038/85820.

Papaemmanuil, E., M. Gerstung, Lars Bullinger, Verena I. Gaidzik, Peter Paschka, Nicola D. Roberts, Nicola E. Potter, et al. 2016. "Genomic Classification and Prognosis in Acute Myeloid Leukemia." *New England Journal of Medicine* 374 (23): 2209–21. https://doi.org/10.1056/NEJMoa1516192.

Papaemmanuil, E., M. Gerstung, L. Malcovati, S. Tauro, G. Gundem, P. Van Loo, C. J. Yoon, et al. 2013. "Clinical and Biological Implications of Driver Mutations in Myelodysplastic Syndromes." *Blood* 122 (22): 3616–27. https://doi.org/10.1182/blood-2013-08-518886.

Pardee, A. B. 1974. "A Restriction Point for Control of Normal Animal Cell Proliferation." *Proceedings of the National Academy of Sciences of the United States of America* 71 (4): 1286–90.

Pasqualucci, L., A. Liso, M. P. Martelli, N. Bolli, R. Pacini, A. Tabarrini, M. Carini, et al. 2006. "Mutated Nucleophosmin Detects Clonal Multilineage Involvement in Acute Myeloid Leukemia: Impact on WHO Classification." *Blood* 108 (13): 4146–55. https://doi.org/10.1182/blood-2006-06-026716.

Passegué, Emmanuelle, Amy J. Wagers, Sylvie Giuriato, Wade C. Anderson, and Irving L. Weissman. 2005. "Global Analysis of Proliferation and Cell Cycle Gene Expression in the Regulation of Hematopoietic Stem and Progenitor Cell Fates." *The Journal of Experimental Medicine* 202 (11): 1599–1611. https://doi.org/10.1084/jem.20050967.

Picelli, Simone, Omid R Faridani, Åsa K Björklund, Gösta Winberg, Sven Sagasser, and Rickard Sandberg. 2014. "Full-Length RNA-Seq from Single Cells Using Smart-Seq2." *Nature Protocols* 9 (1): 171–81. https://doi.org/10.1038/nprot.2014.006.

Pietras, Eric M., Ranjani Lakshminarasimhan, Jose-Marc Techner, Sarah Fong, Johanna Flach, Mikhail Binnewies, and Emmanuelle Passegué. 2014. "Re-Entry into Quiescence Protects Hematopoietic Stem Cells from the Killing Effect of Chronic Exposure to Type I Interferons." *The Journal of Experimental Medicine* 211 (2): 245–62. https://doi.org/10.1084/jem.20131043.

Pietras, Eric M., Matthew R. Warr, and Emmanuelle Passegué. 2011. "Cell Cycle Regulation in Hematopoietic Stem Cells." *The Journal of Cell Biology* 195 (5): 709–20. https://doi.org/10.1083/jcb.201102131.

Redner, R. L., E. A. Rush, S. Faas, W. A. Rudert, and S. J. Corey. 1996. "The t(5;17) Variant of Acute Promyelocytic Leukemia Expresses a Nucleophosmin-Retinoic Acid Receptor Fusion." *Blood* 87 (3): 882–86.

Rieger, M. A., and T. Schroeder. 2012. “Hematopoiesis.” *Cold Spring Harbor Perspectives in Biology* 4 (12): a008250–a008250. https://doi.org/10.1101/cshperspect.a008250.

Robinson, M. D., D. J. McCarthy, and G. K. Smyth. 2010. “EdgeR: A Bioconductor Package for Differential Expression Analysis of Digital Gene Expression Data.” *Bioinformatics* 26 (1): 139–40. https://doi.org/10.1093/bioinformatics/btp616.

Rossi, Derrick J., David Bryder, Jacob M. Zahn, Henrik Ahlenius, Rebecca Sonu, Amy J. Wagers, and Irving L. Weissman. 2005. “Cell Intrinsic Alterations Underlie Hematopoietic Stem Cell Aging.” *Proceedings of the National Academy of Sciences* 102 (26): 9194–99. https://doi.org/10.1073/pnas.0503280102.

Roussel, P. 1994. “Identification of Ag-NOR Proteins, Markers of Proliferation Related to Ribosomal Gene Activity.” *Experimental Cell Research* 214 (2): 465–72. https://doi.org/10.1006/excr.1994.1283.

Rowley, J. D. 1973. “Identificaton of a Translocation with Quinacrine Fluorescence in a Patient with Acute Leukemia.” *Annales De Genetique* 16 (2): 109–12.

Rowley, J. D., H. M. Golomb, and C. Dougherty. 1977. “15/17 Translocation, a Consistent Chromosomal Change in Acute Promyelocytic Leukaemia.” *Lancet (London, England)* 1 (8010): 549–50.

Satoh, Yusuke, Itaru Matsumura, Hirokazu Tanaka, Sachiko Ezoe, Hiroyuki Sugahara, Masao Mizuki, Hirohiko Shibayama, et al. 2004. “Roles for C-Myc in Self-Renewal of Hematopoietic Stem Cells.” *The Journal of Biological Chemistry* 279 (24): 24986–93. https://doi.org/10.1074/jbc.M400407200.

Sauvage, F. J. de. 1996. “Physiological Regulation of Early and Late Stages of Megakaryocytopoiesis by Thrombopoietin.” *Journal of Experimental Medicine* 183 (2): 651–56. https://doi.org/10.1084/jem.183.2.651.

Scheicher, Ruth, Andrea Hoelbl-Kovacic, Florian Bellutti, Anca-Sarmiza Tigan, Michaela Prchal-Murphy, Gerwin Heller, Christine Schneckenleithner, et al. 2015. “CDK6 as a Key Regulator of Hematopoietic and Leukemic Stem Cell Activation.” *Blood* 125 (1): 90–101. https://doi.org/10.1182/blood-2014-06-584417.

Schneider, Caroline A., Wayne S. Rasband, and Kevin W. Eliceiri. 2012. “NIH Image to ImageJ: 25 Years of Image Analysis.” *Nature Methods* 9 (7): 671–75.

Shih, Alan H., Yanwen Jiang, Cem Meydan, Kaitlyn Shank, Suveg Pandey, Laura Barreyro, Ileana Antony-Debre, et al. 2015. “Mutational Cooperativity Linked to Combinatorial Epigenetic Gain of Function in Acute Myeloid Leukemia.” *Cancer Cell* 27 (4): 502–15. https://doi.org/10.1016/j.ccell.2015.03.009.

Shlush, Liran I., Sasan Zandi, Amanda Mitchell, Weihsu Claire Chen, Joseph M. Brandwein, Vikas Gupta, James A. Kennedy, et al. 2014. “Identification of Pre-Leukaemic Haematopoietic Stem Cells in Acute Leukaemia.” *Nature* 506 (7488): 328–33. https://doi.org/10.1038/nature13038.

Siegel, Rebecca L., Kimberly D. Miller, and Ahmedin Jemal. 2017. “Cancer Statistics, 2017.” *CA: A Cancer Journal for Clinicians* 67 (1): 7–30. https://doi.org/10.3322/caac.21387.

Siminovitch, L., E. A. McCulloch, and J. E. Till. 1963. “The Distribution of Colony-Forming Cells among Spleen Colonies.” *Journal of Cellular and Comparative Physiology* 62 (3): 327–36. https://doi.org/10.1002/jcp.1030620313.

Spangrude, G. J., S. Heimfeld, and I. L. Weissman. 1988. “Purification and Characterization of Mouse Hematopoietic Stem Cells.” *Science (New York, N.Y.)* 241

(4861): 58–62.

Spector, D. L., R. L. Ochs, and H. Busch. 1984. “Silver Staining, Immunofluorescence, and Immunoelectron Microscopic Localization of Nucleolar Phosphoproteins B23 and C23.” *Chromosoma* 90 (2): 139–48.

Sportoletti, P., E. Varasano, R. Rossi, O. Bereshchenko, D. Cecchini, I. Gionfriddo, N. Bolli, et al. 2013. “The Human NPM1 Mutation A Perturbs Megakaryopoiesis in a Conditional Mouse Model.” *Blood* 121 (17): 3447–58. https://doi.org/10.1182/blood-2012-08-449553.

Srinivas, S., T. Watanabe, C. S. Lin, C. M. William, Y. Tanabe, T. M. Jessell, and F. Costantini. 2001. “Cre Reporter Strains Produced by Targeted Insertion of EYFP and ECFP into the ROSA26 Locus.” *BMC Developmental Biology* 1: 4.

Subramanian, A., P. Tamayo, V. K. Mootha, S. Mukherjee, B. L. Ebert, M. A. Gillette, A. Paulovich, et al. 2005. “Gene Set Enrichment Analysis: A Knowledge-Based Approach for Interpreting Genome-Wide Expression Profiles.” *Proceedings of the National Academy of Sciences* 102 (43): 15545–50. https://doi.org/10.1073/pnas.0506580102.

Suda, Toshio, Fumio Arai, and Shigeto Shimmura. 2005. “Regulation of Stem Cells in the Niche.” *Cornea* 24 (8 Suppl): S12–17.

Suda, Toshio, Keiyo Takubo, and Gregg L. Semenza. 2011. “Metabolic Regulation of Hematopoietic Stem Cells in the Hypoxic Niche.” *Cell Stem Cell* 9 (4): 298–310. https://doi.org/10.1016/j.stem.2011.09.010.

Sugiyama, Tatsuki, Hiroshi Kohara, Mamiko Noda, and Takashi Nagasawa. 2006. “Maintenance of the Hematopoietic Stem Cell Pool by CXCL12-CXCR4 Chemokine Signaling in Bone Marrow Stromal Cell Niches.” *Immunity* 25 (6): 977–88. https://doi.org/10.1016/j.immuni.2006.10.016.

Sun, Yuqing, Bo Zhou, Fengbiao Mao, Jing Xu, Hongzhi Miao, Zhenhua Zou, Le Tran Phuc Khoa, et al. 2018. “HOXA9 Reprograms the Enhancer Landscape to Promote Leukemogenesis.” *Cancer Cell* 34 (4): 643-658.e5. https://doi.org/10.1016/j.ccell.2018.08.018.

Suri, C., P. F. Jones, S. Patan, S. Bartunkova, P. C. Maisonpierre, S. Davis, T. N. Sato, and G. D. Yancopoulos. 1996. “Requisite Role of Angiopoietin-1, a Ligand for the TIE2 Receptor, during Embryonic Angiogenesis.” *Cell* 87 (7): 1171–80.

Tabe, Yoko, Yue Xi Shi, Zhihong Zeng, Linhua Jin, Masato Shikami, Yasuhito Hatanaka, Takashi Miida, Frank J. Hsu, Michael Andreeff, and Marina Konopleva. 2013. “TGF-β-Neutralizing Antibody 1D11 Enhances Cytarabine-Induced Apoptosis in AML Cells in the Bone Marrow Microenvironment.” Edited by Pranela Rameshwar. *PLoS ONE* 8 (6): e62785. https://doi.org/10.1371/journal.pone.0062785.

Takubo, Keiyo, Nobuhito Goda, Wakako Yamada, Hirono Iriuchishima, Eiji Ikeda, Yoshiaki Kubota, Haruko Shima, et al. 2010. “Regulation of the HIF-1α Level Is Essential for Hematopoietic Stem Cells.” *Cell Stem Cell* 7 (3): 391–402. https://doi.org/10.1016/j.stem.2010.06.020.

Takubo, Keiyo, Go Nagamatsu, Chiharu I. Kobayashi, Ayako Nakamura-Ishizu, Hiroshi Kobayashi, Eiji Ikeda, Nobuhito Goda, et al. 2013. “Regulation of Glycolysis by Pdk Functions as a Metabolic Checkpoint for Cell Cycle Quiescence in Hematopoietic Stem Cells.” *Cell Stem Cell* 12 (1): 49–61. https://doi.org/10.1016/j.stem.2012.10.011.

The Cancer Genome Atlas Research Network. 2013. “Genomic and Epigenomic Landscapes of Adult De Novo Acute Myeloid Leukemia.” *New England Journal of*

Medicine 368 (22): 2059–74. https://doi.org/10.1056/NEJMoa1301689.

Thiede, C. 2006. "Prevalence and Prognostic Impact of NPM1 Mutations in 1485 Adult Patients with Acute Myeloid Leukemia (AML)." *Blood* 107 (10): 4011–20. https://doi.org/10.1182/blood-2005-08-3167.

Thorsteinsdottir, U., G. Sauvageau, and R. K. Humphries. 1999. "Enhanced in Vivo Regenerative Potential of HOXB4-Transduced Hematopoietic Stem Cells with Regulation of Their Pool Size." *Blood* 94 (8): 2605–12.

Till, J. E., and E. A. McCulloch. 1961. "A Direct Measurement of the Radiation Sensitivity of Normal Mouse Bone Marrow Cells." *Radiation Research* 14 (February): 213–22.

Vassiliou, George S, Jonathan L Cooper, Roland Rad, Juan Li, Stephen Rice, Anthony Uren, Lena Rad, et al. 2011. "Mutant Nucleophosmin and Cooperating Pathways Drive Leukemia Initiation and Progression in Mice." *Nature Genetics* 43 (5): 470–75. https://doi.org/10.1038/ng.796.

Venezia, Teresa A, Akil A Merchant, Carlos A Ramos, Nathan L Whitehouse, Andrew S Young, Chad A Shaw, and Margaret A Goodell. 2004. "Molecular Signatures of Proliferation and Quiescence in Hematopoietic Stem Cells." Edited by Bing Lim. *PLoS Biology* 2 (10): e301. https://doi.org/10.1371/journal.pbio.0020301.

Viale, Andrea, Francesca De Franco, Annette Orleth, Valeria Cambiaghi, Virginia Giuliani, Daniela Bossi, Chiara Ronchini, et al. 2009. "Cell-Cycle Restriction Limits DNA Damage and Maintains Self-Renewal of Leukaemia Stem Cells." *Nature* 457 (7225): 51–56. https://doi.org/10.1038/nature07618.

Vogelstein, Bert, Eric R. Fearon, Stanley R. Hamilton, Scott E. Kern, Ann C. Preisinger, Mark Leppert, Alida M.M. Smits, and Johannes L. Bos. 1988. "Genetic Alterations during Colorectal-Tumor Development." *New England Journal of Medicine* 319 (9): 525–32. https://doi.org/10.1056/NEJM198809013190901.

Walter, R B, and E H Estey. 2015. "Management of Older or Unfit Patients with Acute Myeloid Leukemia." *Leukemia* 29 (4): 770–75. https://doi.org/10.1038/leu.2014.216.

Weissmann, S., T Alpermann, V Grossmann, A Kowarsch, N Nadarajah, C Eder, F Dicker, et al. 2012. "Landscape of TET2 Mutations in Acute Myeloid Leukemia." *Leukemia* 26 (5): 934–42. https://doi.org/10.1038/leu.2011.326.

Whitman, S. P., K. J. Archer, L. Feng, C. Baldus, B. Becknell, B. D. Carlson, A. J. Carroll, et al. 2001. "Absence of the Wild-Type Allele Predicts Poor Prognosis in Adult de Novo Acute Myeloid Leukemia with Normal Cytogenetics and the Internal Tandem Duplication of FLT3: A Cancer and Leukemia Group B Study." *Cancer Research* 61 (19): 7233–39.

Wilson, A. 2004. "C-Myc Controls the Balance between Hematopoietic Stem Cell Self-Renewal and Differentiation." *Genes & Development* 18 (22): 2747–63. https://doi.org/10.1101/gad.313104.

Wilson, A., Elisa Laurenti, Gabriela Oser, Richard C. van der Wath, William Blanco-Bose, Maike Jaworski, Sandra Offner, et al. 2008. "Hematopoietic Stem Cells Reversibly Switch from Dormancy to Self-Renewal during Homeostasis and Repair." *Cell* 135 (6): 1118–29. https://doi.org/10.1016/j.cell.2008.10.048.

Wu, Yong, Min Su, ShuX Zhang, Yu Cheng, Xiao Y. Liao, Bao Y. Lin, and Yuan Z. Chen. 2017. "Abnormal Expression of TGF-Beta Type II Receptor Isoforms Contributes to Acute Myeloid Leukemia." *Oncotarget* 8 (6).

https://doi.org/10.18632/oncotarget.14325.

Yamada, Takeshi, Chun Shik Park, and H Daniel Lacorazza. 2013. "Genetic Control of Quiescence in Hematopoietic Stem Cells." *Cell Cycle* 12 (15): 2376–83. https://doi.org/10.4161/cc.25416.

Yamamoto, Y., H. Kiyoi, Y. Nakano, R. Suzuki, Y. Kodera, S. Miyawaki, N. Asou, et al. 2001. "Activating Mutation of D835 within the Activation Loop of FLT3 in Human Hematologic Malignancies." *Blood* 97 (8): 2434–39.

Yamazaki, S., A. Iwama, S.-i. Takayanagi, K. Eto, H. Ema, and H. Nakauchi. 2009. "TGF- as a Candidate Bone Marrow Niche Signal to Induce Hematopoietic Stem Cell Hibernation." *Blood* 113 (6): 1250–56. https://doi.org/10.1182/blood-2008-04-146480.

Yang, L., L. Wang, H. Geiger, J. A. Cancelas, J. Mo, and Y. Zheng. 2007. "Rho GTPase Cdc42 Coordinates Hematopoietic Stem Cell Quiescence and Niche Interaction in the Bone Marrow." *Proceedings of the National Academy of Sciences* 104 (12): 5091–96. https://doi.org/10.1073/pnas.0610819104.

Yang, Liubin, Benjamin Rodriguez, Allison Mayle, Hyun Jung Park, Xueqiu Lin, Min Luo, Mira Jeong, et al. 2016. "DNMT3A Loss Drives Enhancer Hypomethylation in FLT3-ITD-Associated Leukemias." *Cancer Cell* 29 (6): 922–34. https://doi.org/10.1016/j.ccell.2016.05.003.

Yilmaz, Ömer H., Riccardo Valdez, Brian K. Theisen, Wei Guo, David O. Ferguson, Hong Wu, and Sean J. Morrison. 2006. "Pten Dependence Distinguishes Haematopoietic Stem Cells from Leukaemia-Initiating Cells." *Nature* 441 (7092): 475–82. https://doi.org/10.1038/nature04703.

Yoshihara, Hiroki, Fumio Arai, Kentaro Hosokawa, Tetsuya Hagiwara, Keiyo Takubo, Yuka Nakamura, Yumiko Gomei, et al. 2007. "Thrombopoietin/MPL Signaling Regulates Hematopoietic Stem Cell Quiescence and Interaction with the Osteoblastic Niche." *Cell Stem Cell* 1 (6): 685–97. https://doi.org/10.1016/j.stem.2007.10.020.

Yung, Benjamin Yat Ming. 2007. "Oncogenic Role of Nucleophosmin/B23." *Chang Gung Medical Journal* 30 (4): 285–93.

Zhang, Jiwang, Justin C. Grindley, Tong Yin, Sachintha Jayasinghe, Xi C. He, Jason T. Ross, Jeffrey S. Haug, et al. 2006. "PTEN Maintains Haematopoietic Stem Cells and Acts in Lineage Choice and Leukaemia Prevention." *Nature* 441 (7092): 518–22. https://doi.org/10.1038/nature04747.

Zhang, Jiwang, Chao Niu, Ling Ye, Haiyang Huang, Xi He, Wei-Gang Tong, Jason Ross, et al. 2003. "Identification of the Haematopoietic Stem Cell Niche and Control of the Niche Size." *Nature* 425 (6960): 836–41. https://doi.org/10.1038/nature02041.

Zhao, Meng, John M Perry, Heather Marshall, Aparna Venkatraman, Pengxu Qian, Xi C He, Jasimuddin Ahamed, and Linheng Li. 2014. "Megakaryocytes Maintain Homeostatic Quiescence and Promote Post-Injury Regeneration of Hematopoietic Stem Cells." *Nature Medicine* 20 (11): 1321–26. https://doi.org/10.1038/nm.3706.

Zsebo, Krisztina M., David A. Williams, Edwin N. Geissler, Virginia C. Broudy, Francis H. Martin, Harry L. Atkins, Rou-Yin Hsu, et al. 1990. "Stem Cell Factor Is Encoded at the SI Locus of the Mouse and Is the Ligand for the C-Kit Tyrosine Kinase Receptor." *Cell* 63 (1): 213–24. https://doi.org/10.1016/0092-8674(90)90302-U.

Zuber, J., I. Radtke, T. S. Pardee, Z. Zhao, A. R. Rappaport, W. Luo, M. E. McCurrach, et al. 2009. "Mouse Models of Human AML Accurately Predict Chemotherapy Response." *Genes & Development* 23 (7): 877–89. https://doi.org/10.1101/gad.1771409.